Dissertation

submitted to the

Combined Faculty of Natural Sciences and Mathematics

of the Ruperto Carola University Heidelberg, Germany

for the degree of

Doctor of Natural Sciences

Presented by

M.Sc. Felix Funck

born in: Tübingen, Germany

Oral examination: November 15th 2019

Innate immune cell crosstalk induces melanoma cell senescence

Referees:

Prof. Dr. Viktor Umansky

Prof. Dr. Knut Schäkel

Table of Contents

1 Zusammenfassung

Das angeborene Immunsystem stellt die erste Abwehrlinie gegen Infektionen und Krebs dar und ist daher maßgeblich am Erfolg von Tumor-spezifischen Immunantworten beteiligt. Ein kritischer Aspekt der Entstehung von Melanom ist die Fähigkeit, der Zerstörung durch das eigene Immunsystem zu entgehen. An diesem Punkt setzen moderne Therapien an, indem sie die Inhibition des Immunsystems auflösen, wie durch den erfolgreichen Einsatz von Checkpoint Inhibitoren demonstriert wurde. In vielen Patienten häufen sich jedoch Mutationen in Genen für die Antigenpräsentierung, was dazu führt, dass diese Patienten nicht auf T-zell vermittelte Immunantworten reagieren. In diesem Fall könnte die therapeutische Manipulation angeborener Immunantworten eine effektive Methode zur Vorbeugung der Tumorprogression und Metastasierung darstellen. In dieser Studie wird die Wirkung von zwei Immunzellen des angeborenen Immunsystems, slan$^+$ Monozyten (slanMo) und natürlichen Killer (NK) Zellen, gegenüber Melanom untersucht. Außerdem wird deren Aktivierung durch R848 analysiert, einem synthetischen TLR 7/8 Ligand, der aktuell auf seine therapeutische Wirksamkeit bei Melanom hin getestet wird.

Wir werfen die Frage auf, ob slanMo aktiv NK Zellen rekrutieren um angeborene Immunreaktionen zu initiieren, welche dann das Tumorwachstum kontrollieren und Seneszenz in Melanom Zellen induzieren können. Wir detektieren slanMo wiederholt in Melanom befallenem Gewebe, jedoch nur sporadisch in gesunder Haut. Aggressive Formen von Melanom waren durch eine geringere Anzahl infiltrierender slanMo gekennzeichnet, die außerdem mit der Infiltration von NK Zellen korrelierten. Um zu hinterfragen, ob die Korrelation der slanMo und NK Zell Infiltration auf einem zusammenhängenden Migrationsmechanismus beruht, untersuchten wir die Chemokin Sekretion von slanMo. *In vitro* Kultivierung von slanMo führte zur Sekretion von verschiedenen Chemokinen wie zum Beispiel IL-8/CXCL8, was zusätzlich durch Zugabe von R848 erhöht wurde. Konditioniertes Medium von stimulierten slanMo induzierte NK Zell chemotaxis und führte zur herunter Regulierung der IL-8 Rezeptoren CXCR1 und CXCR2 auf NK Zellen, was auf eine Beteiligung der Rezeptoren hindeutet. Neutralisierungsexperimente identifizierten IL-8 als das relevante Chemokin in slanMo CM. Um den Einfluss der slanMo/NK Zell Wechselwirkung auf Melanom Zellen zu untersuchen, übertrugen wir Überstände von R848-stimulierten slanMo/NK Zell Ko-Kulturen auf Melanom Zellen, was das Wachstum der Melanom Zellen stark einschränkte. R848-stimulierte slanMo/NK Zell Ko-Kulturen enthielten hohe Mengen an TNF-α und IFN-γ, die nicht erreicht werden konnten wenn NK Zellen mit CD14$^+$ Monozyten oder slanMo mit T Zellen inkubiert wurden. Experimente mit

neutralisierenden Antikörpern demonstrierten die Seneszenz induzierende Funktion von TNF-α und IFN-γ in slanMo/NK Zell Überständen, welche durch reduzierte Proliferation, gesteigerte Expression von Seneszenz-assoziierter β-Galactosidase und p21, und dem Auftreten eines Seneszenz-assoziierten Sekretorischen Phänotyps in Tumor Zellen gekennzeichnet ist.

Zusammenfassend wurde hier das Potenzial der angeborenen Immunität in Bezug auf die Generierung einer Seneszenz-induzierenden Umgebung, ermöglicht durch Stimulierung mit TLR Liganden, untersucht. Diese Studie bietet Einsichten in den therapeutischen Wirkmechanismus von TLR Liganden, wie zum Beispiel dem TLR 7/8 Liganden Imiquimod, der zur topischen Behandlung von Melanom eingesetzt wird. In diesem Zusammenhang sprechen unsere Ergebnisse für eine optimale Stimulierung von slanMo im Tumor, was dann durch Rekrutierung von NK Zellen zu Seneszenz in Melanom Zellen führen könnte.

2 Summary

Innate immune cells represent the first line of defense against infections and cancer and therefore play a pivotal role in determining the fate of anti-tumor immune responses. As a critical aspect of melanoma biology is represented by the ability to evade immune destruction, modern therapies can benefit from breaking immune suppression, as demonstrated by checkpoint inhibitor therapy. However, many patients acquire defects in antigen presentation and thereby remain unresponsive to T cell mediated immune clearance. For those patients, therapies enabling innate immune responses might prove to be effective in preventing cancer progression and metastasis. Therefore, this study investigated the anti-melanoma effects of two innate immune cell types, slan$^+$ monocytes (slanMo) and natural killer (NK) cells, in combination with stimulation by R848, a synthetic TLR 7/8 ligand for topical application that is currently investigated regarding therapeutic efficacy in melanoma.

Here, we addressed the question whether slanMo actively recruit NK cells in order to initiate an innate immune response that limits tumor growth and induces senescence in melanoma cells. We showed that slanMo are frequently detected in melanoma tissue, but rarely in healthy skin. More invasive forms of melanoma exhibited reduced numbers of infiltrating slanMo that were accompanied by correlating numbers of NK cells. To elucidate whether the correlating infiltration patterns represent a connected migration mechanism, we investigated chemokine production by slanMo. In vitro culture of slanMo resulted in the secretion of various chemokines such as IL-8/CXCL8, which was further increased by stimulation with R848. Stimulated slanMo conditioned medium (slanMo CM) induced chemotaxis of NK cells and led to the downregulation of the IL-8 receptors CXCR1 and CXCR2 on NK cells, indicative of receptor engagement. Neutralization experiments revealed IL-8 as the relevant NK cell chemoattractant in slanMo CM. To investigate the influence of the slanMo/NK cell crosstalk on melanoma cells, we transferred supernatants from R848-stimulated slanMo/NK cell co-cultures to melanoma cells, resulting in strongly attenuated cell growth. We found that R848-stimulated slanMo/NK cell co-culture CM contained high levels of TNF-α and IFN-γ, not reached when NK cells were cultured with CD14$^+$ monocytes or slanMo were cultured with T cells. Neutralization experiments revealed that TNF-α and IFN-γ present in slanMo/NK cell co-culture CM induced senescence in melanoma cells as indicated by reduced proliferation, increased senescence-associated β-Galactosidase expression, p21 upregulation, and induction of a senescence-associated secretory phenotype (SASP) in the tumor cells.

Taken together, this study describes the potential of innate immunity to generate a senescence inducing microenvironment after stimulation with TLR ligands. We provide

insight into the therapeutical mechanism of TLR ligands such as the TLR 7/8 ligand Imiquimod for topical melanoma therapy. Accordingly, our results argue for increased NK cell recruitment as a foundation for eliciting slanMo/NK cell crosstalk induced melanoma cell senescence.

3 Introduction

3.1 The Immune System

The immune system is responsible for defending the body against foreign dangers such as bacteria, viruses, fungi, or parasites. Naturally, it is a race between the pathogen and the host's immune system, where each side developes strategies to evade destruction by the opponent. To protect the organism against damage, the immune system possesses a variety of specialized cells that can be roughly divided into two arms – innate immune cells and adaptive immune cells. The major discriminating factor is that innate immunity offers immediate protection against pathogens in the range of minutes to hours, whereas adaptive immunity requires clonal selection and maturation, delaying adaptive immune responses to a magnitude of days and weeks. Together, both arms of the immune system provide powerful and long lasting immunity, which can again be divided into two parts: (1) Cellular interactions between immune cells and pathogens resulting in direct killing, and (2) the secretion of soluble factors and antibodies recognizing pathogenic motifs and thereby facilitating neutralization and clearance of infections. As a result, immune responses need to be subject to thorough regulation, as misguided or overshooting reactions pose a threat to the host organism. Besides danger-associated functions, the immune system is also involved in tissue homeostasis, i.e. through removing apoptotic cells and supporting tissue regeneration after injury.

3.1.1 Innate Immunity

The innate immune system is the first line of defense against pathogens. Innate immune cells are therefore readily present and active within tissues lining the body surface, which are mainly the skin and the mucosal system. Human white blood cells, also called leukocytes, generally originate from the bone marrow. In human blood, the major innate leukocyte populations are:

Neutrophils

Neutrophils are the most abundant leukocyte population in the blood and often mediate fast, but short-lived reactions. Morphologically, they can be identified by a segmented nucleus, which led to the alternative name of polymorphonuclear leukocytes. Already at steady state, neutrophils possess cytoplasmic granules filled with lytic enzymes and other anti-microbial

agents such as defensins, which allow them to immediately target invading pathogens. The major focus of neutrophils, however, lies in the phagocytosis of pathogens.

Mononuclear Phagocytes

Human Monocytes can be divided in three subgroups identified by the expression of the surface markers CD14 and CD16 (Fcγ Receptor III): (1) classical monocytes are $CD14^{+}CD16^{-}$; (2) intermediate monocytes are $CD14^{+}CD16^{+}$; and (3) non-classical monocytes are $CD14^{-/dim}CD16^{+}$ [1]. Non-classical monocytes can further be subdivided based on expression of the carbohydrate modification 6-sulfo LAcNAc (slan) on PSGL-1 [2]. Those $slan^{+}$ monocytes were termed slanMo and will be discussed together with NK cells in section 3.2. After migration into tissues, monocytes can mature and become macrophages. In addition to monocyte-derived macrophages, organs also harbor specialized tissue resident macrophages that function in tissue homeostasis and local immune reactions, such as microglia in the brain or alveolar Kupffer cells [3, 4]. Similar to neutrophils, monocytes and macrophages are potent phagocytes and often mediate long-term clearance as a supplement to short-lived neutrophil reactions. In addition, secretion of cytokines such as TNF-α, IL-6 and IL-8, allows mononuclear phagocytes to influence local immune reactions and recruit subsequent waves of immune cells, termed acute phase response [5].

In the murine system, monocytes consist of $Ly6C^{high}$ and $Ly6C^{low}$ monocytes, being homologous to human classical and non-classical monocytes, respectively. $Ly6C^{low}$ monocytes are also called patrolling monocytes, which stems from observations of those cells crawling along the endothelium, a phenotype they share with their human counterpart [6]. However, it is still unclear whether a murine homolog for human slanMo exists, since no carbohydrate modification comparable to slan is reported to be present on murine monocytes up to date.

Dendritic cells (DCs)

Dendritic cells (DCs) are specialized antigen-presenting cells (APCs). In that way, they function as a critical relay between the innate and adaptive immune response. APCs, in contrast to MHC-I associated self-peptide display on all cells, can present external molecules to naïve T cells and thereby initiate adaptive immune responses. Conventional DCs (cDCs) are the most abundant DC subset in tissues and lymphoid organs and constantly monitor the surrounding environment for exogenous particles, a behavior that is facilitated by formation of long protrusions, so-called dendrites. Plasmacytoid dendritic cells (pDCs) represent another DC subset in blood and tissue, which are mostly involved in Type I Interferon-mediated anti-viral responses.

Mast cells, Basophils, and Eosinophils

Mast cells are absent in the circulation, but can be found in tissues where they impact local immune reactions, most commonly allergic reactions. Similar to neutrophils, basophils and eosinophils are blood granulocytes characterized by accumulation of lytic granules.

Natural killer (NK) cells

NK cells belong to the lymphocytic system as they together with T and B cells originate from the common lymphoid precursor. NK cells share many functions with T cells but lack the antigen receptor machinery. Therefore, NK cells also count as innate immune cells and will be discussed in more detail in section 3.2, as they are an integral part of this thesis.

3.1.2 Innate immune recognition

The innate immune system is specialized in directly responding to threats without requiring prolonged activation periods. This is enabled by receptors recognizing certain pathogen-associated molecular patterns (PAMPs) and damage-associated molecular patterns (DAMPs). PAMPs are proteins, lipids, or DNA, directly originating from the pathogen, whereas DAMPS are often molecules that become exposed after tissue damage or apoptosis of host cells, such as nuclear or stress-induced proteins. The major pattern recognition receptors (PRRs) are membrane-bound Toll-like receptors (TLRs), C-type lectin-like receptors (CLRs), and scavenger receptors, as well as cytosolic NOD-like receptors (NLRs) and RIG-like receptors (RLRs) [7]. TLRs are special in the way that the receptors can be present on the cell surface as well as on endosomes. In humans, 9 TLRs are known, of which TLR3, 7, 8, 9 appear exclusively on endosomal membranes [8, 9, 10]. Several receptor-ligand pairs have been described to date, i.e. bacterial cell wall-derived lipopolysaccharid (LPS) can trigger the common adapter protein MyD88 via TLR4 signaling and thereby mediate NF-κB activation, leading to the transcription of NF-κB target genes such as the cytokines TNF-α, IL-12, IL-1, IL-6, and chemokines such as CCL2 and CXCL8 (IL-8) [11]. Endosomal TLRs recognize different polynucleotide configurations, i.e. single stranded RNA (ssRNA) binding to TLR7 and TLR8 to induce NF-κB signaling [12].

An important aspect of all those receptors is that they are germ-line encoded and therefore are not dependent on antigen-specific maturation. On the other hand, this also represents a major caveat of innate immunity, namely the inability to react to changes outside the inherent repertoire, i.e. when bacteria acquire mutations that alter protein structure or lipid modifications.

3.1.3 Adaptive Immunity

The common lymphocyte progenitor gives rise to T cells, B cells, and NK cells. Among lymphocytes, T and B cells orchestrate long-lasting immune responses based on highly variable antigen receptors that are generated through gene rearrangement. Even though recent reports also demonstrate certain memory functions for NK cells, the basic concept of immunological memory refers to T and B cell immunity.

As common to all blood cells, lymphocytes are generated in the bone marrow. However T and B cells are unique in that they require specialized lymphoid organs for their development. B cells remain in the bone marrow, whereas T cells migrate to the thymus for their final maturation to take place. In general, both T and B cells undergo certain selection processes to assure that only clones with a functional, yet not excessively strong binding antigen receptor are released to the periphery. This process is called central tolerance and involves several steps: (1) Pre-antigen receptor expression; only cells that express functional pre-receptors, which are composed of only one of the final receptor chains, receive survival signals and evade apoptotic cell death. (2) Antigen receptor expression; at this stage, T and B cells rearrange the genes for the second antigen-receptor chain, called V(D)J recombination. Random combination of V(D)J rearranged single chains generates a theoretical diversity of ~10^{11} B cell receptors (BCR) and ~10^{16} T cell receptors (TCR). (3) Positive selection; T and B cells that express functional antigen-receptors are selected and proliferate to increase the pool of functional cells. (4) Negative selection; In order to prevent immune reactions against own tissues, so called autoimmune reactions, the pool of functional T and B cells is cleared of clones expressing highly reactive antigen-receptors. Those clones that survive both positive and negative selection advance and migrate into the periphery. However, it is not rare that autoreactive T or B cells escape central tolerance. Therefore, it is also important to constantly control immune activity in the periphery. Peripheral tolerance is mostly maintained by T regulatory cells (T regs) that are supposed to regulate chronic or exacerbated immune responses through sercretion of inhibitory cytokines such as IL-10. Additionally, overly active T cells in the periphery can enter a state of anergy, which renders them unresponsive.

As mentioned before, adaptive immune responses require an additional priming phase in the magnitude of days. The high diversity of possible TCRs and BCRs increases the likelihood of reactive T and B cells being present virtually at any time and against any pathogen. However, the need for high diversity also reduces the actual number of reactive cells and therefore, after recognizing its cognate antigen, the lymphocyte first enters several rounds of proliferation and affinity maturation, a process where the specificity of the variable region is further fine-tuned for optimal binding of the exogenous ligands. This priming usually takes

place in secondary lymphoid organs such as lymph nodes and the spleen, where APCs immigrate to present tissue antigens to T cells and to provide co-stimulatory signals. T cells consist of two major subsets, CD4 and CD8 T cells, and the major discriminator is selective binding to peptide-MHC-II and peptide-MHC-I complexes, respectively. However, the subsets also differ functionally. Whereas CD4 T cells are classically viewed as stimulatory cells, characterized by secreting cytokines and activating B cells, earning them the name T helper (Th) cell, CD8 T cells are also called cytotoxic T cells due to their established cytotoxic properties and direct killing of target cells through perforin and granzyme production.

B cells also undergo their priming phase in lymph nodes, where APCs, Th cells, and B cells come together. In this environment, B cells prepare for high scale production of a soluble form of the BCR, called Immunoglobulin (IgG), or antibody. Antibodies can neutralize target pathogens or toxins by opsonization of the targets. Additionally, opsonized pathogens are easy targets for cells carrying special receptors recognizing the constant antibody region. A major hallmark of adaptive immunity are memory responses, meaning that both T and B cells can develop long-lived subpopulations that retain epitope specificity of the first antigen encounter and can mount immediate responses after re-encounter of the same pathogen. In the classical case of vaccination, memory B cells maintain long-lasting immunity through constant secretion of pathogen-specific antibodies that prevent subsequent infections.

Other rare immune cell populations complete the lymphocytic system. Those include NK T cells, innate lymphoid cells (ILCs), and γδ T cells [13, 14, 15]. γδ T cells share the development with conventional αβ T cells. However, γδ TCR rearrangement generates far less variability and γδ TCRs rather resemble PRRs, which is why they are considered part of innate immunity. Of note, also CD4 Th cells are further subdivided into different subsets, most prominently the Th1 and Th2 subsets, but over the recent years more subsets were added, i.e. Th17 cells, which are suggested to possess high inflammatory driving potential, in particular in skin diseases such as psoriasis [16].

3.1.4 Trafficking and tissue homing of immune cells

After their generation in the bone marrow, immune cells enter the blood stream, allowing them to reach virtually all vasculated tissues. Therefore, the immune cell composition in the blood that can be monitored at any given point is the combined result of both the supply of newly generated cells (influx), as well as the egress into tissues (efflux). Extravasation, which describes the exit from the blood stream, generally involves different steps called the leukocyte adhesion cascade [17].

Leukocyte transmigration

The first steps of emigration from the blood stream are defined by interactions with endothelial cells. These interactions involve different adhesion receptors of varying affinity. The interactions are gradually increasing in adhesion strength until the cell remains stationary on the vessel wall. PSGL-1 on leukocytes mediates the interaction with the endothelium by binding to selectins, in particular E- and P-selectin, expressed on inflamed endothelial cells as well as L-selectin expressed on other leukocytes [18]. In addition, integrins and their ligands also support rolling, i.e. very late antigen 4 (VLA4; $\alpha_4\beta_1$-integrin) and lymphocyte function-associated antigen 1 (LFA-1; $\alpha_1\beta_2$-integrin), expressed on lymphocytes, can engage vascular cell-adhesion molecule 1 (VCAM1) and intercellular adhesion molecule 1 (ICAM1), respectively, together mediating firm adhesion and thereby reducing rolling speed [19]. During the rolling process, leukocytes receive signals through their interactions with the endothelium, which in turn transform integrins to higher affinity conformations via inside-out signaling, finally rendering the leukocytes stationary. Those activating signals include integrin signaling via VLA4 and LFA-1. However, the most efficient inside-out signaling is transmitted by g-protein coupled receptor (GPCR)-mediated chemokine signaling relying on ectopic luminal expression of chemokine ligands. Arrested cells then receive outside-in signals through integrins to further strengthen adhesion to the vasculature and prevent detachment [20]. After firm attachment, leukocytes prepare for transmigration through the endothelial layer. Monocytes have been observed to crawl along the vasculature in search for optimal transmigration areas. The transmigration process is initiated by binding of leukocyte integrins to their ligands on endothelial cells together with a local accumulation of ICAM1 and VCAM1, strongly facilitating transmigration [21, 22]. Crossing the endothelial layer can occur in two ways, either between neighboring endothelial cells (paracellular) or directly through individual endothelial cells (transcellular). In general, this whole cascade is predominantly taking place in inflamed areas, where the local environment activates the endothelium to enable attachment against shear stress.

The chemokine system

Circulating immune cells can enter tissues by firm adhesion and subsequent transmigration. However, the concept of homeostatic tissue homing is not well understood and mostly investigated regarding certain immune cell populations such as monocytes or neutrophils. Understandably, in homeostasis, only cells expressing respective adhesion molecules are able to extravasate. Under inflammatory conditions, tissues experience strongly increased leukocyte influx, which is mostly mediated by changes in the endothelium. In those settings, chemokines are involved in recruiting and guiding particular leukocyte subsets to their destination. This is mediated by chemokine receptor – chemokine binding and subsequent

signaling. There are two major groups of chemokines, the C-X-C chemokines and the CC chemokines, referring to a specific sequence motif shared by all chemokines in the group. Only two sets of chemokines are unique and cannot be added to the two groups, namely the C chemokines XCL1 and XCL2, and the CX_3C chemokine fractalkine (CX_3CL1). The specificity of chemokine receptors is heterogeneous, even though certain exclusive receptor – ligand pairs exist, i.e. C-X-C Chemokine receptor 4 (CXCR4) – C-X-C chemokine ligand 12 (CXCL12; also called stromal-derived-factor 1 (SDF-1)) (Fig. 3.1) [23].

Chemokine receptors transmit their signals exclusively via GPCRs. In general, triggering chemokine GPCRs relays signals via phospholipase Cβ2 (PLC2) directed calcium influx and other pathways, such as the mitogen-activated protein kinase (MAPK) pathway [20]. This affects various morphological and migratory features, including changes in adhesion molecule avidity, actin rearrangement and polarization, production of lysosomal enzymes, and increased locomotive behavior.

Chemokine – chemokine receptor interactions are important in many physiological and inflammatory settings. CCR7 is expressed on T cells, B cells, and certain dendritic cells and binds to CCL19 and CCL21 [24, 25]. In secondary lymphoid organs (SLO) like the spleen or lymph nodes, CCR7 is pivotal in guiding T cells to the respective T cell areas, thereby also enabling the formation of SLO architectural structures, for which T cells constitute a major part [26, 27]. *CCR7*$^{-/-}$ mice display strongly altered SLO morphology, which is owed to malfunction in DC and T cell recruitment, in turn disrupting the initiation of the entire adaptive immune response. Interestingly, *CCR7*$^{-/-}$ T cells manage to reach SLOs, are however then trapped and unable to migrate to sub-organ structures [26].

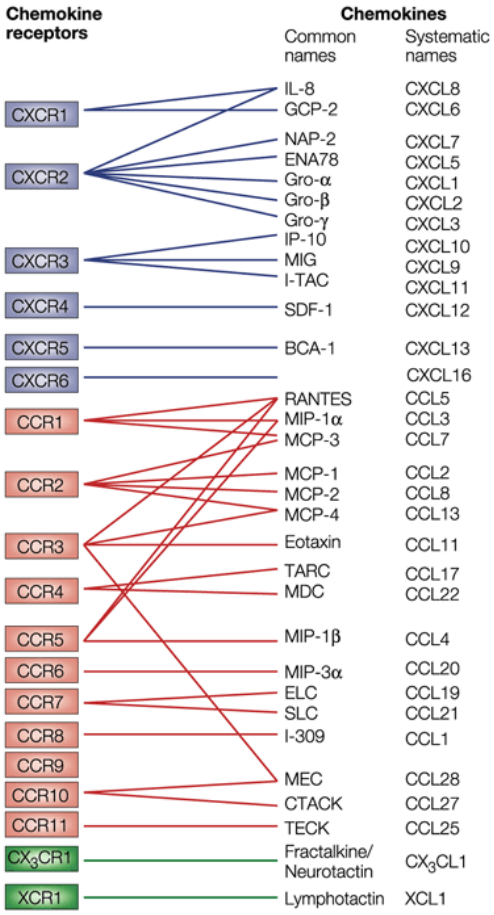

Figure 3.1 – The Chemokine system. Chemokine receptors are either specific for a single chemokine or are heterogenous regarding different chemokine binding ligands. Similarly, chemokine ligand – chemokine receptor pairs can also be specific for one combination or a single chemokine can bind various receptors. Adapted from Proudfoot *et al.*, 2002 [28].

3.1.5 Tumor Immunology

Tumor immunology describes the interactions between transformed cells and the immune system. It is established for a long time that innate and adaptive immunity can recognize and eliminate tumor cells. In this line of thought, it is also conceivable that many initial tumor and metastasis formations are stopped in its tracks by the immune system, which acts as a homeostatic malignancy sensor in the cancer immunosurveillance model.

The concept of tumor immunology expands the immune surveillance model and is typically divided in three stages: Elimination, Equilibrium, and Escape – the three E's (Fig. 3.2) [29, 30].

3.1.5.1 Elimination

Many innate immune cell subsets are readily present in tissues and therefore form the majority of sentinel cells. The process of malignant transformation is often accompanied by severe changes in the affected cells. Transformed cells are known to secrete or present

different stress-associated molecules. Several stress-induced ligands can bind to activating NK cell receptors, which will be a topic in 3.2.2.1. Soluble factors are secreted or released after necrotic tumor cell death. An example is the high mobility group box 1 protein (HMGB1), a protein usually localized in the nucleus, which is released by dying tumor cells [31, 32]. Importantly, HMGB1 can activate monocytes and trigger increased TNF-α production, a process believed to function via binding to the receptor for advanced glycation enproducts (RAGE) and TLR receptors [31, 33].

3.1.5.2 Equilibrium

Tumor clones initially spared by immune cell elimination often enter a state in which they adapt their immunogenicity by mutations in the antigen presentation machinery or even in specific T cell antigens. In the equilibrium phase, tumor cells are forced into a kind of dormant state by cytotoxic T cells, which eliminate proliferating tumor cells. In fact, studies in a tumor mouse model revealed that T cells effectively regulate outgrowth of immunogenic tumor variants, since ablation of T cells in this model led to immediate tumor progression [34]. This effect was further dependent on IFN-γ, yet independent of the innate immune system, since depletion of NK cells had no effect on tumor regression. The low proliferative state facilitates to remain undetected in ongoing immune responses and allows to acquire mutations in order to reduce immunogenicity.

3.1.5.3 Escape

The escape phase describes the recurrent outgrowth of single, low level immunogenic tumor cells. Tumor cells employ different mechanisms to evade destruction by the immune system:

Individual tumor clones can alter their antigen presentation in a way to prevent destruction by T cells and other cytotoxic cells. Specifically, mutation or loss of β2-Microglobulin (β2m) or defects in the IFN-γ signaling pathway (i.e. targeting the IFNGR1 or the JAK1/2 and STAT1 molecules) render T cell mediated immunity ineffective [30]. On the other hand, tumor cells often modulate the entire microenvironment in order to generate an immune suppressive environment. This can involve direct secretion of immune inhibitory factors such as TGF-β, IL-10, Indoleamine 2,3-deoxygenase (IDO), vascular endothelial growth factor (VEGF), or soluble forms of activating ligands like MICA (sMICA), thereby blocking the receptors on NK cells [35, 36]. More prominently, tumor cells can display the inhibitory surface receptors PD-L1 and CTLA-4, both binding to B7 family proteins on T cells. In this regard, PD-L1 and CTLA-4 are considered immune checkpoints and both represent recent targets of novel immunotherapeutics, so called checkpoint inhibitors [37]. In addition to directly secreting immune suppressive cytokines, tumor cells also secrete chemokines to recruit and maintain

myeloid-derived suppressor cells (MDSCs) or Tregs that then regulate immune responses independently, thereby fostering tumor progression [38, 39]. Lastly, other tumor cell intrinsic mechanisms rely on resisting immune-mediated killing mechanisms by upregulation of anti-apoptotic proteins such as Bcl-XL or adapting expression of death receptors (Fas ligand, TNF-related apoptosis-inducing ligand (TRAIL)) [30].

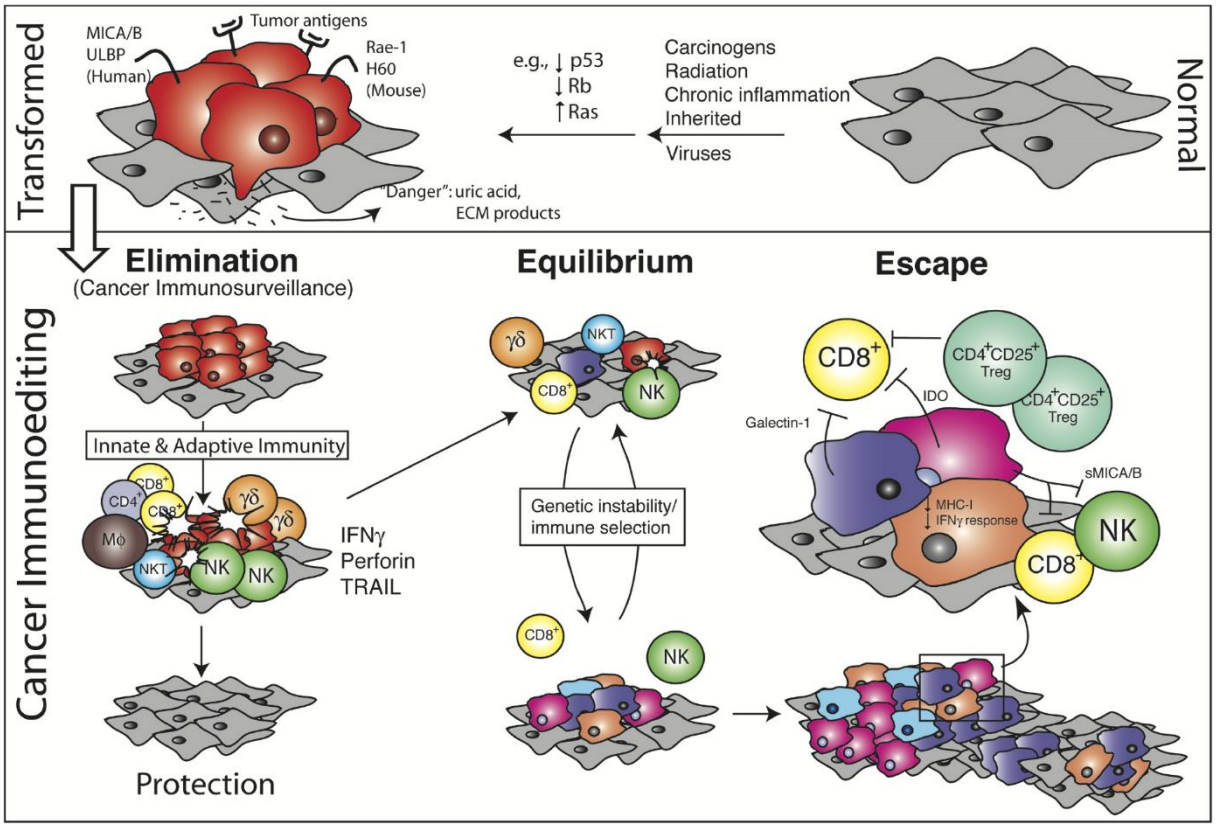

Figure 3.2 – The three E's. Illustration of the classical cancer immunoediting concept. Transformed cells express DAMPs that activate the immune system, resulting in initial tumor regression in the elimination phase. Some tumor clones acquire a low immunogenic state in the equilibrium phase, enabling them to escape immune destruction. Adapted from Dunn *et. al.*, 2004 [29].

3.1.6 Tumor infiltrating leukocytes

According to the concept of tumor immunology, immune cells can mount potent anti-tumor responses. However, this is in the first instance reliant on the presence and activity of specific immune cell populations in the TME, which is a result of active homing and transmigration into solid tumors. Similar to classical inflammatory scenarios, effective anti-tumor-immunity requires both innate and adaptive immunity to cooperate in initiating and maintaining effective immune reactions. Despite their instrumental role in inflammation, the role and frequency of monocytes and macrophages in solid tumors is not well understood, since most studies focus on cytotoxic T cells as the major targets of checkpoint inhibitor therapy. As a consequence, tumors are sometimes classified according to their response rates towards checkpoint inhibitor treatment as cold tumors or hot tumors, representing very

low or very high T cell infiltration and immunotherapy responsiveness, respectively [40]. Exclusion of immune cells, in particular effector T cells, can be facilitated by different mechanisms, such as modulation of the local chemokine milieu and the endothelial composition, together limiting transmigration. Additionally, expression of inhibitory checkpoint ligands and the generation of a highly hypoxic environment in the TME often affects the viability of immune cells, resulting in reduced proliferative capacity and apoptosis, thereby actively reducing the amount of intratumoral immune cells [41]. Another aspect that is the topic of an ongoing debate is the prognostic value of the intratumoral immune cell composition. Naturally, the effectiveness of immune responses heavily relies on the presence and ratios of particular immune cell subsets in the TME, since a high proportion of immune cell functions are associated with immune regulation and inhibition of excessive immune reactions. Similar to classical immune cell recruitment to sites of inflammation, circulating immune cells rely on migratory cues that guide their infiltration into the TME. Recently, different methods including whole tumor transcriptomic analysis as well as single-cell resolution techniques such as single-cell RNA-sequencing, mass cytometry, and *in situ* staining, were used to decipher the immune cell composition for different tumor entities [42, 43, 44]. Importantly, correlation of immune cell signatures with patient survival and therapy responsiveness allows to infer a prognostic value for specific immune cell populations in the TME [45]. While the presence of cytotoxic T cells and NK cells generally argues for a positive prognosis, it is now clear that also the activation status of effector cells, which is regulated by tumor- or immune cell-derived factors, is pivotal for effective tumor clearance [46, 47]. Hence, the presence of immune-inhibitory MDSCs, Tregs, and inhibitory ligands, which skews T cells towards an exhausted phenotype, is associated with a worse outcome, an observation that mirrors the concept of tumor escape from immune destruction by immunoediting [48, 49]. Nevertheless, it remains challenging to allocate specific prognostic values to individual immune cell populations, since many immune cell subsets in humans are poorly characterized regarding their marker and activation profile in tissues and tumors. Therefore, it is often required to include a broad panel of markers to specifically address one cell type, even for single-cell resolution techniques.

The prognostic value of monocytes and macrophages in tumors is still ambigous. For one, classical monocytes are repeatedly associated with chronic, tumor-promoting inflammation [50, 51, 52]. In contrast, the subset of patrolling monocytes has been found to exert anti-metastatic functions, since knockout mice lacking this particular subset showed a severly increased metastatic load [53]. Despite a bias towards a negative prognostic value, monocytes and macrophages are also reported to posses potent anti-tumor function under certain conditions. Macrophages in tissues are often divided into two functional groups; M1 and M2 polarized macrophages, exerting rather an anti-tumorigenic and pro-tumorigenic role,

respectively [54]. In the TME, macrophages are further classified as tumor-associated macrophages (TAMs), which generally represent a tumor fostering, M2-like phenotype [55]. In line with the pro-tumorigenic properties of classical monocytes, Franklin *et al.* demonstrated that TAMs originate from CCR2$^+$ classical monocytes [56].

3.2 Interactions between innate immune cells

Innate and adaptive immunity often interact to establish and support powerful and long-lasting immune responses, as described for DCs priming and supporting antigen specific T cells. Since certain innate immune cell populations also require stimulation and maturation phases, similar synergistic interactions also occur inside the innate immune system.

3.2.1 Origin and function of slan$^+$ monocytes (slanMo)

Around 20 years ago, Schäkel and colleagues generated the monoclonal antibody (mAb) M-DC8 by immunizing mice with a T cell-, B cell-, and CD14$^+$ monocyte-depleted, HLA-DR$^+$ leukocyte fraction [2]. It was later discovered that M-DC8 binds to a hitherto unknown carbohydrate modification on PSGL-1, termed 6-sulfo LacNAc (slan) [57]. Initially, slan+ cells were considered to be part of the DC lineage because of major functional similarities they share with DCs, i.e. efficient T cell priming [2, 57, 58]. However, recent transcriptomic analysis revealed that slan$^+$ cells cluster together with non-classical monocytes, suggesting that slan$^+$ cells originiate from the monocytic lineage [59]. The marker slan is present on roughly 50 % of human non-classical monocytes, which is why slan$^+$ cells are now called slan$^+$ monocytes (slanMo). Considering the ratios of monocytes and non-classical monocytes, slanMo typically constitute around 1.0 – 1.5 % of peripheral blood mononuclear cells (PBMCs) in healthy donors. Compared to classical DC populations, which usually make up less than 1 % of PBMCs, slanMo represent a high frequency, DC-like population in the human system [60].

3.2.1.1 Patrolling monocytes in humans and mice

Human monocytes are conventionally divided into 3 separate groups based on the expression of CD14 and CD16, encompassing classical CD14$^+$CD16$^-$ monocytes, intermediate CD14$^+$CD16$^+$ monocytes, and non-classical CD14$^-$CD16$^+$ monocytes [1]. Recently, it was described that classical monocytes give rise to intermediate and non-classical monocytes, reminiscent of a developmental hierarchy [61]. In mice, monocytes are classified based on the marker Ly6C. Ly6C^{high} cells are homologous to human classical monocytes, whereas Ly6C$^-$ cells are called patrolling monocytes and are suspected to be homologous to human non-classical monocytes [59]. In fact, a similar developmental hierarchy

exists for murine Ly6C^{high} cells, which function as the precursors for Ly6C^{-} patrolling monocytes [62]. As the name already suggests, patrolling monocytes have the ability to crawl along and monitor the vasculature for endothelial damage. This phenotype is described for both human non-classical monocytes and murine Ly6C^{-} monocytes, which is why also human non-classical monocytes are often referred to as patrolling monocytes [63]. By using genetic knockout mice, Hanna et al demonstrated that Ly6C^{-} monocyte development depends on the transcription factor Nur77 (NR4A1), a transcription factor also upregulated in their human counterparts [64]. Both human and murine patrolling monocytes can be identified as CX3CR1^{high}CCR2^{-} cells with high TNF-α production potential [59].

3.2.1.2 Dendritic cell (DC)-like functions of slanMo

As previously mentioned, slanMo were initially regarded as circulating blood DCs based on their cytokine production and T cell priming capability. T cells cultured with autologous slanMo in the presence of recall antigens such as Tetanus toxoid (TT) or keyhole limpet hemocyanin (KLH) exhibited increased proliferation. Exposure to tyrosinase-peptide loaded slanMo greatly increased antigen-specific T cell responses. In both stimulation techniques, slanMo were superior to CD14+ monocytes in promoting T cell function [2]. Compared to cDCs as the classical APCs, slanMo proved to be slightly inferior in T cell priming [57].

Another hallmark of DC biology is the release of stimulatory cytokines, in particular IL-12, which is a potent T cell and NK cell activating factor. It was demonstrated that slanMo account for even stronger IL-12 production than cDCs *in vitro* [58]. However, this is reliant on a pre-incubation period of several hours, reminiscent of a maturation phase often required for monocyte development. If left undisturbed for 6 hours before stimulation, slanMo can become the major producers of IL-12 among PBMCs [58]. As part of the innate immune system, slanMo carry several PRRs, with TLRs being the strongest drivers of cytokine responses [65, 66]. In this context, strong induction of IL-12 is reported for various ligands, including LPS signaling via TLR4 and R848 signaling via TLR7 and TLR8, reaching concentrations not matched by equally stimulated DC populations or CD14^{+} monocytes [58, 65, 66]. Of note, also CD40-CD40 ligand interactions are capable of triggering IL-12 expression [58]. Similar to IL-12, slanMo are also potent producers of the pro-inflammatory cytokine TNF-α, which is secreted at low levels in steady state and at strongly elevated levels after TLR stimulation [2, 67]. Autocrine TNF-α is important for expression of other cytokines, such as IL-23 [68]. Other reports were not able to reproduce this major role in cytokine production and T cell stimulation for slanMo [59, 69]. However, these experiments lacked the necessary maturation period prior to stimulation, thus rendering the results incomparable to previous findings.

In the blood, slanMo are regulated by erythrocytes, which control their activation via CD47 – signal-regulatory protein α (SIRPα) interactions. SIRPα signaling on slanMo efficiently reduces TNF-α and IL-12 production, thereby regulating the inflammatory potential of those cells in the circulation [58].

3.2.1.3 Tissue distribution of slanMo

Research on the tissue distribution of non-classical monocytes is still hampered by the lack of specific markers, since conventional gating strategies using multiple markers are not feasible for histological analysis up to date. In this context, the stable marker slan, which can be detected with the specific clones M-DC8, DD1 and DD2 [2, 57], opens up the possibility to investigate the slanMo subset *in situ*.

slanMo, and non-classical monocytes in general, strongly express the CX_3C receptor 1 (CX_3CR1), a feature that additionally separates monocytes subsets because classical monocytes lack this receptor completely [70]. The respective ligand, CX_3CL1 (fractalkine), is reported to be expressed on the endothelial lumen in a membrane bound form and pro-inflammatory cytokines such as TNF-α and IFN-γ can upregulate CX_3CL1 surface expression [71]. $CD16^+$ monocytes (including non-classical and intermediate monocytes) that express CX_3CR1 strongly adhere to the vasculature. However, active transmigration is reported to be hampered in the context of endothelial CX_3CL1 expression, preferentially allowing $CX_3CR1^-CD14^+$ monocytes to extravasate to sites of inflammation [71].

In line with the previously described DC phenotype, slanMo can acquire either a DC-like or a macrophage-like phenotype in tissues, being described as either $CD163^{low}CD14^{low}CD64^{low}CD^{low}$ or $CD163^{high}CD14^{high}CD64^{high}CD16^{high}$, respectively [70]. Morphologically, $slan^+$ cells acquire a dendritic shape with visible dendrites in tissues [72, 73]. However, $slan^+$ cells can also exhibit a round, more monocytic appearance, in particular in close proximity to vessels. In steady state, slanMo numerously populate tonsils, but are rare in other tissues. In an inflammatory setting, slanMo were shown to infiltrate multiple sclerosis lesions [74], lupus nephritis [75], atopic dermatitis [76], psoriasis [65], and different tumor entities [70]. Regarding their presence in the tumor microenvironment (TME), a predominant role in lymph node metastasis appears prevalent, as a big study detected slanMo solely in metastatic tumor draining lymph nodes of carcinoma patients but not in the primary tumor [73]. Additionally, slanMo are present in affected lymph nodes of B-cell lymphoma patients and mediate anti-tumor responses [72].

3.2.1.4 Interactions of slanMo with tumor cells

slanMo can carry out versatile anti-tumor functions. As described before, slanMo possess effective T cell stimulatory potential, which allows them to prime cytotoxic T cells for specific tumor antigens. Combination with a modular slan targeting antigen delivery system greatly increases antigen specific T cell proliferation [77].

The general activation status of slanMo in the tumor microenvironment is still largely unclear. However, cellular interactions with tumor cells can activate slanMo *in vitro* in the presence of additional IFN-γ and stimulate TNF-α production [60]. In addition, slanMo mediate direct tumor cell lysis via a TNF-α mediated mechanism. Due to very high expression of the Fc γ Receptor III (CD16) on the surface of slanMo, tumor cell lysis is far increased for opsonized tumor cell targets, referred to as antibody-dependent cellular cytotoxicity (ADCC) [61]. In this case, slanMo receive additional activation signals through CD16-mediated ITAM signaling leading to increased TNF-α production [61]. This mode of activation is also of relevance in other settings, i.e. in lupus nephritis, where immune complexes represent a major hallmark of the disease [57]. As part of the mononuclear phagocyte lineage, slanMo are also specialized at phagocytizing tumor cells and tumor cell debris. This function is documented for different tumor types *in vitro* and *in vivo* [54, 55].

Tumors can also exert immune suppression, a phenomenon well described for T cell exhaustion in the TME. Similarly, it is reported that circulating slanMo exhibit reduced numbers and function in multiple myeloma patients [80]. Another factor of immune suppression can stem from chemotherapeutic therapy affecting immune cells as a side effect. Here, a heterogenous picture arises because slanMo are reported to be functionally impaired *in vitro* by doxorubicin, vinblastine, and bortezomib, whereas mitomycin-c, methothrexate, and paclitaxel have no impact on slanMo function [81].

3.2.2 Natural Killer (NK) cells

In humans, NK cells comprise around 10-15 % of PBMCs and are classically divided into 2 subsets based on expression of the neural cell adhesion molecule (NCAM), which is also expressed on glia cells and neurons in the brain. In the case of NK cells, NCAM is most often referred to as CD56. A smaller subset of around 10-15 % of total NK cells expresses strong levels of CD56 and very low levels of CD16, thus being identified as $CD56^{high}CD16^{neg}$. In contrast, the majority of NK cells exhibit intermediate CD56 and high CD16 expression, hence being referred to as the $CD56^{dim}CD16^{high}$ subset [82, 83].

NK cells are part of the lymphocytic lineage despite relying on innate mechanisms, which has generated for them the term innate lymphoid cells (ILCs). However, the group of ILCs

contains additional subpopulations, notably ILC1, ILC2, ILC3, and lymphoid tissue inducer (LTi) cells, all defined by different combinations of surface molecules [84, 85].

3.2.2.1 Activating and inhibitory receptors on NK cells

Human NK cells are regulated by a multitude of germline-encoded cell surface receptors transmitting either activating or inhibitory signals, thereby allowing to precisely fine-tune their activation status. A group of receptors called natural-cytotoxicity receptors (NCR) includes Nkp46, Nkp44, and Nkp30, which all represent major activating receptors. Additionally, NKG2D and DNAM-1 bind to stress-induced ligands on tumor or virus-infected cells and are known to stimulate NK cells and induce cytotoxicity [86]. Expression of CD16 enables recognition of antibody-coated target cells. In particular, CD16 binding to Fc parts of bound IgG greatly increases killing of target cells by ADCC and cytokine secretion. In general, NK cell activating receptors use different intracellular adapter molecules to transmit activating signals, including ITAM and DNAX-activating proteins (DAP) 10 and DAP12 [87].

Besides activation through cellular contacts, NK cells also strongly respond to cytokines. Consequently, NK cells express an array of cytokine receptors, notably IL-1 receptor (IL-1R), IL-2R, IL-12R, IL-15R, IL-18R, IL21R, IFN-α receptor (IFNAR) [88]. Cytokine signaling in NK cells is required for different biological processes. The cytokines IL-2 and IL-15, whose respective receptors also share the same β-chain (CD122) and γ-chain (CD132) receptor sub-complexes, are important for NK cell maturation and proliferation [89, 90]. However, IL-15 has stronger activation capability when presented in trans on the membrane bound to the IL-15R α-chain [91]. IL-2 is provided by activated T cells, whereas monocytes and DCs are the major source of IL-15.

The activating IL-12R and IL-18R bind to IL-12 and IL-18, respectively, which are cytokines produced by monocytes, macrophages, and DCs. IL-12, in particular, is pivotal in inducing cytotoxicity and cytokine production by NK cells. It is composed of two subunits, IL-12p35 (IL-12A) and IL-12p40 (IL-12B), together forming the bioactive p70 heterodimer. The p40 subunit is shared with another cytokine, IL-23, which is composed of IL-12p40 and IL-23p19. In general, IL-12R signals via phosphorylated STAT4 and thereby triggers cytokine production, predominantly IFN-γ, and cytotoxicity by upregulation of activating receptors [92]. Recently, a special role of synergistic cytokine combinations became apparent. In particular combined IL-12, IL-15, and IL-18 are uniquely potent in stimulating both human and murine NK cell anti-tumor immune responses [93, 94, 95]. Of note, IL-12 can potentially also act regulatory, as NK cell apoptosis after combined IL-12 and IL-2 exposure is reported, suggesting a mechanism to prevent excess or chronic IL-12 mediated inflammation [96].

NK cell cytotoxic and pro-inflammatory function can pose severe threats to tissues. Therefore, to balance NK cell activity under extensive presence of activating ligands, NK cells readily express inhibitory receptors responsible for preventing tissue damage [86]. Most prominently, killer immunoglobulin-like receptors (KIRs) recognize MHC I molecules and convey inhibitory signals to NK cells via immunoreceptor tyrosine-based inhibitory motifs (ITIM) signaling [97]. Owing to constant expression of MHC I on all nucleated cells, the loss or downregulation of MHC I on tumor or virus-infected cells is recognized by NK cells through omitting inhibitory signals. Other major inhibitory receptors include CD94/NKG2A, Killer cell lectin-like receptor subfamily G member 1 (KLRG1), and T cell immunoreceptor with Ig and ITIM domains (TIGIT), all of which signal via ITIMs to regulate the activation status of NK cells [86].

3.2.2.2 Cytokine-production by NK cells

The signature cytokine produced by NK cells is generally considered to be the type II Interferon IFN-γ [98]. Consequently, NK cells represent an immediate innate source of IFN-γ, before Th1 immunity takes over. Other cytokines and chemokines secreted by NK cells after appropriate stimulation include TNF-α, granulocyte macrophage-colony stimulating factor (GM-CSF), CCL3/4/5, IL-8, and the C-type chemokines XCL1 and XCL2. While the secreted chemokines can mediate recruitment of other immune cell populations, i.e. DCs via the CCR5 ligands CCL3/4/5, IFN-γ and TNF-α are largely involved in initiating and maintaining immune responses [99]. TNF-α is considered an acute phase protein due to its early expression in inflammation and its effects on the endothelium, where it mediates vasodilation and activation of endothelial cells. IFN-γ predominantly activates monocytes, macrophages, and DCs, thereby often supporting maturation and fueling cytokine production.

3.2.2.3 Migratory aspects of NK cells and presence in tissues

Since NK cells constitute around 10 % of PBMCs, they form a major circulating population capable of infiltrating distant tissues in large numbers, especially in inflammation. Under homeostatic conditions, NK cells readily populate the liver, lung, lymphoid tissues, and uterus [100]. Owing to fundamental differences in chemokine receptor expression between the two NK cell subsets, homing of $CD56^{bright}$ and $CD56^{dim}$ cells deviates strongly in both steady-state and inflammation [101, 102]. Whereas $CD56^{bright}$ NK cells can be detected in SLOs owed to expression of CXCR3, CCR7, and L-selectin, $CD56^{dim}$ NK cells are rather characterized by a receptor repertoire allowing them to infiltrate inflamed tissues [103, 104]. Specifically, $CD56^{dim}$ NK cells express CXCR1, CXCR2, CXCR4, CCR2, CX_3CR1, and chemerin receptor 23 (Chem23), of which Chem23 binds to the unconventional chemokine chemerin [102, 103, 105, 106, 107]. Interestingly, chemokine receptor variations relatively accurately align with differential

tissue distribution. In this way, under steady state, CD56^{bright} NK cells form the major NK cell subset in mucosa-associated lymphoid tissue (MALT), liver, kidney, uterus, adrenal gland, and visceral adipose tissue [100]. On the other hand, CD56^{dim} NK cells preferentially populate the bone marrow, spleen, lung, and breast.

Inflamed vasculature is prepared for increased influx of immune cells. Typical chemotactic mediators of inflammation are IL-8, CCL2-5, and CXCL10, broadly matching with CD56^{dim} NK cell receptor expression [102]. In line with this, in many inflammatory mouse models, such as herpes simplex virus or influenza, NK cells were critical in mediating anti-viral immunity [108]. Besides the well-documented role of NK cells in virus infection, detailed descriptions of NK cell infiltration in chronic inflammatory diseases, autoimmune diseases and cancer, are less well studied. Infiltration into tumor tissue is dictated by different factors. On the one hand, tumor cells often dampen immune responses through an anti-inflammatory environment, thereby also hampering immune cell chemokine crosstalk. On the other hand, tumor cells are capable of directly modifying the tumor microenvironment by selective secretion of chemokines, which allows them to modulate immune cell infiltration. Finally, NK recruitment into tumor tissue is often rendered futile due to NK cells also suffering under tumor mediated immunesuppression. However, NK cells are reported to be present in cervical cancer [109], breast cancer [110], melanoma metastasis [111, 112], and other tumor entities [84]. An increasing body of evidence suggests that NK cells exert a pivotal role in protection from metastasis. Various reports state absence of NK cells in the primary tissue, but active infiltration into, and reduction of, metastasis [113]. However, the reason why NK cells are most often ineffective in primary tumor tissue and appear to only exert anti-metastatic activity remains largely unknown.

Apart from NK cells, other ILC populations are less well characterized in human tissues and pathologies. This is majorly owed to their recent discovery and the requirement to include multiple markers for reliable detection of individual ILC population [84]. However, the phenotype and composition of ILCs in human tissues appears to be very heterogenous, as an initial study suggests [114].

3.2.2.4 Anti-tumor functions of NK cells

NK cells are important for two major anti-tumor functions, notably direct cytotoxicity and IFN-γ production. The mechanisms by which NK cell mediated tumor-directed cytotoxicity can occur are well studied and either involve secretion of lytic granules filled with perforin and granzymes or surface expression of death receptors [115]. Perforin and granzymes are the classical NK cell and cytotoxic CD8 T cell effector molecules, which induce apoptotic cell death in target cells [116]. Mechanistically, NK cells form cytotoxic synapses through which the

secretion of lytic granules is spatially controlled. Perforin released after degranulation permeabilizes the target membrane by forming pores through which granzymes can enter the cytoplasm. Inside the target cell, granzyme B (GzmB) activates the key apoptosis-inducing caspase-3, thereby initiating GzmB-mediated apoptosis [116]. Importantly, cathepsin B and LAMP-1 (CD107a) protect the effector cells against perforin-associated damage [117, 118]. Cytotoxicity via death receptors relies on direct binding of target cells. This can occur with different receptor-ligand interactions, most prominently Fas-FasL, TRAIL-TRAILR, and TNF-TNFR. In general, triggering of death receptors culminates in the formation of the death-inducing signaling complex (DISC), which then initiates apoptosis [116]. Both modes of inducing cell death have been reported to mediate tumor destruction in mouse models [119, 120].

Besides direct cytotoxicity, NK cells can influence tumor cells by secretion of IFN-γ. IFN-γ can increase MHC I expression on target cells, thereby facilitating adaptive immune responses. Besides, IFN-γ increases the sensitivity of target cells towards apoptosis by upregulation of death receptors [99]. Interestingly, IFN-γ was also found to restrict proliferation in different cell types, and the combination of TNF-α and IFN-γ, both of which are also produced by NK cells, is reported to induce a senescent state in tumor cells [121, 122, 123]. In line with this, an anti-proliferative role of NK cells stimulated with PDGF-DD is reported against tumor cells [124].

3.2.3 The slanMo/NK cell crosstalk in the tumor microenvironment

The crosstalk between innate immune cells often solely relies on soluble interactions, since no direct cell-cell contact like in antigen-receptor mediated T cell priming is required. Therefore, innate immunity possesses a versatile cytokine and chemokine system ideally suited to initiate immune responses.

slanMo are major producers of IL-12 among PBMCs [58]. Even though no experimental evidence for their cytokine-production in tissues is available, it can be assumed that they can achieve a potent pro-inflammatory state after exiting the periphery. NK cells respond with strong IFN-γ production towards IL-12 [92]. In turn, IFN-γ potently stimulates slanMo responses. In line with this, slanMo/NK cell co-cultures exhibit a synergistic positive feedback fueled by slanMo-derived IL-12 and NK cell-derived IFN-γ (Fig. 3.3). It is reported that this bidirectional crosstalk is started by presentation of membrane-bound TNF-α (mTNF-α) on the surface of slanMo after appropriate stimulation with TLR ligands such as LPS [125]. Concomitantly, NK cells upregulate TNF receptor (TNFR2) during the co-culture, leading to NFκB signaling. This results in expression of common NFκB targets, of which GM-CSF supports IL-12 production by slanMo [125]. At this point, the positive feedback loop takes over, reaching very high levels of IL-12 and IFN-γ.

In addition, NK cells upregulate the activation marker NKp46, NKp44, and NKp30 after contact with TLR-activated slanMo [126]. In line with this, tumor-directed cytotoxicity is also significantly increased after co-culture. In a reciprocal fashion, NK cells support slanMo maturation by increasing slanMo surface expression of CD83, CD86, ICAM-1, and HLA-DR, and reducing inhibitory IL-10 production. While NK cell activation is IL-12 mediated and therefore largely cell-contact independent, the reciprocal slanMo stimulation is partially cell-cell contact dependent [126].

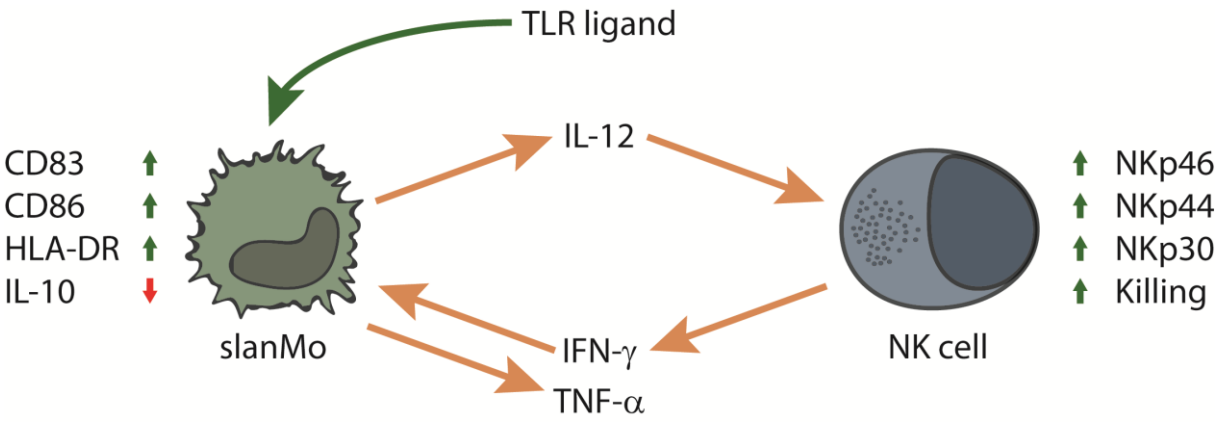

Figure 3.3 – Graphical illustration of the slanMo / NK cell crosstalk. The synergistic bidirectional stimulation is mediated by IL-12 and TNF-α produced by TLR-activated slanMo and NK cell-derived IFN-γ that activates slanMo. This interaction elevates the expression of HLA-DR and the maturation markers CD83 and CD86 on slanMo. Immunosuppressive IL-10 production by slanMo is reduced after contact with NK cells. NK cells upregulate the surface markers NKp46, NKp44, NKp30, and exhibit higher cytotoxicity.

3.2.3.1 The patrolling monocyte / NK cell crosstalk in mice

Mouse models often give valuable mechanistic insights that can be translated to the human system. Based on previous studies, murine patrolling monocytes appear to exhibit a high functional homology to human non-classical monocytes, and therefore also to the subpopulation of slanMo [59]. Murine patrolling monocytes are involved in detection and elimination of metastasis in tumor models of lung carcinoma and melanoma [53]. Interestingly, this mechanism further relied on recruitment of NK cells to the site of metastasis. In line with this, another study reported a role for the murine patrolling monocyte and NK cell crosstalk in reducing metastatic load [127]. In detail, primary tumors were required to stimulate IL-15 production by murine patrolling monocytes, which then activated NK cell IFN-γ production. Furthermore, it is reported that murine patrolling monocytes can become activated by cancer exosomes and thereby limit metastasis. However, this effect was reliant on pigment epithelium-derived factor (PEDF) on the surface exosomes, which was interestingly only present on exosomes from non-metastatic cancers [128].

Together, this strongly suggests a major role of patrolling monocytes in mediating metastasis rejection, in particular through interaction with NK cells.

3.3 Tumor biology

3.3.1 Malignant transformation

The process of malignant transformation turns healthy cells into cancers with uncontrolled proliferation, often leading to mortality in patients. Several safeguard mechanisms exist, which usually prevent that single mutations result in malignancy. Thus, for single cells to achieve a malignant state requires the accumulation of multiple mutations, together nullifying all relevant safeguard mechanisms. Mutations arise through DNA damage. Despite several DNA repair mechanisms existing in healthy cells, DNA damage can ultimately result in permanent genetic modifications. There are ample causes of mutagenesis, most common factors are however ultraviolet- (UV-) or γ-irradiation from the sun, and ingested or inhaled genotoxic substances. Oncogenesis-related genes are classified in two groups, oncogenes and tumor-suppressor genes:

Mutations in oncogenes, leading to upregulation or continuous activation, are the major drivers of malignant transformation. Often, oncogenes provide constant proliferative signals, thereby enabling unrestricted proliferation. A prominent example are mutations in the protein NRAS in melanoma. Despite KRAS being most commonly mutated over all cancer entities, highest RAS mutation frequencies in melanoma occur in NRAS [129, 130]. Mutations that render NRAS constitutively active initiate downstream signaling predominantly via RAS-RAF-MAPK and PI3K pathways. Continuous signaling then provides pro-survival signals, affects cell-cycle deregulation, and thereby induces proliferation [129, 130]. In this regard, NRAS mutations alone already cover many of the hallmarks of cancer described in 2011 by Hanahan and Weinberg, which state that tumor cells require the ability to sustain proliferative signaling, evade growth suppression, resist cell death, induce angiogenesis, enable replicative immortality, activate invasion and metastasis, deregulate cellular energetics, and avoid immune destruction [131]. Due to this, mutations in targets such as NRAS are often called driver mutations.

Similarly, tumors frequently exhibit loss of or inactivating mutations on tumor suppressors. Tumor suppressors represent safeguard mechanisms that prevent unrestricted growth in healthy cells. The transcription factor p53 is also referred to as “guardian of the genome”, a name that stems from its integral role in the DNA damage response [132]. In the event of DNA damage, p53 becomes activated and arrests cell growth through induction of target genes

such as the cyclin-dependent kinase (CDK) inhibitor (CDKI) p21 (CDKN1A) [121, 133, 134]. The arrest in cell cycling allows the DNA repair machinery to correct mutagenic events. However, if DNA repair is unsuccessful, p53 can dictate the cell's fate in one of two ways: Either apoptosis pathways become activated and eliminate potentially mutagenic cells, or the cells enter a state of permanent growth arrest called senescence [135]. Senescent cells are arrested in the G0/G1 state of the cell cycle and are believed to have lost the ability to re-enter the active cell cycle.

3.3.2 Melanoma

Melanoma is a tumor originating from melanocytes in the skin. Other common types of skin cancer include squamous cell carcinoma (SCC) and basal cell carcinoma (BCC). Yet both are generally considered to be less aggressive than melanoma.

Activation of oncogenes and suppression of tumor suppressors together form the path for oncogenesis. In this regard, each tumor entity has different signatures of commonly mutated genes, and also individual tumors often exhibit markedly different mutational patterns than tumors of the same origin. Interestingly, also the general mutational load varies strongly between tumor entities. Melanoma typically exhibits one of the highest mutational burden of all types of tumors, which appears reasonable considering the constant UV irradiation exposure of the skin as a major mutagenic factor. As mentioned before, melanomas commonly incorporate specific driver mutations, most prominently BRAF, NRAS, p16INK4A, and p53. In fact, around 50% of melanoma patients harbor a BRAF V600E mutation, highlighting the importance of constitutively active signaling kinases in melanoma development [129].

From a clinical perspective, melanoma is classified regardless of mutational status. Due to the easy visual accessibility of melanocytic tumors, the basic determination of malignancy is made upon visual examination. Discriminating factors include the size, shape, contour and color. Malignant cutaneous tumors are then further classified according to the stage of progression. For stages prior to metastasizing, this relies the size of the tumor, summarizing non-ulcerated tumors below 1 mm in radius as stage I melanoma and tumors above 1 mm as stage II. Stage III encompasses melanomas with involvement of regional lymph nodes. With the detection of distant metastasis, melanomas fall under the stage IV category [136].

3.3.3 Melanoma Therapy

Melanomas very frequently incorporate driver mutations in the serine/threonine-protein kinase BRAF. This high prevalence of a single driver mutation with a pivotal role in initiating and maintaining a malignant state also opens up avenues for therapeutic intervention. First targeted therapies against melanoma were approved in 2011, are still developed further and are applied in the clinics today. Vemurafenib is a selective BRAF-mutant inhibitor that achieves initial tumor regression in around 90 % of patients. However, tumor regression is generally transient, since melanomas rapidly acquire additional mutations in other pathways which substitute for the key role of BRAF [137].

Another more recent therapeutic approach arises from tumor immunology. Immune checkpoint inhibitors neutralize surface molecules that would otherwise severely dampen local immune reactions. Two types of therapeutics, either binding to PD-1 or CTLA-4, are currently used in the clinic with unprecedented response rates in melanoma. Mechanistically, PD-1 and CTLA-4 are expressed by activated T cells and cause T cell exhaustion through binding to PD-L1 on tumor cells and CD80/86 on antigen presenting cells. This inhibitory axis is relieved through blocking with neutralizing antibodies, which boosts T cell responses. However, still only a fraction of patients respond to checkpoint inhibitor therapy and side effects are immense, typically including chronic inflammatory diseases triggered by overshooting immune responses. Nevertheless, checkpoint inhibitor immunotherapy represents the biggest breakthrough in cancer therapy over the last years [137].

Another rare line of therapy involves topical application immune stimulatory agents such as the TLR 7/8 ligand Imiquimod for cutaneous melanoma [138]. This application is under investigation for its use as supportive treatment after initial melanoma excision and to induce melanoma regression where operation is not feasible [139, 140].

3.4 Senescence in tumors

Senescence describes a permanent stop in cell cycle progression, where the cells remain in a G0/G1 arrest. This has important implications with regard to oncogenesis, since senescence is a common response to mutations and oncogene activity, a process called oncogene-induced senescence (OIS). OIS is only one trigger that can cause cellular senescence. Additionally, senescence can be a result of the DNA damage response, it can occur as replicative senescence induced by telomere shortening, or it can be triggered through tumor suppressor activation or oxidative stress [141]. Senescent cells are characterized by strongly reduced proliferation reminiscent of a complete growth arrest, changes in

heterochromatin organization, and through an enlarged and flattened morphology. Another widely used marker for senescent cells is senescence-associated β-Galactosidase (SA-β Gal), a lysosomal enzyme consistently upregulated in senescent cells [142]. Recently, the secretome of senescent cells has become a major field of study. The so called senescence-associated secretory phenotype (SASP) is characterized by the secretion of a range of particular soluble factors. The SASP includes inflammatory cytokines and chemokines such as IL-6, IL-8, IL-1α, IL-1β, and CXCL-1, extracellular matrix (ECM) modifying enzymes such as the matrix metalloproteinases (MMPs) MMP-1 and MMP-2 [143], angiogenesis-related factors such as VEGF, and immune suppression mediators such as TGF-β [144].

3.4.1 Regulation of the cell cycle

During the mammalian cell cycle, different groups of proteins cooperate to initiate, maintain, and regulate cell division after receiving mitotic signals. The cell cycle is divided in four phases (Fig. 3.4): The G_1 phase, where cells grow in volume in order to prepare for the second phase, the S phase. During the S phase, the diploid (2n) genetic material is duplicated in a way that each daughter cell receives a complete diploid set of chromosomes. In the subsequent G_2 phase, the cells continue to grow and accumulate organelles before entering mitosis, which is called the M phase, and which ultimately yields the generation of two identical daughter cells. Importantly, the cell cycle has safeguard mechanisms in the form of checkpoints that restrict progression to the next phase in order to prevent transmission of mutated genetic material to the progeny. During the G_1/S phase transition, cells examine the DNA for damage and proceed with DNA replication only in the absence of DNA-damage response signals. Similarly, cells control successful DNA synthesis during the S phase and prolong the G_2 phase in case of DNA damage prior to entering the M phase.

Progression to the next phase is mediated by cyclically expressed cell cycle proteins called cyclins and cyclin-dependent kinases (CDKs) (Fig. 3.4). Importantly, specific cyclin – CDK pairs are active during defined cell cycle phases and are required for advancing to the next phase. D Cyclins coupled to CDK4 and CDK6 are active during the G_1 phase. CDK2-cyclin E and CDK2-cyclin A complexes are required for G_1/S transition and the S phase, respectively. Finally, CDK1 can interact with cyclin A and cyclin B to initiate and undergo mitosis. Despite control through constant degradation of cyclins, CDKs are thoroughly regulated by CDK inhibitors (CDKi). Two groups of CDKi's control CDK-enabled cell cycle progression. $p16^{INK4a}$ (CDKN1A), short p16, belongs to the INK4 protein family and inhibits CDK4/6 – cyclin D complexes [145]. This arrests cells in the G1 phase by preventing progression to the S phase. In fact, p16 expression can terminally arrest proliferation and keep the cells in a senescent

G_0/G_1 arrest. Similarly, p21, as a member of the CIP/KIP family, encompassing p21, p27, and p57[146], predominantly targets CDK1- and CDK2 - cyclin complexes [146]. In this way, p21 can prolong both the G_1 and G_2 phase and thereby mediate senescence through a G_0/G_1 and G_2/M arrest, respectively.

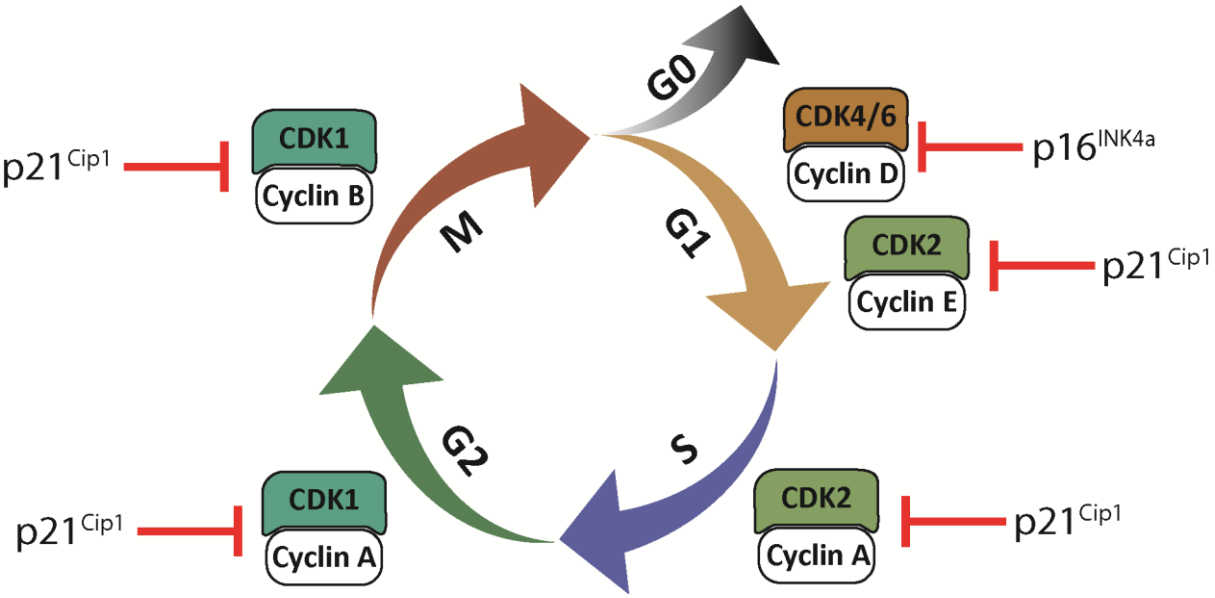

Figure 3.4 – Modulation of the cell cycle by CDK inhibitors. General scheme of the cell cycle including G1 phase, where cells prepare for DNA replication during the S phase. This is a followed by second preparation phase, the G2 phase, after which the cells undergo mitosis in the M phase. As depicted, different cyclin – CDK complexes control each cell cycle phase. $p21^{cip1}$ and $p16^{INK4a}$ represent CDK inhibitors (CDKI) that regulate CDKs during cell cycle progression. CDK (Cyclin-dependent kinase).

3.4.2 Senescence pathways

p21 and p16 are downstream effectors of the two major senescence pathways: The p53-p21 and the p16-Retinoblastom (Rb) pathway. As mentioned before, p53 is activated during the DNA-damage response and mediates the decision between apoptosis and senescence. Apoptosis is mediated through induction of pro-apoptotic targets such as the BH3-only members BIM, PUMA, and NOXA, which inhibit anti-apoptotic Bcl-2, thereby ultimately triggering apoptotic cell death [147].

Alternatively, p16 can be triggered by cellular stress, i.e. DNA damage, oncogenic stress, and as a homeostatic factor during aging. By targeting Cyclin D – CDK complexes, p16 inhibits phosphorylation of the tumor suppressor Rb. Rb phosphorylation is required to release the transcription factor E2F, which is required for progression to the S phase. In this way, consistent p16 expression induces a permanent G_0/G_1 arrest [148].

3.4.3 Deregulation of the cell cycle in tumor cells

Due to several levels of cell cycle regulation, tumor cells are often forced to acquire multiple mutations in cell cycle genes, of which many are considered driver mutations [149]. Most prominently, melanoma, but also other tumor entities, often incorporate loss of function mutations in p53, p16, and less frequently p21, thereby crippling the two major DNA-damage response-associated pathways [150]. On the other hand, tumors can also directly modify cell cycle progression mediators by overexpression of D cyclins and CDK4/6. This shows that tumor cells frequently target the G_1/S checkpoint, highlighting the importance of the G_0/G_1 arrest in limiting propagation of mutations. As a result, several CDK inhibitors are currently tested in clinical trials [151]. Despite limited success to date, CDK inhibitors could profit from observations gained in mouse studies that suggest that development and growth of most tissues are only dependent on CDK1 for functional cell division and can compensate for loss of CDK2/4/6 [152]. This opens up avenues for selectively targeting of specific CDKs. However, it is unclear whether tumors actually require certain CDKs to be deregulated, or if compensatory mechanisms would be able to substitute [150].

3.4.4 Cytokine-induced senescence

Senescence is commonly triggered to prevent propagation of defective genetic material. Recently, Röcken *et al.* demonstrated that the combination of the pro-inflammatory cytokines TNF-α and IFN-γ, secreted by Th1 cells, induces senescence in a β-islet cancer mouse model [123]. In this model, senescence is strictly reliant on both TNF receptor (Tnfr) and IFN-γ induced STAT1 signaling. Besides, TNF-α and IFN-γ were previously also independently associated with cell cycle regulation and senescence. IFN-γ can induce p27 upregulation in rat embryonic fibroblasts and senescence in melanocytes through p21 [122, 153]. Similarly, TNF-α upregulates p21 and p27 in glioblastoma cell lines and mediates senescence in human umbilical vein endothelial cells (HUVECs) through maintaining a chronic DNA-damage response. In addition, common SASP factors, such as TGF-β, IL-6, and IL-8, are also associated with inducing senescence [144]. This generates an interesting concept, in which senescence is maintained through senescence-induced autocrine factors.

3.5 Aim of the Study

Despite recent breakthroughs associated with checkpoint inhibitor therapy of melanoma, treatment only achieves long-term survival in a fraction of patients, which is largely owed to frequent evasion of T cell responses through mutations in the antigen presentation machinery. Thus, novel avenues for targeting T cell resistant patient populations are urgently needed. Innate immunity is not dependent on antigen-specific receptors and clonal proliferation, but instead relies on a broad variety of germline encoded receptors adapted to recognize disease-associated patterns. slanMo and NK cells are innate immune cells that engage in a synergistic crosstalk increasing both tumor-directed cytotoxicity and cytokine production. However, the influence and anti-tumor potential of this crosstalk in malignant melanoma is poorly explored.

Here, we aim to elucidate the following aspects of the intratumoral crosstalk between slanMo and NK cells:

1) The detection and quantification of slanMo and NK cells in melanoma, including the resolution of kinetic aspects by analyzing all stages of melanoma development.

2) The characterization of the chemokine milieu generated by slanMo combined with migration analysis of NK cells. In detail, we pursued the hypothesis that R848-stimulated slanMo recuit NK cells to the TME.

3) Evaluation of the influence of the R848-stimulated slanMo/NK cell crosstalk on melanoma cells. In particular, we wanted to evaluate whether the cytokine milieu generated by slanMo and NK cells elicits a senescence phenotype in melanoma cells.

4) Characterizing the secretion of SASP factors in senescent melanoma cells.

These investigations will combine functional *in vitro* data with validation of our cell types in patient samples. Together, this provides relevant insight into the modes of action of therapeutics aiming at activating innate immune cells, such as the TLR 7/8 ligand imiquimod that is used for topical melanoma therapy.

4 Materials and Methods

4.1 Materials

4.1.1 Cell lines

Cell line	Origin	Medium
SK-Mel-25	Human Melanoma cell line	RPMI
SK-Mel-28	Human Melanoma cell line	RPMI
SK-Mel-30	Human Melanoma cell line	RPMI
Ma-Mel-86b	Human Melanoma cell line	RPMI

All culture medium was supplemented with 10 % FCS, 2 mM L-glutamine, and 1 % Penicillin/Streptomycin, unless otherwise stated in 4.2.

4.1.2 Cell culture consumables

Product	Company	Catalogue
Conical tubes (15 ml, 50 ml)	Cellstar, Frickenhausen, Germany	227261
Serological pipets (5 ml)	Greiner, Frickenhausen, Germany	4487
Serological pipets (10 ml)	Greiner, Frickenhausen, Germany	4488
Serological pipets (25 ml)	Greiner, Frickenhausen, Germany	4489
Pipette tips (20 µl)	Gilson, Limburg, Germany	F161450
Pipette tips (200 µl)	Gilson, Limburg, Germany	F161930
Pipette tips (1000 µl)	Gilson, Limburg, Germany	F161670
6-well Tissue culture plate	Corning, Kaiserslautern, Germany	353046
12-well Tissue culture plate	Corning, Kaiserslautern, Germany	353043
24-well Tissue culture plate	Corning, Kaiserslautern, Germany	353047
48-well Tissue culture plate	Corning, Kaiserslautern, Germany	353078
96-well microplate, flat-bottom	Corning, Kaiserslautern, Germany	353072
96-well microplate, round-bottom	Corning, Kaiserslautern, Germany	353077
Culture flask (25, 75, 175 cm^2)	Thermo Fisher, Waltham, MA, USA	156367, 156499, 159910
96 well migration plates, ChemTx	Neuroprobe, Gaithersburg, MD, USA	101-5

Transwell Permeable Suppport, 5 µm, 24 well	Costar, Corning, Kaiserslautern, Germany	3421
Diagnostic slides 8 well	Gerhard Menzel GmbH, Braunschweig, Germany	X1XER301B

4.1.3 Cell culture reagents

Product	Company	Catalogue
Fetal bovine serum	Sigma, Steinheim, Germany	F7524
EDTA	Applichem, Darmstadt, Germany	A2937
Phosphate buffered saline (PBS)	Thermo Fisher, Waltham, MA, USA	14190144
Biocoll seperating solution	Biochrom, Berlin, Germany	L6115
Human Serum	Sigma, Steinheim, Germany	H4522
Penicillin/Streptomycin	GE Healthcare, Munich, Germany	P11-010
L-Glutamine	GE Healthcare, Munich, Germany	M11-004
MEM non-essential amino acids	Sigma, Steinheim, Germany	M7145
Sodium pyruvate	Sigma, Steinheim, Germany	S8636
RPMI 1640	Biochrom, Berlin, Germany	F1215
Human albumin	Octapharma, Langenfeld, Germany	00200331
Trypan Blue	Thermo Fisher, Waltham, MA, USA	15250-061
Trypsin EDTA (10x)	GE Healthcare, Munich, Germany	L11-003
Cryomedium (Cryo-SFM)	Promocell, Heidelberg, Germany	C-29912
Annexin V reagent	Sartorius, Goettingen, Germany	4641

Human and fetal bovine serum was inactivated at 56 °C for 30 minutes prior to application in cell culture experiments.

Cell culture medium for primary human cells:

Complete RPMI	RPMI 1640, 10% human serum, 2 mM L-glutamine, 1 % Penicillin/Streptomycin, 1x MEM amino acids, 1 mM sodium pyruvate

4.1.4 Magnetic activated cell sorting (MACS)

Product	Company	Catalogue
autoMACS columns	Miltenyi, Bergisch Gladbach, Germany	130-021-101
NK cell isolation kit	Miltenyi, Bergisch Gladbach, Germany	130-092-657
Anti-mouse IgM Microbeads	Miltenyi, Bergisch Gladbach, Germany	130-047-301
CD4+ T cell isolation kit	Miltenyi, Bergisch Gladbach, Germany	130-096-533
CD14 Microbeads, Human	Miltenyi, Bergisch Gladbach, Germany	130-050-201

4.1.5 Kits

Cytokine measurement kits

Product	Company	Catalogue
LEGENDplex™ Human Anti-Virus Response Panel	Biolegend, San Diego, CA, USA	740390
LEGENDplex™ Human Cytokine Panel 2	Biolegend, San Diego, CA, USA	740102
LEGENDplex™ Human Proinflammatory Chemokine Panel	Biolegend, San Diego, CA, USA	740003
Human TNF ELISA Set	BD Biosciences, Heidelberg, Germany	555212
Human IFN-γ ELISA Set	BD Biosciences, Heidelberg, Germany	555142

Histology kits and reagents

Product	Company	Catalogue
Dako REAL Detection System	Dako, Jena, Germany	K5005
Vectastain® ABC:HRP Mouse IgM	Linaris, Mannheim, Germany	PK-4010
Goat anti-Rabbit IgG (H+L):Biotin	Linaris, Mannheim, Germany	BA-1000
Histogreen	Linaris, Mannheim, Germany	E109
Avidin/Biotin blocking kit	Linaris, Mannheim, Germany	SP-2001
Roti-Histol	Carl Roth, Karlsruhe, Germany	6640.5
Hematoxylin Gill 3	Thermo Scientific, Waltham, MA, USA	6765009

Aquaous mounting medium	Aquatex, Merck, Darmstadt, Germany	108562
Xylene based mounting medium	Consul Mount, Thermo Scientific	9990440
Immunofluorescence Mounting Medium	Dako, Jena, Germany	S3023

Western Blot kits and reagents

Product	Company	Catalogue
BCA Protein Assay	Thermo Fisher, Waltham, MA, USA	23225
ProSieve Color Protein marker	Lonza, Basel, Switzerland	850537
ECL Substrate	GE Healthcare, Munich, Germany	RPN2235

Other kits and reagents

Product	Company	Catalogue
CellTiter-Glo Luminescent Cell Viability Assay	Promega, Mannheim, Germany	G7571
β-Galactosidase staining kit	US Biological, Salem, MA, USA	G1041-76
TMB solution ELISA	BD Biosciences, Heidelberg, Germany	555214
Scintillation solution	Perkin Elmer, Waltham, MA, USA	1205-440

4.1.6 Antibodies

Antibodies for flow cytometry (FACS)

Primary antibody	Clone	Company	Species	Final conc.
CD56 PE-Cy7	HCD56	Biolegend, San Diego, CA, USA	Mouse IgG1κ	2 µg/ml
CD56 FITC	HCD56	Biolegend, San Diego, CA, USA	Mouse IgG1κ	4 µg/ml
CD3 APC	UCHT1	BD, Heidelberg, Germany	Mouse IgG1κ	1:10
CD16 PE	3G8	BD, Heidelberg, Germany	Mouse IgG1κ	1:10
CXCR1 FITC	8F1	Biolegend, San Diego, CA, USA	Mouse IgG2b	4 µg/ml
CXCR2 PE	5E8	Biolegend, San Diego, CA, USA	Mouse IgG1κ	1.4 µg/ml

Isotype control	Clone	Company	Species	Final conc.
mIgG2b FITC	MPC-11	Biolegend, San Diego, CA, USA	Mouse IgG2b	As CXCR1 FITC
mIgG1 PE	MOPC-21	BD, Heidelberg, Germany	Mouse IgG1κ	As CXCR2 PE

Sec. control	**Cat.**	**Company**	**Species**	**Final conc.**
Anti mIgM (anti-slan)	731822	Beckman Coulter, Fullerton, CA, USA	Goat $F(ab)_2$	2.5 µg/ml

Antibodies for Histology and Western Blot

Primary antibody	**Clone**	**Company**	**Species**	**Final conc.**
CD56	123c3	Invitrogen, Carlsbad, CA, USA	Mouse IgG1κ	IF: 13.3 µg/ml
slan	DD2	Hybridoma supernatant	Mouse IgM	IHC: 50 µg/ml
CD3	SP7	Abcam, Cambridge, UK	Rabbit IgG	IHC: 1:200
p21	EPR362	Abcam, Cambridge, UK	Rabbit IgG	IF/IHC: 5 µg/ml WB: 0.5 µg/ml
Ki67	MIB-1	Dako, Jena, Germany	Mouse IgG1κ	IF/IHC: 0.6 µg/ml
β-actin HRP	C4	SantaCruz, Heidelberg, Germany	Mouse IgG1	WB: 0.2 µg/ml

Isotype control	**Clone**	**Company**	**Species**	**Final conc.**
mIgM	MM-30	Biolegend, San Diego, CA, USA	Mouse IgM	As primary
mIgG1κ	MOPC-21	BD, Heidelberg, Germany	Mouse IgG1κ	As primary
rbIgG	EPR25A	Abcam, Cambridge, UK	Rabbit IgG	As primary

Sec. antibody	Cat.	Company	Species	Final conc.
Goat anti-rabbit A488	111-545-003	Dianova, Hamburg, Germany	goat	IF: 2.5 µg/ml
Goat anti-mouse A647	115-605-062	Dianova, Hamburg, Germany	goat	IF: 2.5 µg/ml
Goat anti-rabbit HRP	111-035-144	Dianova, Hamburg, Germany	goat	WB: 1 µg/ml

Antibodies for neutralization experiments

Antibody	Clone	Company	Species	Final conc.
Adalimumab	D2E7	Humira, Abbvie, Chicago, IL, USA	Human IgG1	10 µg/ml
Human IFN-γ	B133.5	Hoelzel Diagnostika, Cologne, Germany	Mouse IgG1	10 µg/ml
Human IL-8	6217	R&D, Abingdon, UK	Mouse IgG1	10-20 µg/ml
Human CCR5	45531	R&D, Abingdon, UK	Mouse IgG2b	20 µg/ml

Isotype control	Clone	Company	Species	Final conc.
Human IgG1 isotype	Cat: BE0297	Hoelzel Diagnostika, Cologne, Germany	Human IgG1	As primary
Mouse IgG1 isotype	MOPC-21	Hoelzel Diagnostika, Cologne, Germany	Mouse IgG1	As primary
Mouse IgG2b isotype	Mg2b-57	Biolegend, San Diego, CA, USA	Mouse IgG2b	As primary

4.1.7 Chemical reagents and biological compounds

Product	Company
DAPI (4′,6-Diamidin-2-phenylindol)	Sigma, Steinheim, Germany
Paraformaldehyde (PFA)	Sigma, Steinheim, Germany
Recombinant TNF-α	Promocell, Heidelberg, Germany
Recombinant IFN-γ	Immunotools, Friesoythe, Germany
R848	Life Technologies, Carlsbad, CA, USA
Lipopolysaccharid (LPS)	Sigma, Steinheim, Germany

CCL3	Immunotools, Friesoythe, Germany
CCL4	Immunotools, Friesoythe, Germany
CXCL-8 (IL-8)	Immunotools, Friesoythe, Germany
CXCL12 (SDF-1)	Immunotools, Friesoythe, Germany
BSA (Bovine Serum Albumin)	Sigma, Steinheim, Germany
Tween 20	Carl Roth, Karlsruhe, Germany

4.1.8 Buffers and solutions

Buffer	**Composition**
PBS	137 mM NaCl, 2.7 mM KCL, 12 mM H_2PO_4, pH 7.4
TBS	50 mM Tris, 150 mM NaCl, pH 7.5
PBS-Tween (PBS-T)	PBS + 0.05 % Tween 20
TBS-Tween (TBS-T)	TBS + 0.05 % Tween 20

Cell culture

Buffer	**Composition**
PBS/EDTA	PBS + 2 mM EDTA
MACS Buffer	PBS + 2.5 % human albumin + 2 mM EDTA
FACS Buffer	PBS + 2.5 % human albumin + 2 mM EDTA + 0.1 % sodium azide

SDS-PAGE and Western Blot

Buffer	**Composition**
Hot lysis buffer	10 mM Tris (pH 8.0), 1 % SDS, 1 mM sodium orthovanadate
SDS sample buffer	0.15 M Tris, 1.2 % (v/v) SDS, 4 mM glycerol, 2 mM β-mercaptoethanol, 0.02 µM bromophenolblue, pH 6.8
15 % Resolving gel	15 % (v/v) acryl-bisacrylamid, 0.1 % (w/v) SDS, 25 % (v/v) of 1.5 M Tris (pH 8.8), 0.1 % (w/v) ammonium persulfate (APS), 0.04 % TEMED
5 % Stacking gel	5 % (v/v) acryl-bisacrylamid, 0.1 % (w/v) SDS, 12,5 % (v/v) of 1.5 M Tris (pH 8.8), 0.1 % (w/v) ammonium persulfate (APS), 0.1 % TEMED
SDS running buffer	2.5 M Tris, 192 mM glycine, 0.1 % (v/v) SDS

Blocking solution	TBS + 5 % (w/v) BSA
Transfer buffer	47 mM Tris, 20 % (v/v) methanol, 1.3 mM SDS, 34 mM glycine
Stripping Buffer	2 % (w/v) SDS, 6.3 % of 1 M Tris (pH 6.7), 0.7 % (v/v) β-mercaptoethanol

4.1.9 Oligonucleotides

All human forward and reverse primers were purchased from Metabion.

Gene	**Forward Sequence (5' → 3')**	**Reverse Sequence (5' → 3')**
hIL6	AGACAGCCACTCACCTCTTCAG	TTCTGCCAGTGCCTCTTTGCTG
hIL8	TTGGCAGCCTTCCTGATTTC	TCTTTAGCACTCCTTGGCAAAAC
hIL1A	TGTATGTGACTGCCCAAGATGAAG	AGAGGAGGTTGGTCTCACTACC
hIL1B	CCACAGACCTTCCAGGAGAATG	GTGCAGTTCAGTGATCGTACAGG
hTGFβ1	CGGAGTTGTGCGGCAGTGGT	GTTGGTGTCCAGGGCTCGGC
hVEGF-A	AGTTCATGGATGTCTATCAGCGC	TCCGCATAATCTGCATGGTG
hMMP1	ATGAAGCAGCCCAGATGTGGAG	TGGTCCACATCTGCTCTTGGCA
hMMP2	CCACTGCCTTCGATACAC	GAGCCACTCTCTGGAATCTTAAA
hMMP9	GCCACTACTGTGCCTTTGAGTC	CCCTCAGAGAATCGCCAGTACT
hMMP3	CACTCACAGACCTGACTCGGTT	AAGCAGGATCACAGTTGGCTGG
hPAI1	GGCCATTACTACGACATCCTG	GGTCATGTTGCCTTTCCAGT
hPAI2	GCTGTTTGGTGAGAAGTCTGCG	CTGCACATTCTAGGAAGTCTACTG
hCXCL1	AGCCAACGTCAAGCATCTCAA	AATCCACTTTAGCTTCGGGTCAA
hCXCL2	GGCAGAAAGCTTGTCTCAACCC	CTCCTTCAGGAACAGCCACCAA
hL1CAM	TCGCCCTATGTCCACTACACCT	ATCCACAGGGTTCTTCTCTGGG
hICAM-1	AGCGGCTGACGTGTGCAGTAAT	TCTGAGACCTCTGGCTTCGTCA
hITGβ3	CATGGATTCCAGCAATGTCCTCC	TTGAGGCAGGTGGCATTGAAGG
hCCL2	CCGAGAGGCTGAGACTAAC	CTTGCTGCTGGTGATTCTTC
hCCL7	ACAGAAGGACCACCAGTAGCCA	GGTGCTTCATAAAGTCCTGGACC
hOPN	CTGACATCCAGTACCCTGATGC	GGCCTTGTATGCACCATTCA
hGAPDH	CGACCACTTTGTCAAGCTCA	AGGGGTCTACATGGCAACTG

4.1.10 Laboratory Instruments, equipment and materials

Instrument	Commercial Name	Company
Centrifuge	Z233 MK-2	Hermle, Wehingen, Germany
Centrifuge	Rotina 420R	Hettich, Tuttlingen, Germany
Centrifuge	Multifuge 3S-R	Heraeus, Newport, GB
Counting chamber	Neubauer Improved	Neolab Migge, Heidelberg, Germany
Incubator	MCO-20AIC	Sanyo, Osaka, Japan
ELISA plate	Nunc MaxiSorp	Thermo Fisher, Waltham, MA, USA
Multiplate ELISA Reader	Multiskan EX	Thermo Fisher, Waltham, MA, USA
Luminescence plate	CulturPlate-96 Black	Perkin Elmer, Waltham, MA, USA
Luminescence Reader	1450 LSC & Luminescence Counter	Perkin Elmer, Waltham, MA, USA
Gel reader	ChemiDoc XRS	BIORAD, Hercules, CA, USA
Microtome	SLIDE 2003	Pfm medical, Cologne, Germany
Flow Cytometer	Gallios 4L	Beckman Coulter, Sinsheim, Germany
Brightfield microscope	Axioskop 40	Zeiss
Brightfield microscope	Leica DM IRB	Leica, Wetzlar, Germany
Fluorescence microscope	Leica DM 5500 B	Leica, Wetzlar, Germany
Live cell imaging system	IncuCyte® Live-cell analysis system	Sartorius, Goettingen, Germany

4.2 Methods

4.2.1 Patient samples

Formalin-fixed paraffin-embedded (FFPE) tissue sections from melanoma patients of all stages (I-IV) were provided by Prof. Dr. Hassel from the National Center for Tumor Diseases. Patient's written informed consent was obtained prior to sample acquisition and use of samples was reviewed by the Ethic Board of the University of Heidelberg (S-091/2011). Melanoma samples included primary stage I (n=10), stage II (n=16) and stage III (n=10) melanoma specimens, stage III lymph node (LN) metastasis (n=10), and stage IV distant metastasis (n=8) samples. In addition, we included healty skin (n=7) as control tissue.

4.2.2 Immunohistochemistry (IHC)

Paraffin-embedded samples were cut into sections of 2-5 microns. After rehydration, antigen retrieval was performed by boiling the samples for 30 minutes in citrate buffer at pH 6, followed by washing in water and blocking with 5 % goat serum for 30 minutes. Blocking was done by carefully removing all residual liquid, then encircling the tissue with a hydrophobic pen and carefully adding the blocking solution inside the circle. The slides were prepared for overnight incubation with the primary antibody as listed in 4.1.6. This was done by removing all residual goat serum solution and then adding the antibody, again diluted in blocking solution. The next day, the slides were washed in TBS-T and treated with the Dako REAL™ Detection System according to the manual. Typically, development with the chromogen solution was performed for 5-7 minutes and coloring was monitored under a microscope to prevent excessively weak or strong stainings. For single color IHC, the samples were then counterstained with Haematoxylin for 15 seconds, then washed under running water and embedded in an IHC embedding medium.

Alternatively, for double color IHC, the AP Red developed slides were blocked for endogenous peroxidase activity for 5 minutes with 3% H2O2. Then, the biotin-Streptavidin sites from the first reaction were blocked with the Avidin/Biotin Blocking Kit according to instructions, followed by overnight incubation with purified anti-slan (DD2) or anti-CD3, as described for single color IHC. The slides were washed and the mouse IgM antibody clone DD2 was then detected with a goat anti-mouse IgM specific detection system and rabbit anti-human CD3 with a goat anti-rabbit specific system. The slides were washed in TBS-T and green color was developed with the chromogen Histogreen. After this, the cells were shortly washed in TBS-T, before haematoxylin counterstain and embedding in xylene-based solution was performed.

For image analysis, 3 representative images of double stained (slan + CD56) FFPE samples were digitalized and the density of cells/mm^2 was analyzed and correlated for slanMo and CD56$^+$ NK cells. *p* and r^2 values were calculated using linear regression in Graphpad Prism.

4.2.3 Cell culture methods

4.2.3.1 Thawing of cells

Cells were removed from liquid nitrogen storage. The cryovial was disinfected with ethanol and placed in a 37 °C waterbath until the content was almost thawed completely. Then, the cells were transferred to fresh, pre-warmed culture medium and centrifuged (1300 rpm, 8 minutes, RT). After resuspension of the cell pellet in pre-warmed medium, the cells were transferred to appropriate flasks for culture in the incubator (37 °C, 5 % CO_2).

4.2.3.2 Passaging of cell lines

Adherent cells in culture were washed with PBS before addition of 1 ml trypsin per 75 cm^2 flask. For trypsin to catalyze adhesion molecule shedding, the flasks were placed at 37 °C until cells became round and detached from the plastic through gentle rocking of the flask. Trypsin activity was neutralized by addition of sufficient culture medium and transferred to tubes for centrifugation (1300 rpm, 8 minutes, RT). Typically, after supernatant removal, the cells were then resuspended in 10 ml fresh pre-warmed medium and 1 ml cell solution was transferred to a fresh flask, yielding a 1:10 dilution. The dilution factor was adjusted for each cell line and current confluency, ranging generally from 1:5 to 1:20.

Regularly, samples were taken for Mycoplasma contamination tests.

4.2.3.3 Freezing of cells

After trypzination, 1 – 5x10^6 cells in suspension were centrifuged (1300 rpm, 8 minutes, RT) and taken up in 1 ml Cryomedium. Then, the cells were immediately transferred to cryovials and placed at -80 °C in a freezing container for 1-2 days, before being transferred to liquid nitrogen for long-term storage.

4.2.3.4 Counting of cells by Trypan blue

Cells in suspension were counted by Neubauer chambers. Therefore, 10 µl cell suspension was diluted in trypan blue. The dilution factor was chosen based on the estimated cell number, ranging from 1:3 to 1:100. The mixture was then given into a readily prepared

Neubauer chamber and cells per area were counted on a 100x magnification. Cell number was calculated as follows:

$$total\ cell\ number = \frac{cell\ count}{counted\ squares} * (dilution\ factor) * 10^4$$

4.2.4 Purification and co-culture of human immune cell populations

4.2.4.1 Density gradient centrifugation

Peripheral blood mononuclear cells (PBMCs) were isolated in the evening from fresh (< 5 h after drawing blood) buffy coats of healthy donors by density gradient centrifugation with Biocoll separating solution. The content of the buffy coat was transferred carefully on top of 15 ml Biocoll and then centrifuged (800 rcf, 25 minutes, RT, without brakes). After separation, the intermediate cellular layer was removed and washed 3 times with PBS/EDTA (1300 rpm, 11 minutes, 4 °C) and then resuspended in 25 ml cold medium for storage overnight on ice.

4.2.4.2 Isolation of slanMo

For slanMo isolation on the next day, PBMCs were incubated with diluted M-DC8 hybridoma supernatant in MACS buffer in a ratio of $1*10^8$ cells/ml for 15 minutes at 4 °C. After incubation, the cells were washed with PBS/EDTA (1300 rpm, 10 minutes, 4 °C) and then incubated with rat anti-mouse IgM (1:21 in MACS Buffer and 420 µl per $1*10^8$ cells) at 4 °C for 15 minutes. After a second washing step, the cells were resuspended in MACS buffer and placed in an AutoMACS for separation with an individual protocol performing positive selection. The eluted cells were counted and taken up in fresh complete medium. The purity ($slan^+CD3^-$) of $slan^+$ cells was determined by FACS staining with an anti-IgM FITC antibody targeting the bound hybridoma antibody together with staining for CD3 and CD16. Only donors with a purity >90 % were used. The untouched flow through was used for separation of other populations.

4.2.4.3 Isolation of NK cells, $CD14^+$ monocytes, and T cells

NK cells were isolated with the NK cells isolation kit according to the instructions. However, only 75 % of the original volume in the manual was used. A defined fraction of the slanMo separation flow through was removed and used for NK cell isolation. The cells were separated in an AutoMACS using the ‘Depletes’ configuration for depletion of all non-NK cells. Purity ($CD56^+CD3^-$) of NK cells was analyzed by FACS and was typically >90 %.

$CD14^+$ monocytes were isolated by using the CD14 Microbeads kit according to the vendor's instructions. Separation was performed in an AutoMACS running a positive selection protocol.

T cell isolation was performed with the CD4+ T cell isolation kit according to the instructions. Separation was again achieved by running the negative selection protocol 'Depletes' on an AutoMACS.

4.2.4.4 Co-culture of different immune cell populations

For cytokine testing or conditioned medium (CM) generation, co-cultures of (1) slanMo + NK cells; (2) $CD14^+$ monocytes + NK cells; (3) slanMo + T cells; and (4) $CD14^+$ monocytes + T cells, and mono-cultures of all cell types, were prepared in complete medium. 6 hours after initial seeding of the first immune cell population, each culture setup was either stimulated with 1 µg/ml R848 or 100 ng/ml LPS, or left unstimulated.

For both mono- and co-cultures, slanMo and CD14+ monocytes were both seeded at t=0 h with a density of $3x10^5$ cells/cm^2 and a concentration of $0,5x10^6$ cells/ml, whereas NK cells and T cells were seeded concomitant with either R848 or LPS stimulation at t=6 h, both with a density of $6x10^5$ cells/cm^2 and a concentration of $1x10^6$ cells/ml. This yielded a 1:2 ratio of slanMo/$CD14^+$ monocytes to NK cells/T cells.

At t=24 h, the medium was transferred to tubes and centrifuged (2000 rpm, 12 minutes, 4 °C). Then, the cell-free supernatant was removed and either used directly or stored at -80 °C.

4.2.5 Fluorescence-activated cell sorting (FACS)

For fluorescence staining of suspension cells, $1*10^5$ - $2*10^5$ cells were transferred to a 96-well V-bottom plate and washed with ice-cold FACS buffer (1300 rpm, 5 minutes, 4 °C). Then, the cells were incubated for 30 minutes at 4 °C in the dark with a primary antibody mixture diluted in FACS buffer. If necessary, a secondary antibody incubation step was performed for unlabeled primary antibodies under the same conditions as for the first incubation period. The cells were washed again and transferred in FACS buffer into FACS tubes for analysis on a Beckman Coulter Gallios™ or a BD FACS Canto™. Shortly prior to measurement, 2 µl 7-AAD was added to each tube for live/dead discrimination.

4.2.6 Cytokine-measurement assays

4.2.6.1 Enzyme-linked immunosorbent assay (ELISA)

For measurement of TNF-α and IFN-γ concentrations in slanMo/NK cell co-culture CM, the supernatants were analysed by ELISA. In an ELISA, plate bound capture antibodies bind to their targets in the samples and are then visualized via detection antibodies targeting a different epitope.

4.2.6.2 Flow cytometry based cytokine measurement

Multi-analyte measurements were performed with LEGENDplex™ kits for flow cytometry according to the instructions provided by the vendor. Here, cytokine concentrations are determined with a mixture of pre-labeled beads coupled to cytokine-specific antibodies. Bound cytokines are then detected with a detection antibody mix, which is subsequently fluorescently labeled. The individual fluorescence signal can then be determined for each bead type. Flow cytometry analysis was performed on a Gallios™ FACS.

4.2.7 Migration assays

4.2.7.1 Neuro probe migration assay

For quantifying NK cell migration in 96-well scale, 1-day cultured NK cells were adjusted to a concentration of $2*10^6$ cells/ml. Conditioned medium from R848-activated slanMo (slanMo CM) was provided as chemoattractant in the bottom well of the 96-well plate. In some conditions, a CCR5 or IL-8 neutralizing antibody was added directly to the slanMo CM in a concentration of 20 µg/ml. Then, a second layer providing a porous support for every well was mounted on top. The NK cell solution was added as a drop on each well in a way that both liquid phases are connected. The plate was incubated for 2.5 hours in an incubator at 37 °C and 5 % CO_2 to allow for NK cells to migrate. Then, the cells were transferred to a luminescence plate and total ATP content was measured with the Cell Titer Glo Luminescenct cell viability assay in a black culture plate, optimized for luminescence signal detection. In order to calculate exact cell numbers, a standard curve was generated by providing defined numbers of NK cells in the measurement plate. Specific migration was defined as:

$$specific\ migration\ (\%) = \left(\frac{number\ of\ cells\ [sample] - number\ of\ cells\ [control]}{number\ of\ cells\ [input]}\right) * 100$$

4.2.7.2 Transwell migration assay

Alternatively to a 96-well format, NK cell migration was also tested with regard to changes in chemokine receptor expression. To this end, NK cells were used in a 24-well permeable support assay. Again, IL-8 in the slanMo CM was neutralized or not with an anti-IL-8 antibody (10 µg/ml) or the respective isotype control. The slanMo CM was provided as bottom chamber chemoattractant. As positive control, recombinant IL-8 (100 ng/ml) was used. Then, $2*10^5$ NK cells in 100 µl volume were carefully added on top of the porous insert, thereby connecting the top NK cells with the bottom chamber solution. After 4 hours incubation at 37 °C and 5 % CO_2, the migrated NK cells from the bottom chamber were removed and then stained for CXCR1 and CXCR2. Samples were then analyzed on a Gallios™ FACS.

4.2.8 Conditioned medium (CM) or cytokine treatment of melanoma cells

4.2.8.1 In vitro assay for multiple cell lines

SK-Mel-28, Ma-Mel-86b, SK-Mel-25, and SK-Mel-30 were seeded in appropriate plates at a density of $1x10^4$ cells/cm^2 and $3{,}125x10^4$ cells/ml in medium (5 % FCS only). After a brief settlement and initial attachment phase at RT, the recombinant cytokines (50 ng/ml TNF-α + 500 ng/ml IFN-γ) were added in 1/5 of the cell suspension volume, thereby yielding a final concentration of 10 ng/ml TNF-α + 100 ng/ml IFN-γ and a final concentration of $2{,}5*10^4$ cells/ml. When the cells grown in unmodified control medium reached ~90 % confluency, all samples were trypsinized, washed, counted and reseeded equally at a concentration of $2*10^4$ cells/cm^2 in fresh culture plates and fresh medium. This was repeated for up to 3 passages and growth curves were calculated by projecting future growth of the initially seeded population.

4.2.8.2 Standardized SK-Mel-28 CM Treatment

SK-Mel-28 were seeded at a density of $1x10^4$ cells/cm^2 and $3{,}125x10^4$ cells/ml in 6, 12, 24 well plates, or 55 cm^2 culture dishes in medium (5 % FCS only). After a brief settlement and attachment phase at room temperature, the CM or recombinant cytokines (50 ng/ml TNF-α + 500 ng/ml IFN-γ) were added in 1/5 of the cell suspension volume, thereby yielding a 1 to 5 dilution and a final concentration of 10 ng/ml TNF-α + 100 ng/ml IFN-γ in a final density of $2{,}5*10^4$ cells/ml. The CM was used diluted in order to reduce potential growth inhibiting effects stemming from already exhausted co-culture medium. In order to prevent premature confluency of the control cultures during the passages, the overall growth conditions were limited by using RPMI containing 5 % instead of 10 % FCS. For neutralizing experiments,

both anti-human TNF-α (Adalimumab, 50 µg/ml) and anti-human IFN-γ (50 µg/ml) were directly added to the CM prior to addition to the respective wells, yielding a final concentration of 10 µg/ml each. The cells were then cultured for 4 days at 37 °C, 5 % CO_2 in an incubator. At the first passage, control cells were typically confluent. For passaging, cells were trypsinized, counted, and then reseeded in fresh medium (5 % FCS) at a density of $1*10^4$ cells/cm^2 for cell number analysis after 8 days. Alternatively, the cells were seeded at $2*10^4$ cells/cm^2 and $4*10^4$ cells/ml in appropriate plates for downstream analysis.

At day 8, the cells were again trypsinized and counted in order to calculate growth curves.

4.2.8.3 ^{3}H Thymidine incorporation assay

For measuring proliferation via radioactive ^{3}H Thymidine incorporation, SK-Mel-28 were treated with CM as described before (chapter 4.2.7.2). 1 day after reseeding in 96 well plates, the adherent cells were pulsed for 12 hours with ^{3}H Thymidine (1:5 diluted in medium) solution. After the incubation period, the adherent cells were thoroughly trypsinized and transferred to a 96-well format membrane Filtermat. In detail, the filter was adjusted in the vacuum pump device and washed 3x with water. Then, the soluble cell suspension was sucked through and the filter was again washed 3x with water. Then, filter was dried in a dry oven at 60 °C for 1 hour. The dry filtermat was sealed in a plastic bag after addition of Betaplate Scint Solution. The fully sealed filtermat was then measured for luminescence signal in a luminescence reader. The time for each well was set to 1 second.

4.2.8.4 Senescence-associated β-Galactosidase (SA β-Gal) assay

SA β-Gal staining was performed on SK-Mel-28 cells reseeded in 48 well plates for 1 day after CM treatment (chapter 4.2.7.2). Adherent cells were washed with PBS and then stained with the SA β-Gal staining kit by following the manufacturer's instructions. After overnight staining, the staining solution was removed and the wells were filled with 70% Glycerol for preservation. The plates were stored at 4 °C in a fridge for later imaging.

4.2.8.5 Quantification of SA β-Gal positive cells

For Image acquisition, three representative 100x images were taken. The unmodified images were loaded in ImageJ software and total cells were counted manually with cell counter plug-in. Then, a color threshold encompassing the green/cyan SA β-Gal staining was applied and particles (> 40-60 pixel) were counted as positive cells.

4.2.8.6 Incucyte time kinetic

To visualize the kinetics of morphological changes and apoptosis occurring in SK-Mel-28 during the 4 days exposure to CM, we used the IncuCyte® Live cell analysis system in combination with an Annexin V dye to visualize apoptotic cells. Therefore, SK-Mel-28 were treated and seeded as described before in flat-bottom 96 well plates in triplicates. After addition of CM +/- neutralizing antibodies, IncuCyte® Annexin V Red reagent was added to each well according to the manual and the plate was placed in the Incucyte inside an incubator at 37 °C, 5 % CO_2. Images were taken every two hours for a total of 96 hours with a total magnification of 100x and 4 images per well. Data analysis was performed with Incucyte software.

4.2.9 Immunofluorescence (IF)

4.2.9.1 IF staining

For p21 and Ki67 IF staining, CM-treated and TNF-α/IFN-γ neutralized melanoma cells were seeded on 8 well glass diagnostic slides at $2x10^4$ cells/cm^2 covered in a drop of medium. After 1 day of culture that allowed the cells to adhere to the glass slide, the slide was carefully washed by removing the liquid drop with a vacuum pump and then adding PBS-T. The cells were fixed with 4% PFA for 20 minutes at RT and then permeabilized with 0,1 % (w/v) Triton-X 100 for 10 minutes at RT. Incubation with primary antibody was performed overnight at 4 °C. Either p21 was stained separately or together together with Ki67 and diluted as listed in table 4.1.6. The next day, the slide was washed again and incubated with secondary antibody g-a-m for Ki67 and g-a-rb for p21 for 30 minutes at RT in the dark. In general, after secondary antibody labeling, the slides were kept as dark as possible to prevent fluorophor bleaching. The slides were washed and incubated for 5 minutes with DAPI diluted 1:20000 in DI water at RT. After nuclear staining with DAPI, the cells were washed with DI water, mounted in IF mounting medium and then stored at 4 °C in the dark until images were taken.

4.2.9.2 Digital quantification

Image acquisition was standardized in a way that the same exposure and settings were used for all images from one experiment, allowing to compare fluorescence intensities and number of positive cells between conditions. p21 and Ki67 positive cells were quantified digitally with the software ImageJ. Therefore, unmodified images were loaded and a threshold intensity for each channel separately was defined, including DAPI for quantifying total cells. Then, the threshold was applied and particles (> 20 pixel) in each channel were quantified.

4.2.10 Western Blot

For Western Blot analysis of p21 expression, cells taken from CM or cytokine treatment experiments were lysed in hot lysis buffer. In detail, hot lysis buffer was pre-heated at 100 °C in a thermo block. The cells were washed with PBS, centrifuged (1300 rpm, 8 minutes, 4 °C) and then resuspended in boiling hot lysis buffer (1 ml per $5*10^6$ cells). The mixture was boiled in a thermo block for 15 minutes with regular mixing of the suspension and then centrifuged (14000 rpm, 15 minutes, 4 °C). Afterwards, the supernatant was transferred to fresh tubes without disturbing the white smear in the bottom. The protein concentration was determined by BCA assay according to the instructions and the samples were stored at -20 °C until application in Western Blot analysis.

For size-separation of proteins in the lysates, the protein samples were diluted in SDS buffer and run on a 15 % SDS gel. Then, the proteins were further transferred to a 0.2 µm pore-size nitrocellulose membrane. For the transfer of proteins by western blotting, the membrane was pre-activated with pure methanol and then placed on top of three Whatman paper pre-soaked in blotting buffer, followed by the SDS gel and covered again with three soaked Whatman paper. Blotting was performed for 1 h at 100 mA, after which the membrane was quickly rinsed in TBS-T and then blocken in 5 % BSA for 1 h at RT. The primary antibody p21 was added and the membrane was sealed in a plastic foil and incubated overnight on a shaking table at 4 °C. The next day, the membrane was washed 3x 5 minutes in TBS-T and then incubated with the HRP-labeled secondary antibody diluted in TBS-T for 1 hour at RT. After washing, the membrane was developed by addition of HRP substrate in the form of a 1:1 mixture of ECL reagent and chemiluminescent signals were detected in a chemiluminescence imager. In order to quantify protein content, the membrane was incubated in stripping buffer for 30 minutes at 56 °C to remove previously bound antibodies. A directly HRP-labelel β-actin antibody was used as housekeeping marker and incubated for 2 hours at RT. Then, ECL signal was again detected as described before. Signal intensity was quantified using ImageJ.

4.2.11 Quantitative polymerase chain reaction (qPCR)

qPCR experiments were performed by Lenka Kyiacova in Mannheim:

Total RNA was isolated using TRIzol reagent (Thermo Fisher Scientific), following manufacturers' instructions. RNA was treated with RNase-free DNase I, followed by EDTA deactivation for 10 min at 65°C (both from Thermo Fisher Scientific). First strand cDNA was synthesized from 2000 ng of total RNA with random hexamer primers, using dNTP mix and RevertAid H Minus Reverse transcriptase (all from Thermo Fisher Scientific). qRT-PCR was

performed in a Stratagene Mx3500P qPCR machine (Agilent) using SYBR Select Master Mix containing SYBR GreenE dye (Applied Biosystems). The relative quantity of cDNA was estimated using the ΔΔCT method and data were normalized to GAPDH as housekeeping gene.

4.2.12 Statistical analysis

All Data were analyzed in GraphPad Prism 5 and are presented as mean ±SEM. Heatmaps were created in GraphPad Prism 7. Statistical significance was evaluated by *p* values, which were assessed using 1 way Anova with Bonferroni's multiple comparison *post hoc* test for groups of 3 and paired t test for groups of 2, unless otherwise indicated. *$p<0.05$, **$p<0.01$, ***$p<0.001$.

5 Results

5.1 slanMo and NK cells infiltrate human melanoma

Malignant melanoma is strongly infiltrated by immune cells. With extensive data being present on T cell infiltration into melanoma, rather little is known about infiltration of minor innate immune cell subsets. In particular subsets capable of initiating immune responses and maintaining a pro-inflammatory environment are important for effective anti-tumor responses.

5.1.1 slan$^+$ and CD56$^+$ cells can be detected in primary and metastatic melanoma

We hypothesized a contribution of the slanMo/NK cell crosstalk in anti-melanoma immune responses and therefore aimed at gaining a comprehensive overview of slanMo and NK cell infiltration in melanoma. We collected formalin-fixed parafin embedded (FFPE) samples from all four stages of melanoma development. Detection of slanMo in tissues is facilitated by the monoclonal antibody DD2 that specifically targets the slan antigen and also allows staining of FFPE material (Fig. 5.1 A). NK cells were detected by staining for CD56 (NCAM) (Fig. 5.1 B). Morphologically, slan+ cells exhibited a monocytic-like shape, yet defined cell populations also displayed a DC-like or macrophage-like morphology (Fig. 5.1 A). Interestingly, the lumen of vessels often stained positive for slan and individual slan positive cells appeared to be lining vessel walls repeatedly (data not shown). CD56 staining consistently identified a population of small and round infiltrating cells, consistent with a lymphocytic morphology (Fig. 5.1 B). However, CD56 staining intensity was often weak, suggesting the presence of CD56^{dim} NK cells in the tissues. When investigating melanoma samples ranging from cutaneous stage I, stage II, and stage III melanoma lesions to stage III lymph node and stage IV distant metastasis, we could detect slan+ (Fig. 5.1 C) and CD56+ (Fig. 5.1 D) cells over all stages of melanoma development. In contrast, both mouse IgM (mIgM) and mouse IgG (mIgG), isotypes for DD2 and anti-CD56 antibody, respectively, were negative (Fig. 5.1 E, F). Individual stage I, stage II, and stage III samples consistently contained both slan+ and CD56+ cells. Distant metastasis samples from stage IV melanoma patients were however repeatedly devoid of both cell types.

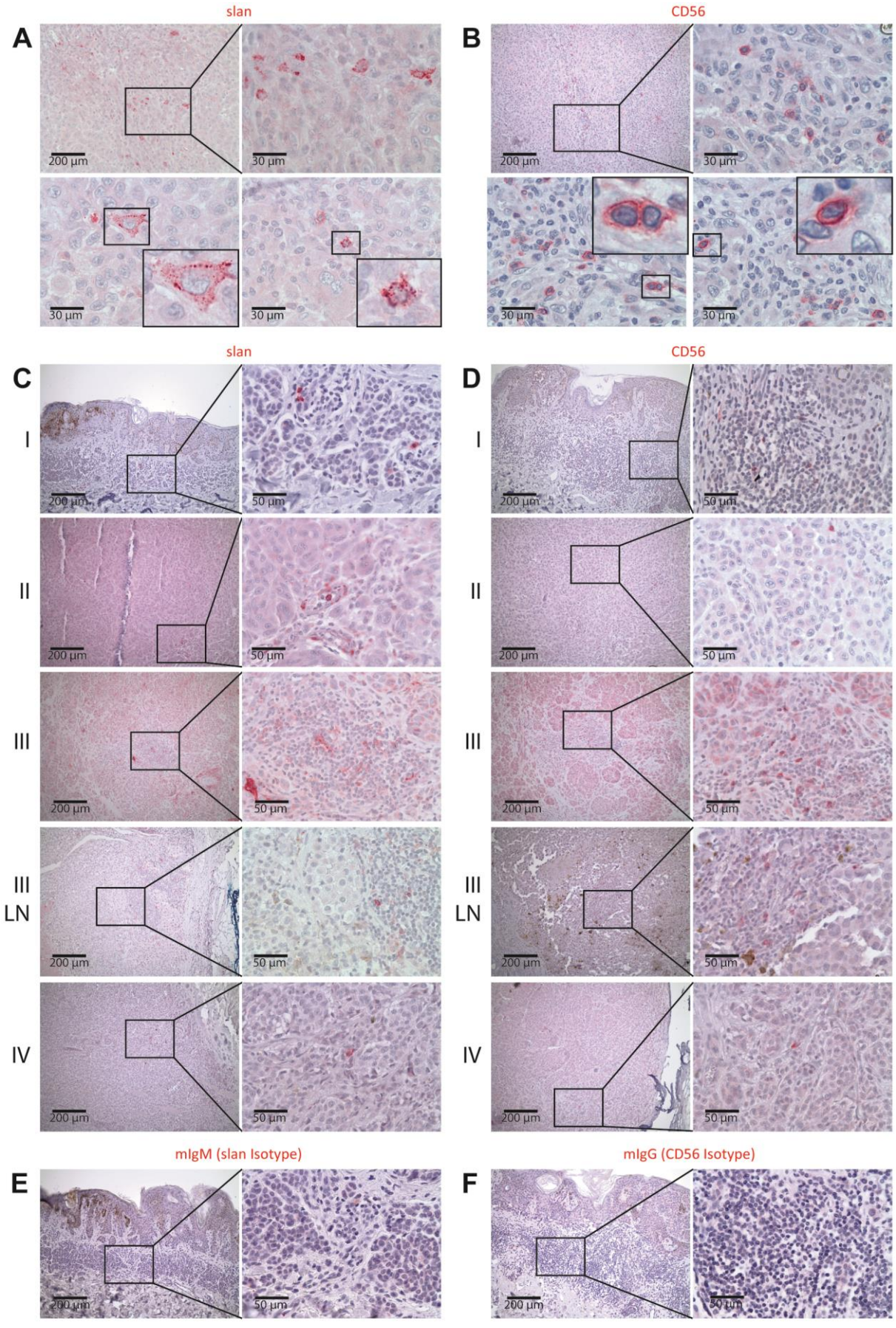

Figure legend on next page.

Figure 5.1 – Detection of slanMo and NK cells in melanoma samples. FFPE samples from melanoma patients were incubated with the **(A, C)** anti-slan monoclonal antibody DD2 (slan) or with an **(B, D)** anti-CD56 monoclonal antibody (CD56). **(A-B)** Representative sections from melanoma patients showing morphological features of slan+ and CD56+ cells. Original magnification 200x and 630x. **(C-D)** Depicted are melanoma samples including stage I (I), stage II (II), stage III (III) cutaneous melanoma, stage III lymph node metastases (III LN), and stage IV distant metastases (IV). Isotype staining with **(E)** mouse IgM (mIgM; isotype for slan staining) and **(F)** mouse IgG (mIgG; isotype for CD56) was performed. An alkaline phosphatase detection system was in combination with a chromogen generating a red color was used for detection of positive cells in the samples. **(C-F)** Original magnification of the first and third column is 100x and of the second and fourth is 400x.

5.1.2 Frequency and correlation of slanMo and NK cells over all stages of melanoma development

Since slanMo and NK cells can enter a synergistic crosstalk facilitating slanMo maturation, cytokine production, and NK cell anti-tumor functions, we investigated whether we can also observe a co-localization of slanMo and NK cells in melanoma tissue. Therefore, we established a two-color IHC system that allows us to detect slanMo and NK cells together with the histological information provided by immunohistochemistry but not immunofluorescence. Using the NK cell marker CD56 in combination with slan in a two-color IHC system does not allow to differentiate between $CD56^+$ NK cells and $CD56^+CD3^+$ NK T cells. However, co-staining of CD56 with CD3 showed that the vast majority of $CD56^+$ cells were CD3 negative and therefore not NK T cells (Fig. 5.2 A). We were also taking into account that melanoma cells can stain positive for CD56. However, it was feasible to differentiate between $CD56^{+/dim}$ tumor cells and $CD56^+$ immune cells based on general morphology and size dicrimination (Fig. 5.2 B). Together, this allowed us to specifically identify NK cells by CD56 staining in tissues. Furthermore, slanMo and NK cells exhibited similar morphological features when comparing single color staining (Fig. 5.1) with the CD56/slan two-color IHC system (Fig. 5.2 C). As expected, slanMo often acquired a larger, macrophage-like morphology (Fig. 5.2 D left image), whereas CD56+ cells appeared lymphocytic (Fig. 5.2 D right image).

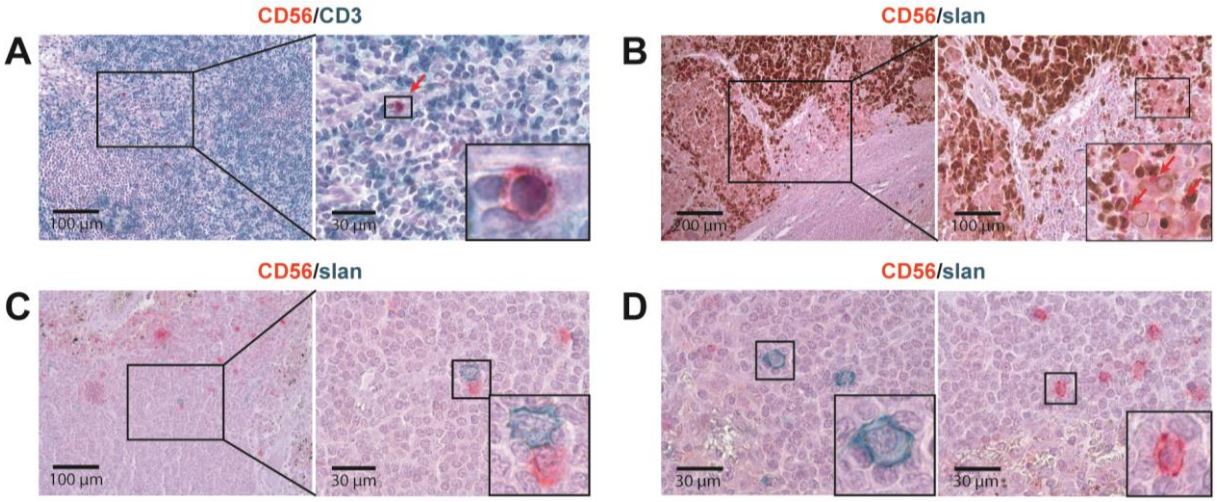

Figure 5.2 – Verification of CD56⁺ NK cell staining in a two-color IHC system. A two-color IHC system was established by using first a red-color detection system in combination with subsequent detection of mIgM or rabbit IgG with a green detection system. **(A)** CD56 was co-stained with CD3 in order to differentiate CD56⁺ NK cells from CD56⁺CD3⁺ double positive NK T cells on FFPE lymph node tissue. Original magnification: left (200x), right (630x). **(B)** CD56 was co-stained with slan in a weak CD56 positive stage III lymph node metastasis melanoma sample. Original magnification: left (100x), right (200x). **(C-D)** Representative images of stage III lymph node metastasis samples of slan+ and CD56+ cells as detected in the two-color IHC system. Original magnification: **(C)** left image (200x), right (630x), **(D)** (630x).

We then collected a larger panel of melanoma samples again covering all four clinical stages for two-color IHC staining. In total, we accumulated 10 stage I (Fig. 5.3 A), 16 stage II (Fig. 5.3 B), 10 stage III (Fig. 5.3 C), 10 stage III lymph node metastasis (Fig. 5.3 D), and 8 stage IV distant metastasis samples (Fig. 5.3 E). We inlcuded healthy human skin samples from 7 donors as control tissues (Fig. 5.3 F). When quantifying the number of slanMo for all stages, we observed a strong accumulation of slanMo in stage I melanoma lesions, which then dropped heavily in stage II and remained constant over the rest of disease progression (Fig. 5.3 G). On the other hand, NK cells were detected in very low numbers in stages I and II, but increased in frequency in stage III. In comparison, healthy human skin was virtually void of NK cells and contained only sparse, isolated slanMo, arguing that the high numbers of slanMo and of NK cells in cutaneous tumors and metastasis is due to anti-tumor immune responses and active infiltration (Fig. 5.3 H). We observed similar numbers of slanMo and NK cells in stage III lymph node metastasis compared to cutaneous stage III melanoma. In stage IV distant metastasis, including the skin, lung, and liver as metastatic sites, both slanMo and NK cells were rare. Interestingly, we found a significant correlation for slanMo and NK cell numbers in stage III melanoma samples (Fig. 5.3 A-F). An explanation for this could be provided by a migration mechanism, in which slanMo attract NK cells towards advanced melanoma metastasis. Interestingly, this would be in line with the observations of high slanMo density in melanoma stage I and increasing NK cell numbers in later stages.

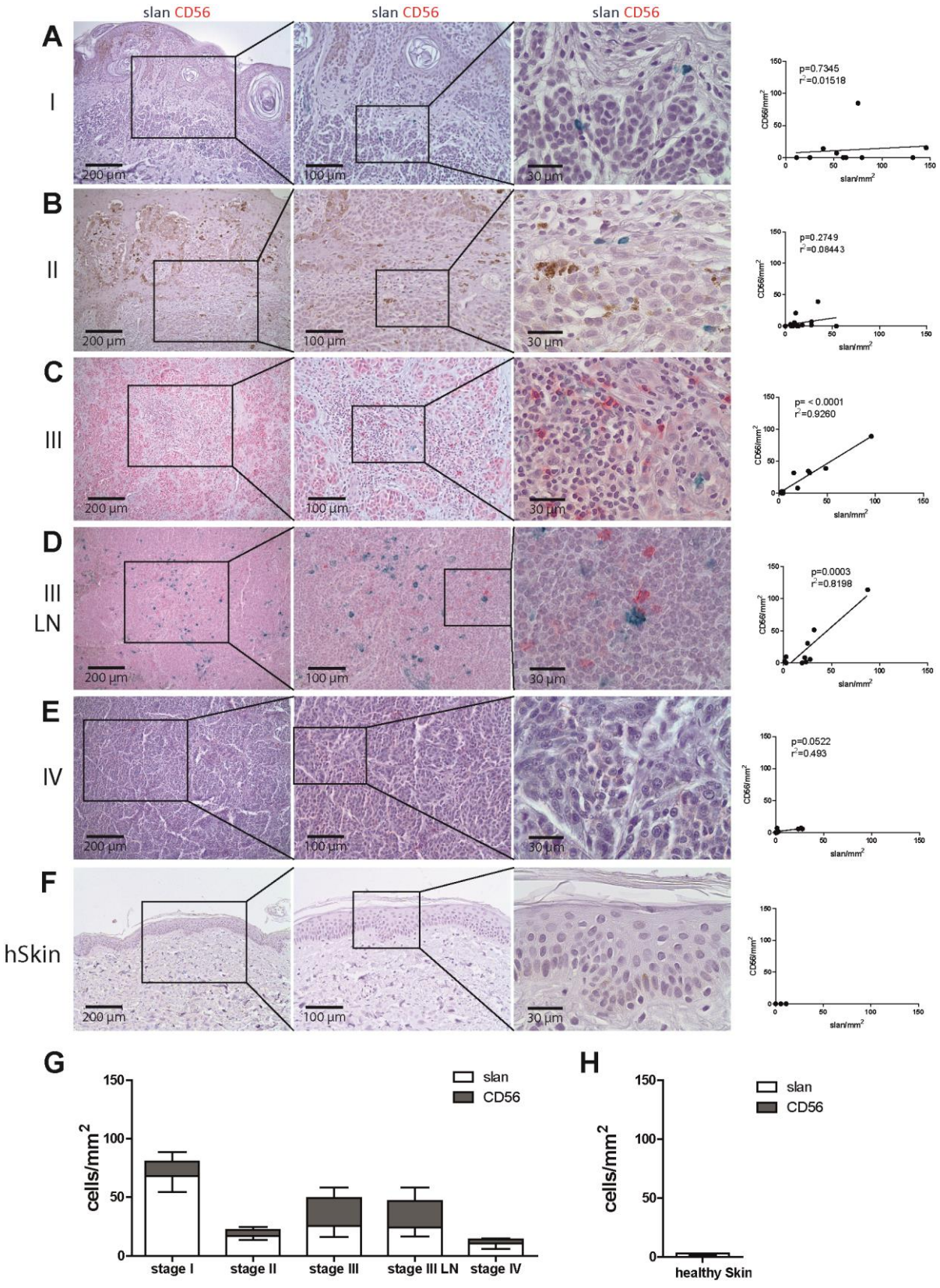

Figure 5.3 – Frequency and correlation of slanMo and NK cells infiltrating melanoma. FFPE melanoma samples from representative stage I **(A)**, stage II **(B)**, stage III **(C)**, stage III lymph node metastases **(D)**, and stage IV distant metastases **(E)** were double stained for slan (green) and CD56 (red). Healthy skin samples were included controls **(F)**. Original magnifications: left column (100x), middle column (200x), right column (630x). Graphs on the right depict the correlation of frequencies in cells/mm^2 correlated for slan and CD56 seperately for (A) – (F). **(G)** Frequencies of slan+ and CD56+ cells/mm^2 as depicted in (A) – (E). **(H)** Frequencies of slan+ and CD56+ cells/mm^2 as depicted (F).

Taken together, we discovered that slanMo and NK cells strongly accumulate in melanoma lesional skin. Additionally, we observed a correlation of slanMo and NK cell infiltration in stage III lesions. This could suggest a connected migration mechanism for slanMo and NK cells.

5.2 slanMo recruit NK cells via IL-8

5.2.1 Characterization of the slanMo chemokine milieu

The finding that slanMo were present at increased numbers in early stages of melanoma and that slanMo and NK cell infiltration correlated in advanced stages of melanoma lead us to study whether slanMo are capable of instructing recruitment of NK cells into tissues. To get a first overview of the chemokine production of slanMo, we performed multiplex chemokine screens of cell-free supernatants from non-activated and TLR 7/8 (R848)-activated slanMo. slanMo require a maturation phase that starts after initial settling on culture plates. Interestingly, slanMo are not capable of producing IL-12 if stimulated directly after seeding, whilst they produce high level IL-12 when stimulated 6 hours after seeding. Since we aimed at detecting maximum chemokine levels, we kept the 6 hour maturation phase protocol (Fig. 5.4 A). Thus, slanMo were stimulated with 1 µg/ml R848 6 hours after seeding and the resulting slanMo conditioned medium (CM) was harvested after a total culture of 24 hours. We then analyzed the cell-free supernatants for expression of different chemokines (Fig. 5.4 B). The heat map in Fig. 5.4 B displays strong expression of CXCL8 (IL-8) and intermediate expression of CCL3 and CCL4, all of which are upregulated after TLR 7/8 stimulation with R848 (Fig. 5.4 C). We then tested whether NK cells can migrate towards the respective ligands discovered in the chemokine screen. By using a 5 µm pore size migration system where we provided recombinant CCL3, CCL4, IL-8, and SDF-1 (CXCL-12) in the bottom chamber (Fig. 5.4 D), we observed concentration-dependent specific NK cell migration for IL-8, whereas CCL3 and CCL4 only induced minor NK cell migration (Fig. 5.4 E). SDF-1 was used as a positive control chemoattractant and accordingly yielded the highest frequencies of migrating NK cells.

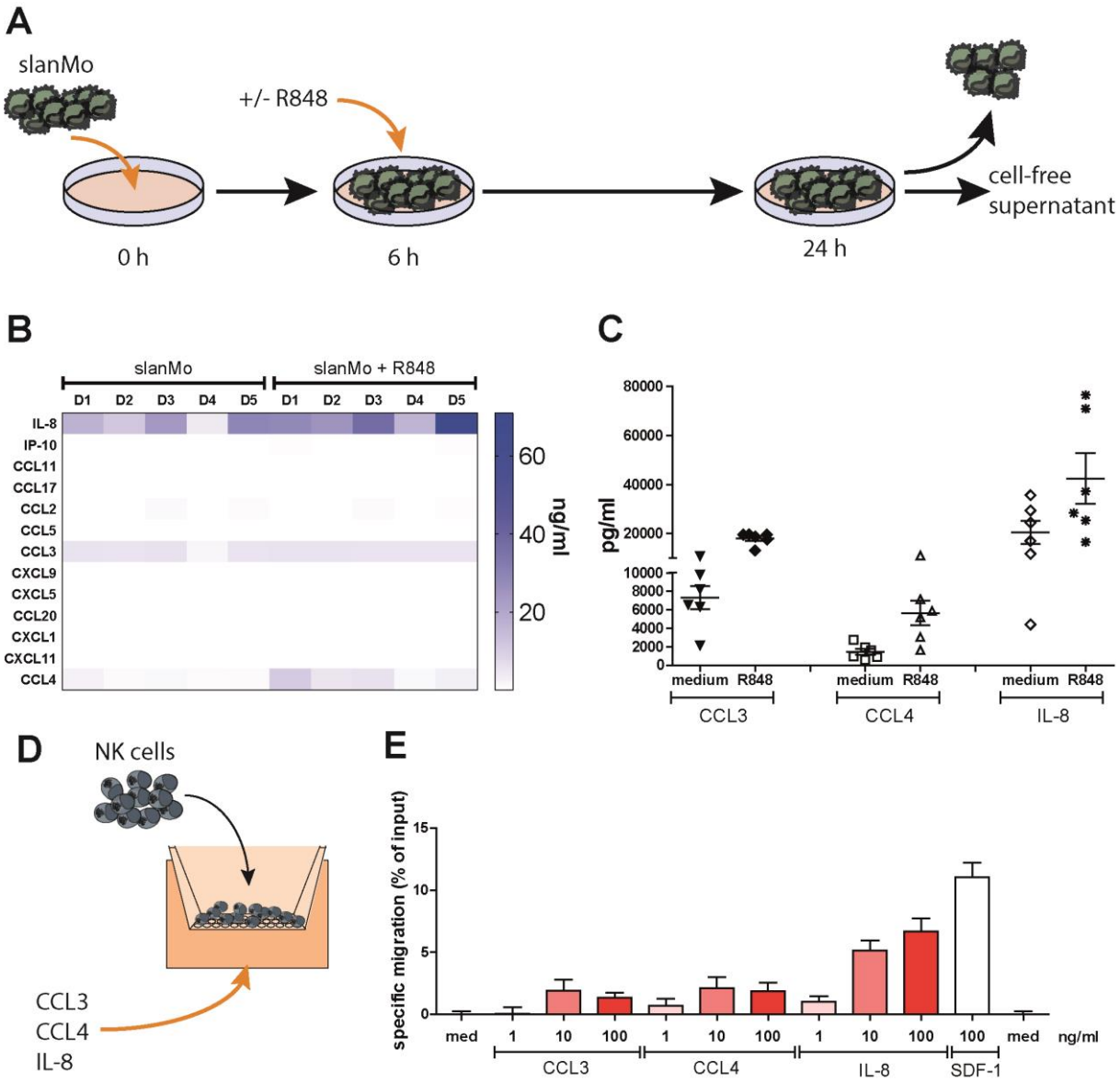

Figure 5.4 – Chemokines secreted by activated slanMo recruit NK cells. (A) Time scheme for slanMo culture and cell-free supernatant generation. **(B)** Heat map depicting concentrations of chemokines analyzed in the multiplex chemokine screen in slanMo-derived cell-free supernatants with and without stimulation with 1 µg/ml R848 from five healthy donors. **(C)** Graph showing concentrations of CCL3, CCL4, and IL-8 from individual donors. **(D)** Scheme of the experimental setup for NK cell migration towards recombinant chemokines. **(E)** Percentage of NK cells that migrated (substracted of medium control values) towards different concentrations of CCL3, CCL4, IL-8, and SDF-1 (CXCL-12). SDF-1 was used as positive control.

5.2.2 Mechanism of slanMo-mediated NK cell attraction

Based on the observation of directed NK cell migration towards chemokines present in the activated slanMo CM, we hypothesized that the slanMo supernatant alone can attract NK cells. Importantly, NK cells are reported to express the respective receptors binding to CCL3/CCL4 (CCR5) and IL-8 (CXCR1/CXCR2) [105]. We provided activated slanMo CM in the bottom chamber and seeded NK cells on a porous membrane, as described before. To

investigate the relevance of CXCR1/CXCR2 – IL-8 and CCR5 – CCL3/CCL4 signaling, we added neutralizing antibodies either against IL-8 or against CCR5, or respective isotype controls, directly to the supernatant (Fig. 5.5 A). NK cells showed a strong specific migration (9,0 % of total input cells normalized to control) towards slanMo CM, which was not affected by the presence of isotype control antibodies (Fig. 5.5 B, C and data not shown). Interestingly, when we neutralized IL-8, this effect was abolished and migration was almost at baseline level (Fig. 5.5 B). In contrast, neutralization of CCR5 had no significant impact on NK cell migration (Fig. 5.5 C). Together, this strongly argues for an essential function of IL-8 in inducing slanMo-mediated NK cell migration.

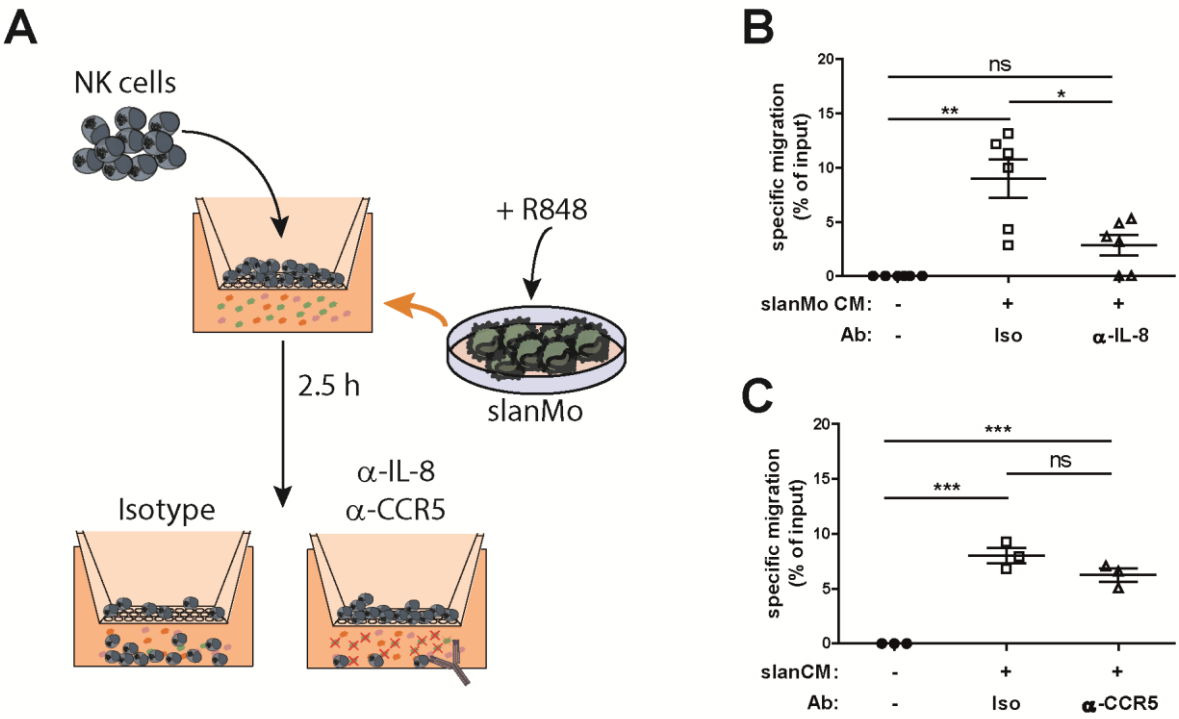

Figure 5.5 – NK cell migration towards slanMo CM is mediated by IL-8. (A) Scheme illustrating the migration assay for NK cell recruitment towards slanMo conditioned medium (slanMo CM) under IL-8 and CCR-5 neutralizaing conditions. **(B)** Graph depicting percentage of migrated NK cells towards slanMo CM with a neutralizaing antibody against IL-8 or respective isotype control. **(C)** Graph depicting percentage of migrated NK cells towards slanMo CM with a neutralizaing antibody against CCR5 or respective isotype control.

IL-8 binds to the chemokine receptors CXCR1 and CXCR2, subsequently mediating internalization and directed migration [154, 155]. Consistent with previous findings, we found that NK cells express CXCR1 and CXCR2 (Fig. 5.6 A). In order to assess which receptors were involved in the IL-8 dependent slanMo CM migration mechanism, we investigated receptor expression of NK cells harvested after migration under IL-8 neutralizing and isotype conditions, as illustrated in Figure 5.5 B. We observed that NK cells migrating in the medium control well were still expressing high levels of both CXCR1 and CXCR2 (Fig. 5.5 C). However, migration towards slanMo CM significantly reduced expression of both CXCR1 and

CXCR2, and IL-8 neutralization in the slanMo CM efficiently prevented receptor downregulation (Fig. 5.5 C, D). For CXCR1, receptor downregulation was completely negated, whereas CXCR2 still exhibited ~50 % reduced receptor expression, as depicted by mean fluorescence intensity values (Fig. 5.5 D). By relying on both quantification of migrated cells and receptor engagement, we were able to demonstrate that IL-8 provided by TLR 7/8-activated slanMo is capable of recruiting NK cells.

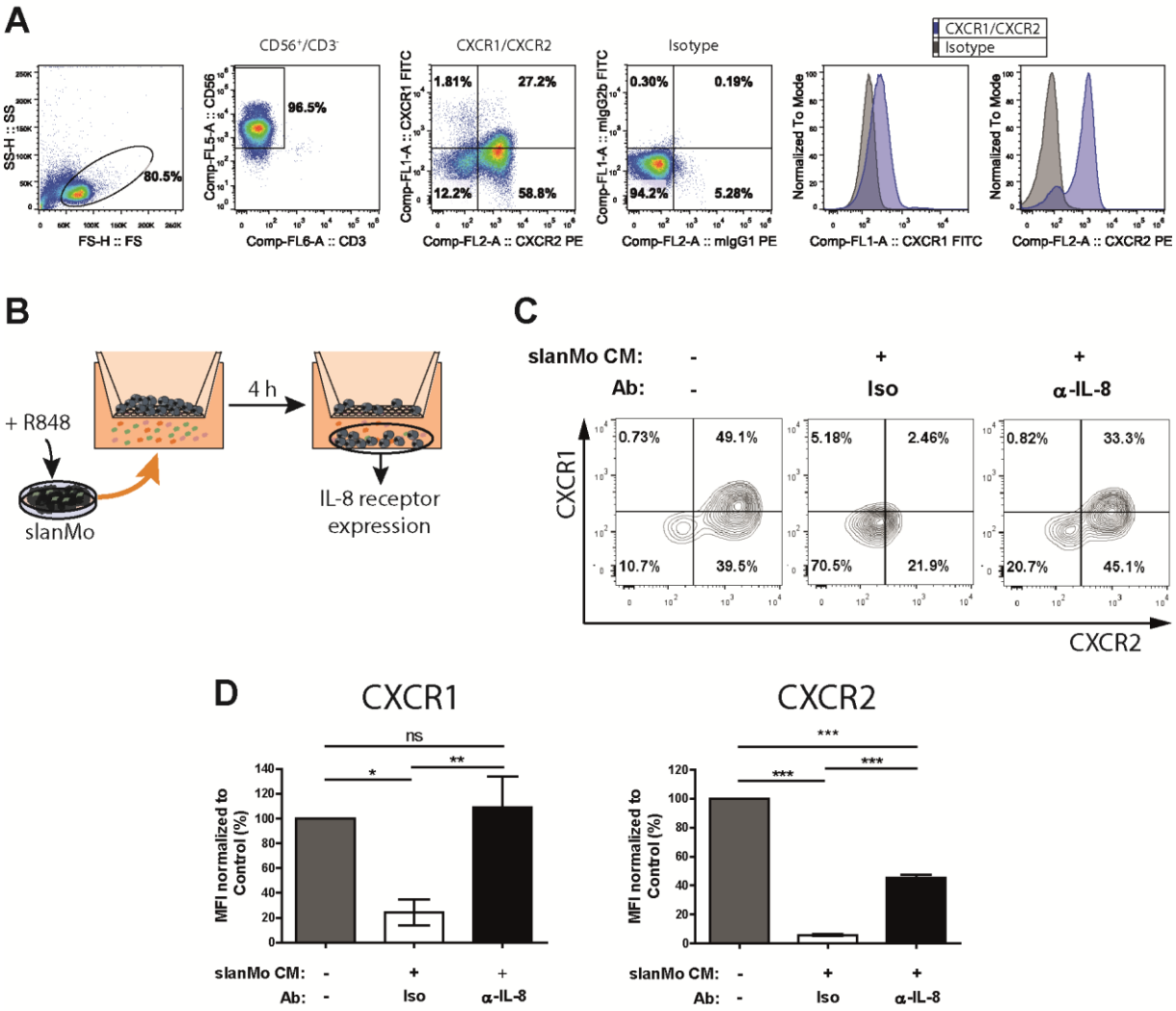

Figure 5.6 NK cell recruitment by slanMo requires CXCR1/CXCR2. (A) FACS staining for CXCR1 and CXCR2 expression on $CD56^{+}CD3^{-}$ NK cells. Histograms show CXCR1/CXCR2 staining (violet) together with respective isotype control staining (gray). **(B)** Schematic for illustration of receptor expression analysis on migrated NK cells. **(C)** CXCR1/CXCR2 staining on NK cells that migrated towards slanMo CM with a neutralizaing antibody against IL-8 or respective isotype control. **(D)** Mean fluorescence intensity (MFI) values for CXCR1 and CXCR2 FACS plots depicted in (C).

5.3 NK cells and slanMo together limit melanoma growth

5.3.1 Effect of conditioned medium treatment on melanoma cells

The TME heavily influences tumor cells, both through soluble factors and cellular interactions. We therefore investigated whether the cytokine milieu generated by slanMo and NK cells in a synergistic crosstalk affects melanoma cells. We incubated SK-Mel-28 melanoma cells for a period of 3-4 days with co-culture conditioned medium (CM), which was harvested from previous co-cultures of R848-stimulated slanMo and NK cells. After this culture in CM, the melanoma cells were harvested and cultured at equivalent cell numbers in normal medium (Fig. 5.7 A). We observed that melanoma cells initially exposed to co-culture CM stopped proliferating and remained in a growth arrest, whereas control cells grew exponentially (Fig. 5.7 B, left graph). In contrast, incubation with slanMo or NK cell mono-culture conditioned medium (slanMo CM or NK cell CM) had only minor or no influence on cell growth, respectively, showing that the observed growth arrest is slanMo/NK cell crosstalk dependent (Fig. 5.7 B).

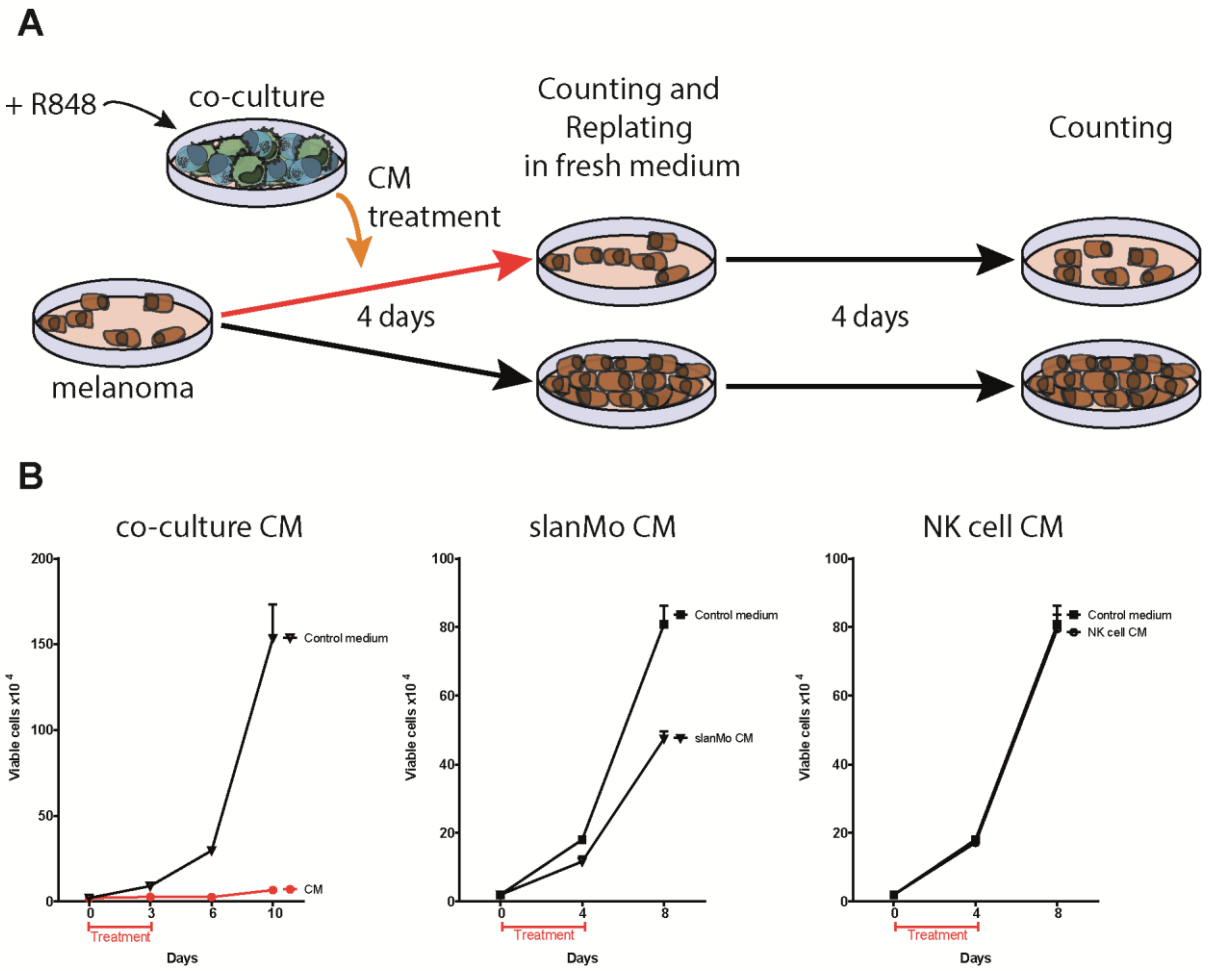

Figure 5.7 - R848-stimulated co-culture CM arrests melanoma growth. (A) Scheme for melanoma cell CM treatment. **(B)** Treatment of SK-Mel-28 with conditioned medium (CM) from different sources, including CM harvested from slanMo/NK cell co-cultures (co-culture CM), slanMo mono-cultures (slanMo CM), and NK cell mono-cultures (NK cell CM), all stimulated with 1 µg/ml R848.

5.3.2 Identification of factors that induce a melanoma growth arrest

In order to identify the factors in the slanMo/NK cell CM that inhibit melanoma growth, we studied its cytokine content by multiplex analysis. To further shed light on the contribution of these cells in the TME, we also included other immune cell mono- and co-cultures, including $CD14^+$ monocytes as slanMo replacements and T cells as NK cell replacements. We found that R848- and LPS-stimulated slanMo strongly upregulate TNF-α, IL-1β, and IL-12. Furthermore, the slanMo cultures and the slanMo/NK cell co-cultures were characterized by high TNF-α, IFN-γ, and IL-12p70 levels compared to $CD14^+$ monocyte ($CD14^+$ Mo) cultures and $CD14^+$ Mo/NK cell co-cultures (Fig. 5.8 A). Interestingly, the slanMo/NK cell co-culture yielded higher levels of IFN-γ, TNF-α, and IL-12p70 compared to slanMo/T cell as well as $CD14^+$ Mo/T cell co-cultures, highlighting the pro-inflammatory cytokine production of the slanMo/NK cell crosstalk. In contrast, NK cells or T cells alone produced only negligible cytokine concentrations compared to slanMo and $CD14^+$ Mo (Fig. 5.8 B).

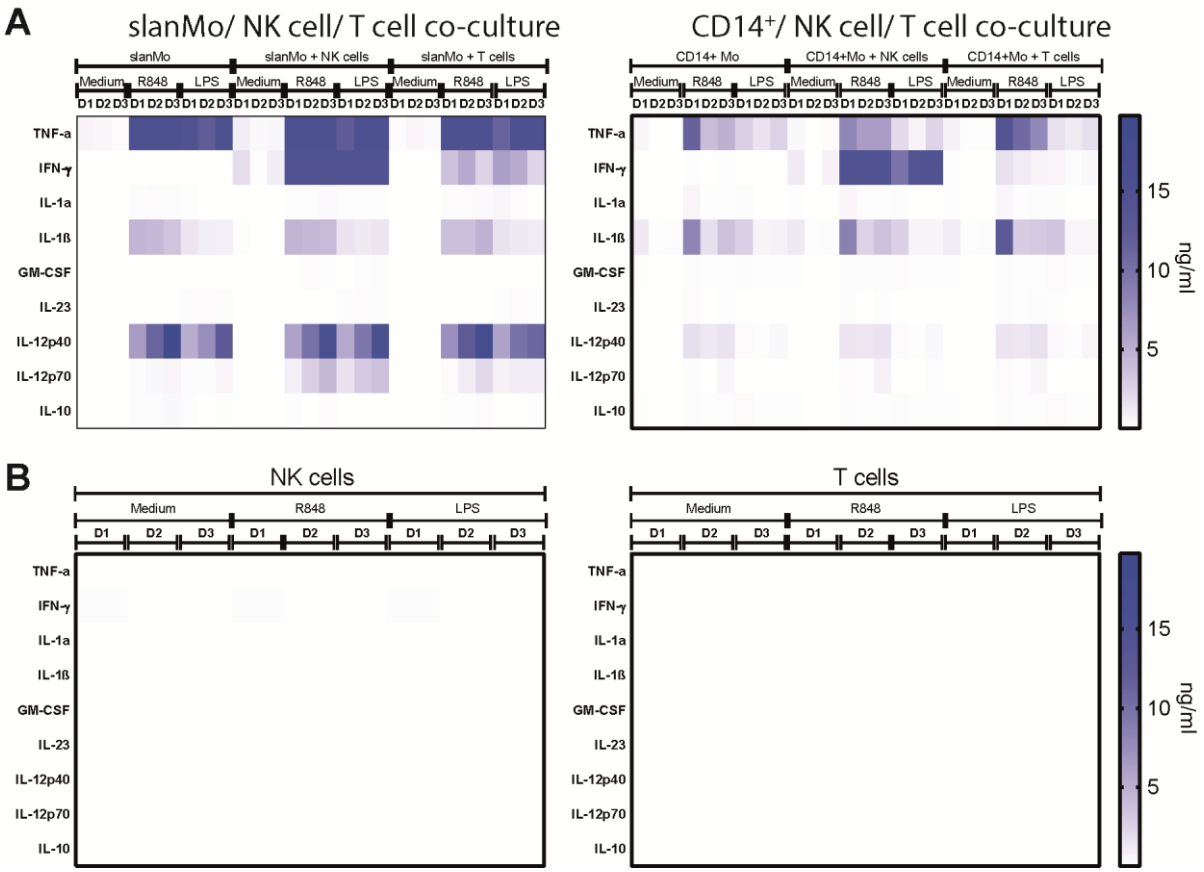

Figure 5.8 – Analysis of the cytokine production of slanMo and CD14+ Mo cultured alone or in combination with NK cells or T cells. Different combinations of co-cultures and individual respective mono-cultures were cultured for 24 h, before cell-free supernatants were harvested. All cultured were stimulated 6 hours after seeding either with 1 µg/ml R848, 100 ng/ml LPS, or left unstimulated. Protein levels were measured by multiplex analysis based on labeled beads binding to the analytes in the supernatant.

As TNF-α and IFN-γ were expressed at particularly high levels in TLR-activated slanMo/NK cell co-cultures, we hypothesized that these cytokines are the major factors mediating the strong growth inhibition effect observed with the co-culture but not mono-culture CM. When we incubated melanoma cells with recombinant TNF-α + IFN-γ, this efficiently reduced cell numbers over several passages in different melanoma cell lines, including SK-Mel-28, Ma-Mel-86b, SK-Mel-25, and SK-Mel-30 (Fig. 5.9 A). In order to demonstrate whether TNF-α and IFN-γ as major constituents of the co-culture CM mediated the CM treatment growth arrest, we added TNF-α + IFN-γ neutralizing antibodies to the initial melanoma culture. Therefore, we established an experimental protocol for SK-Mel-28 with a total culture time of 8 days and a medium exchange after 4 days (Fig. 5.9 B). Neutralization of TNF-α and IFN-γ completely abolished the growth arrest and almost restored exponential growth (Fig. 5.9 C). Interestingly, the CM induced growth inhibition was even more pronounced than with recombinant cytokines (Fig. 5.9 C), suggesting that the median concentrations in the CM exceed the experimental concentrations (10 ng/ml TNF-α and 100 ng/ml IFN-γ) or that other factors secreted by the slanMo/NK cell crosstalk exacerbate the inhibition.

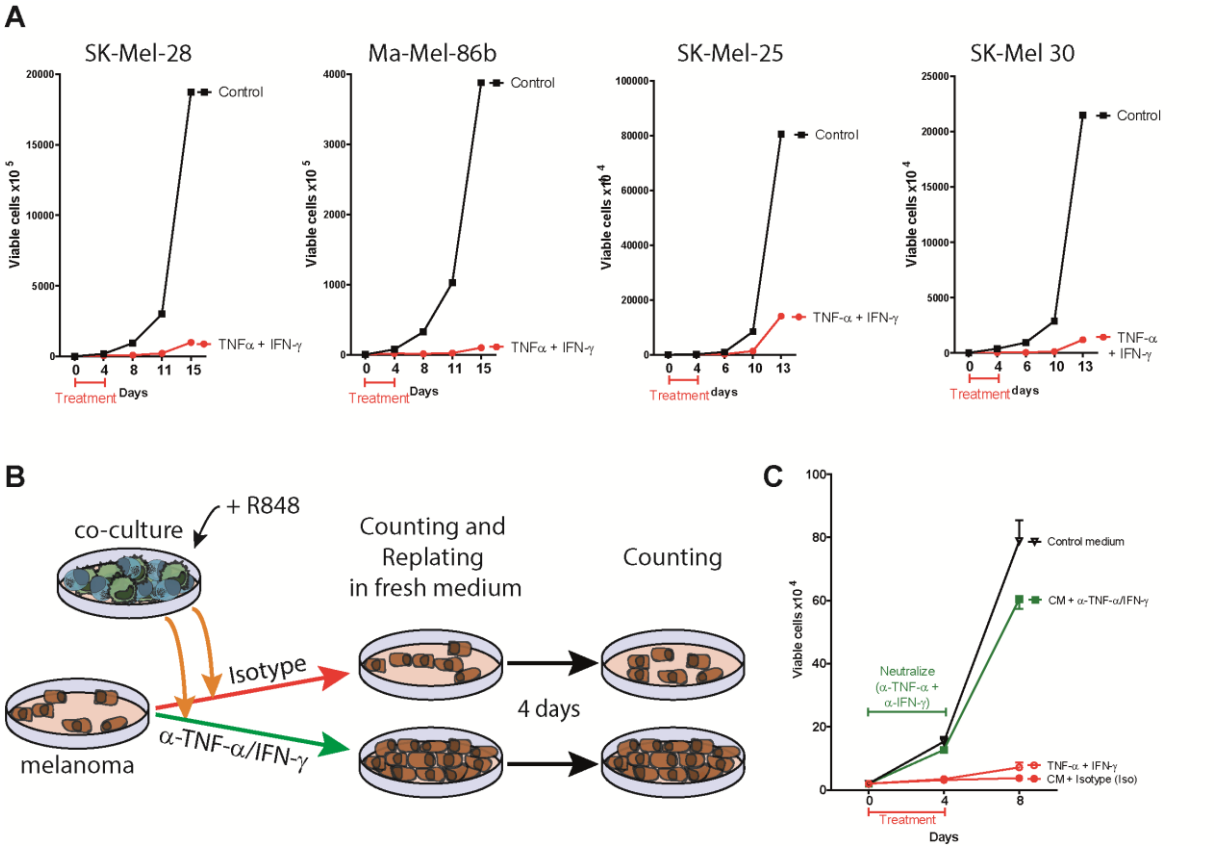

Figure 5.9 – TNF-α and IFN-γ expressed by slanMo and NK cells induce a melanoma cell growth arrest. (A) The melanoma cell lines SK-Mel-28, Ma-Mel-86b, SK-Mel-25, and SK-Mel-30 were cultured in medium containing recombinant TNF-α and IFN-γ (10 ng/ml and 100 ng/ml, respectively). After 4 days, the cells were seeded in fresh medium and cultured for additional three passages. **(B)** Schematic illustrating the experimental procedure for cell growth cytokine neutralization culture assays. **(C)** SK-Mel-28 melanoma cells were cultured for 4 days in diluted co-culture CM together with neutralizing antibodies against TNF-α and IFN-γ or respective isotype controls. After 4 days of culture, cells were counted and reseeded in fresh medium for prolonged culture, before repeated counting after 8 days of total culture time.

5.3.3 Analysis of proliferative markers in growth arrested melanoma cells

Based on the consistent growth arrest induced by co-culture CM treatment, we were interested in quantifying alterations in melanoma cell proliferation. Therefore, we performed Ki67 immunofluorescence staining on CM-treated SK-Mel-28 cells reseeded on microscopic glass slides (Fig. 5.10 A). Consistent with slower cell growth displayed in growth curves, the percentage of Ki67 positive cells was reduced by ~40 % when the cells were cultured in CM (Fig. 5.10 B). The same trend was observed when using recombinant TNF-α and IFN-γ (Fig. 5.10 C). Similar to previous neutralization experiments, addition of anti-TNF-α/IFN-γ antibodies restored normal proliferation (Fig. 5.10 B).

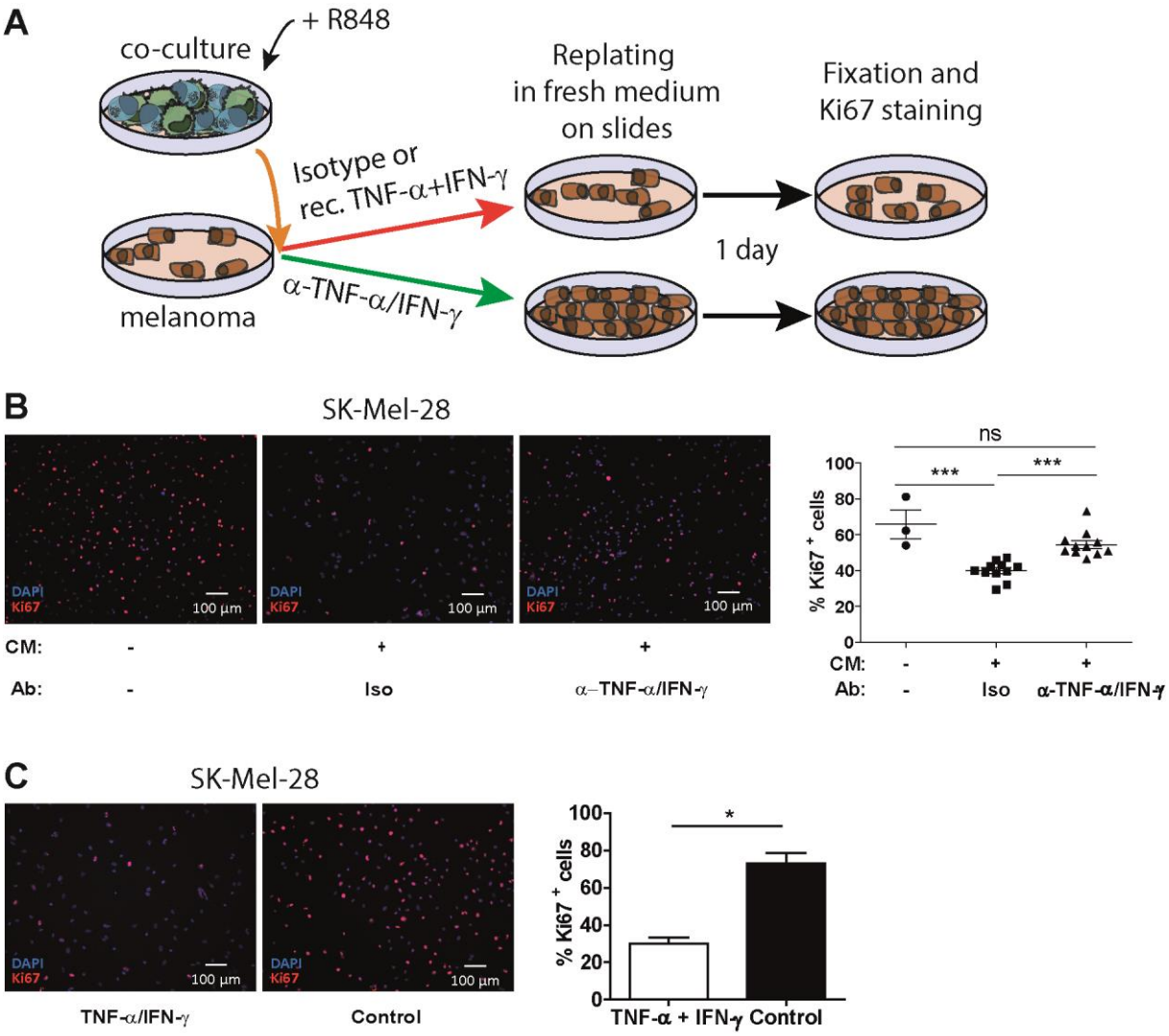

Figure 5.10 – CM treatment reduces the fraction of Ki67-positive cells. (A) Illustration of SK-Mel-28 treatment for Ki67 IF staining. **(B)** Representative images of Ki67 IF staining on SK-Mel-28 cells grown on microscopic glass slides and pre-treated with CM and neutralization against TNF-α and IFN-γ as depicted in (A). Positive cells were quantified using Fiji and a fluorescence intensity threshold combined with a minimal particle size. Results are depicted in the right graph. **(C)** SK-Mel-28 cells were treated with recombinant TNF-α and IFN-γ (10 ng/ml and 100 ng/ml, respectively) before Ki67 IF staining and quantification as described in (B).

We corroborated these results with ^{3}H-Thymidine incorporation as another method to quantify proliferation. Therefore, we applied standard CM treatment with TNF-α/IFN-γ neutralization, after which the cells were pulsed for 12 hours prior to measurement (Fig. 5.11 A). This resulted in significantly reduced proliferation after co-culture CM treatment, which was successfully prevented by TNF-α/IFN-γ neutralization (Fig. 5.11 B). In contrast, mono-culture CM from slanMo or NK cells was not sufficient to limit proliferation (Fig. 5.11 C). Analogous to cytokine neutralization, addition of recombinant TNF-α + IFN-γ efficiently reduced proliferation in several melanoma cell lines (Fig. 5.11 D). In summary, this demonstrates that TNF-α and IFN-γ directly affect melanoma cells by reducing the fraction of proliferating cells.

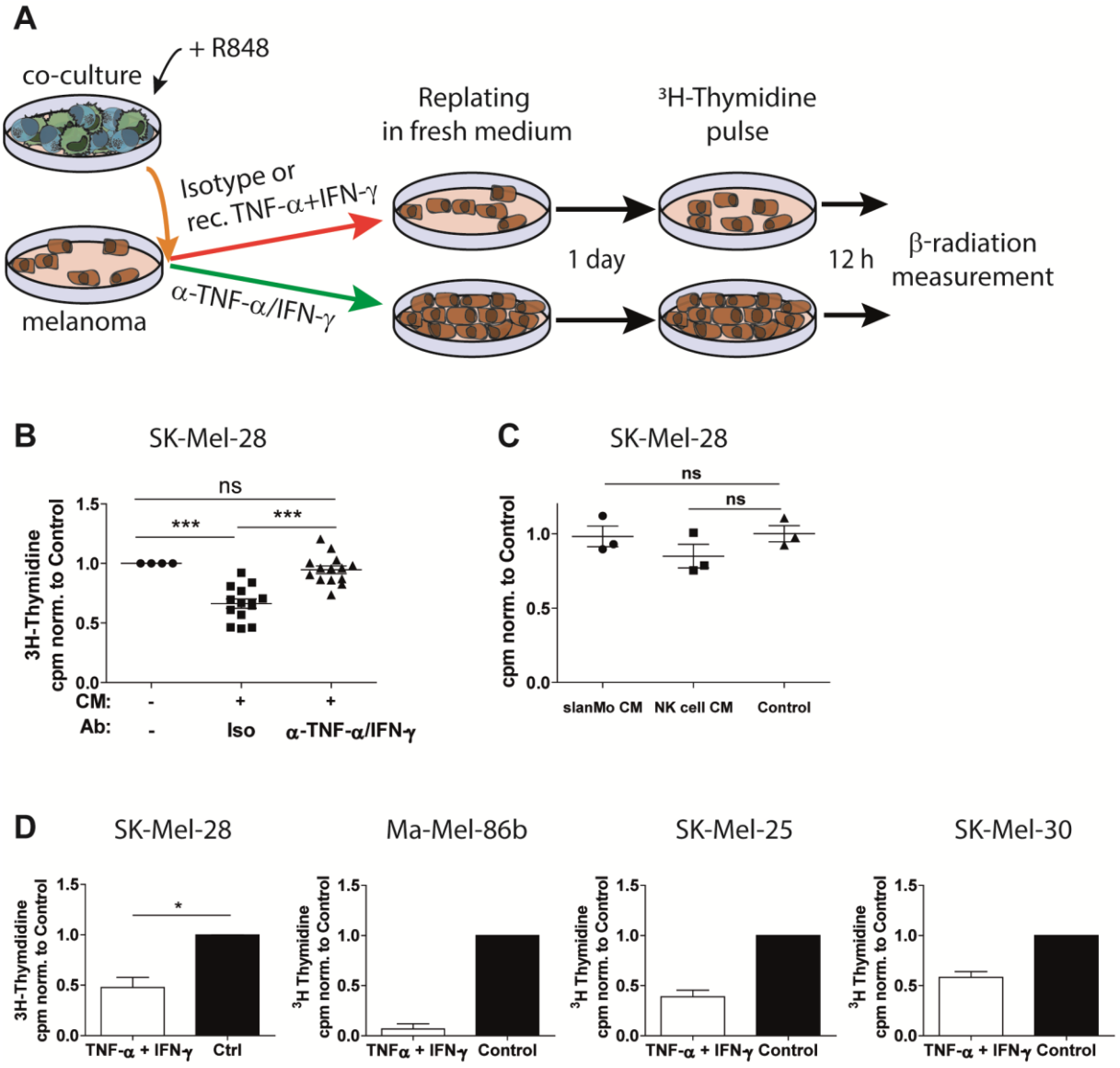

Figure 5.11 – CM treatment reduces melanoma cell proliferation. (A) Illustration of melanoma cell treatment protocol for ^{3}H-Thymidine incorporation assay. SK-Mel-28 cells were treated with **(B)** R848-stimulated co-culture CM + TNF-α/IFN-γ neutralization as described in (A) or with **(C)** R848-stimulated slanMo or NK cell mono-culture CM and pulsed for 12 h with ^{3}H-Thymidine. β-radiation counts were normalized to control values. **(D)** Different melanoma cell lines were treated with recombinant TNF-α and IFN-γ (10 ng/ml and 100 ng/ml, respectively) and ^{3}H-Thymidine incorporation was measured after a 12 h pulse.

5.4 Growth arrested melanoma cells exhibit a senescence phenotype

5.4.1 Kinetics of cytokine-induced melanoma cell growth arrest

In order to further characterize the phenotype of the CM-mediated growth arrest, we placed SK-Mel-28 cells during the 4 days treatment phase in a culture device that repeatedly acquires images and thereby allows to monitor morphological changes and confluence analysis. When we analyzed tumor growth, we observed a higher frequency of Annexin V positive apoptotic cells in the CM and recombinant TNF-α + IFN-γ condition in comparison to control medium and TNF-α and IFN-γ neutralization, which might explain a partial drop in proliferating cells (Fig. 5.12 A). For both CM and recombinant cytokine treatment, we observed slower cell growth and cultures only reached ~ 60 % confluence, in contrast to confluent cell densities in medium control and TNF-α/IFN-γ neutralization conditions (Fig. 5.12 A, B). Additionally, we observed that CM treatment changed cell morphology and resulted in the accumulation of an enlarged and flattened SK-Mel-28 population that often appeared multinucleated (Fig. 5.12 A inlet). Those morphological features are reminiscent of a senescence phenotype, which is often characterized by the same morphological characteristics. This observation offers an additional explanation for the reduced cell growth, as the accumulation of senescent cells in our cultures induced by TNF-α + IFN-γ would reduce the fraction of proliferating cells and thereby mimic limited overall proliferation.

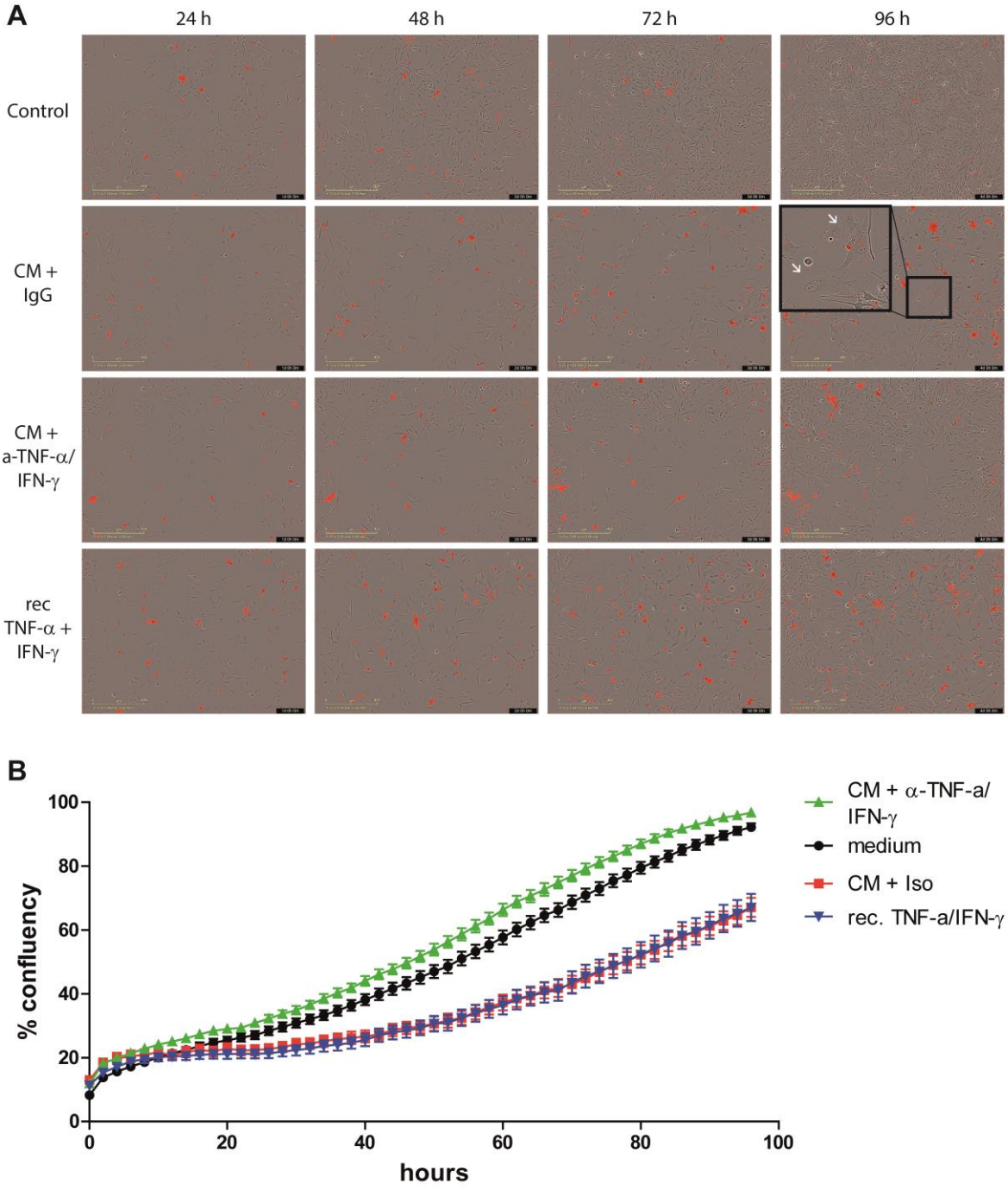

Figure 5.12 – CM treatment affects melanoma viability and cell morphology. (A) SK-Mel-28 cells were treated with co-culture CM (CM) + TNF-α/IFN-γ neutralization or recombinant TNF-α/IFN-γ as described before. Cell growth was visualized over a culture period of 4 days in a IncuCyte® live cell analysis system and images were taken every 2 hours with 100x magnification. An AnnexinV red antibody was included in the culture to visualize apoptotic cells. Representative images after 24h, 48 h, 72 h, and 96 h are depicted. **(B)** The confluency over time was analyzed by the IncuCyte® Software for all conditions.

5.4.2 Evaluation of senescence-associated β-galactosidase staining

For demonstrating senescence as a growth inhibiting mechanism in our cultures, we tested whether CM treatment induced the expression of senescence-associated β-galactosidase (SA β-gal) in SK-Mel-28 cells. SA β-Gal is a common marker for senescent cells that can be visualized at pH 6 through its activity to metabolize X-Galactosidase, which ultimately results in a green staining inside senescent cells. To this end, we performed CM treatment and reseeded the cells in normal medium for 1 day prior to fixation and SA β-gal staining (Fig. 5.13 A). We found that SA β-gal positivity increased significantly with CM treatment (Fig. 5.13 B). Importantly, TNF-α/IFN-γ neutralization effectively reduced the percentage of positive cells, showing that those cytokines are responsible for the observed effect (Fig. 5.13 B). When we used mono-culture CM from slanMo, we observed slightly increased SA β-gal positive cells, however strikingly less pronounced than for co-culture CM (Fig. 5.13 C). In contrast, NK cell CM showed no effect (Fig. 5.13 C). As TNF-α and IFN-γ neutralization significantly reduced SA β-gal staining, we were expecting and could demonstrate that addition of recombinant TNF-α + IFN-γ resulted in higher cell numbers positive for SA β-Gal (Fig. 5.13 D). This suggests that the cytokine cocktail generated from co-culturing slanMo and NK cells contains high amounts of TNF-α and IFN-γ that can lead to senescence in melanoma cells.

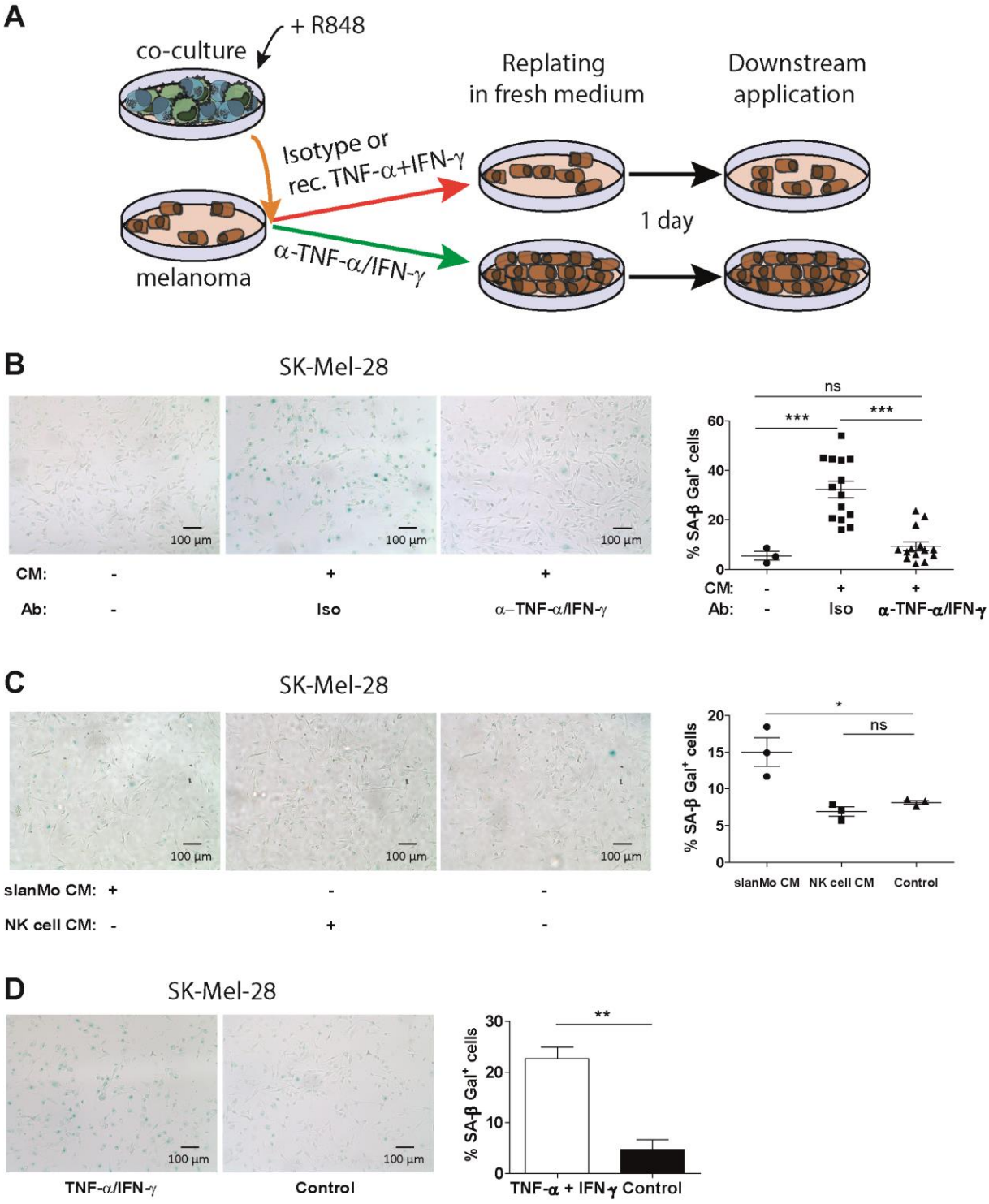

Figure 5.13 – SA β-Galactosidase is upregulated after CM treatment. **(A)** Schematic depicting the protocol for SK-Mel-28 treatment. **(B)** SK-Mel-28 cells were treated with CM + TNF-α/IFN-γ neutralization as described in (A) and cells were stained for SA β-Galactosidase (SA β-Gal) over night. SA β-Gal positive cells were quantified with Fiji and percentages are displayed on the right. SK-Mel-28 cells were treated with **(C)** R848-stimulated slanMo or NK cell mono-culture CM or with **(D)** recombinant TNF-α + IFN-γ, stained for SA β-Gal, and quantified as described in (B).

5.4.3 Molecular markers of cytokine-induced melanoma cell senescence

In order to substantiate the senescent phenotype observed for SK-Mel-28, we analyzed expression of p21 (CDKN1A) as a downstream target of p53 (tp53) in the p53 senescence pathway. Treating SK-Mel-28 with CM significantly upregulated p21 expression, as visualized by Western Blot and densitometric quantification (Fig. 5.14 A). TNF-α and IFN-γ neutralization was able to normalize p21 levels (Fig. 5.14 A). Additionally, recombinant TNF-α + IFN-γ induced p21 expression in SK-Mel-28, Ma-Mel-86b, SK-Mel-25, and SK-Mel-30 (Fig. 5.14 B), indicating that p21 represents a more common regulator of non-proliferative, senescence states in melanoma cells.

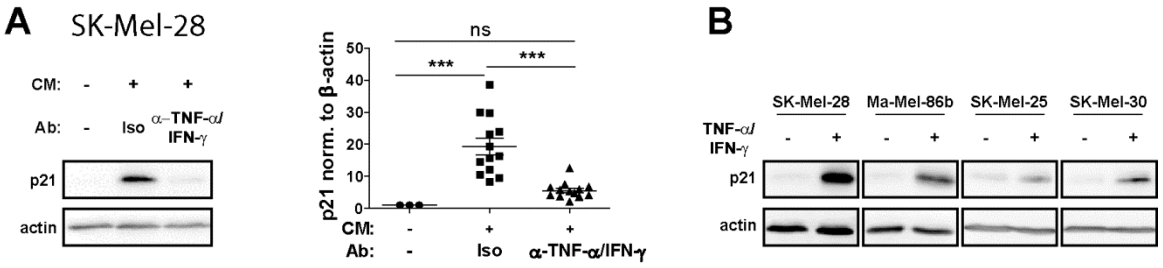

Figure 5.14 – Western Blot analysis of p21 expression after CM and TNFα + IFN-γ treatment. (A) SK-Mel-28 cells were treated as described in Figure 5.13 (A) with CM + TNF-α/IFN-γ neutralization. After 4 days culture, the cells were lysed and lysates were analyzed for p21 in Western Blot (WB). WB was performed by blotting proteins separated via SDS page onto a nitrocellulose membrane and incubating the mebrane with an anti-p21 antibody overnight. Band intensity was quantified by using Fiji and was normalized to β-actin measured on the same sample. Graph depicting normalized band intensity values is shown on the right. **(B)** Different melanoma cell lines were treated as described in Figure 5.13 (A) with recombinant TNF-α + IFN-γ and WB for p21 was performed as stated in (A).

As p21 is localized in the nucleus where it modulates cell cycle progression, we were interested whether we also observe nuclear p21 accumulation under CM treatment conditions. Therefore, p21 was stained by immunofluorescence after fixation of CM-treated cells grown on microscopic slides. Consistent with western blot data, p21 increased after exposure to CM and TNF-α/IFN-γ neutralization reversed p21 positivity (Fig. 5.15 A). In line with this, recombinant TNF-α and IFN-γ strongly increased p21 positive cells (Fig. 5.15 B). In summary, these data demonstrate that the growth arrest observed in response to our crosstalk is a senescence state characterized by high p21 levels.

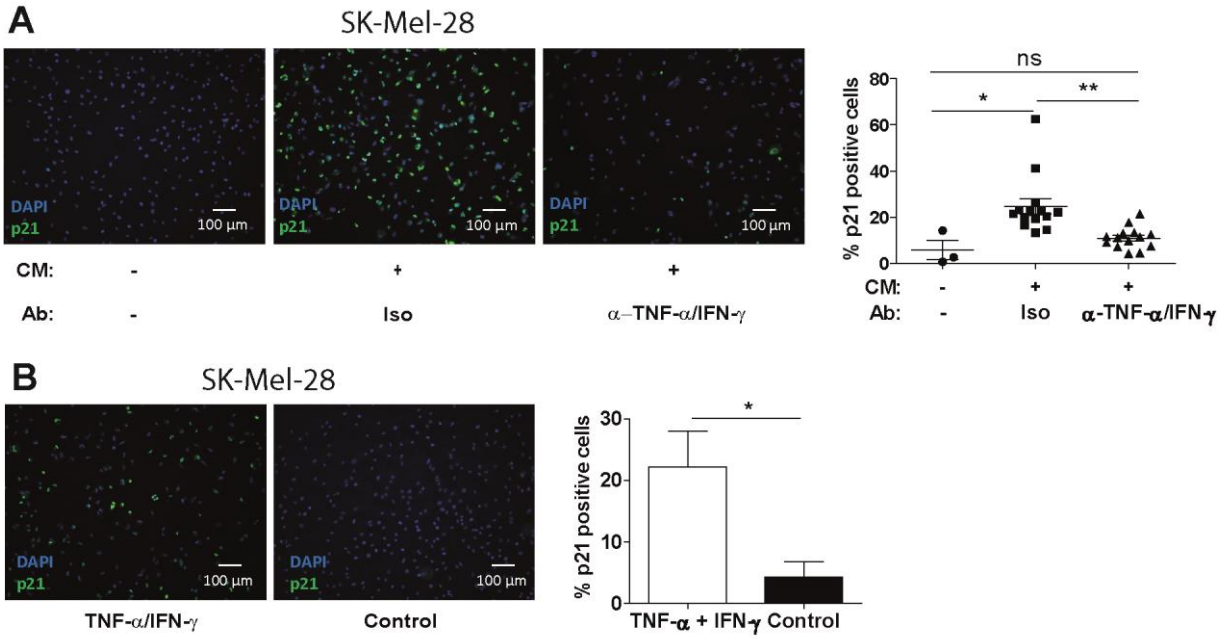

Figure 5.15 – p21 IF staining of CM and TNFα + IFN-γ treated melanoma cells. SK-Mel-28 cells were treated as described in Figure 5.10 (A) with **(A)** CM + TNF-α/IFN-γ neutralization or with **(B)** recombinant TNF-α + IFN-γ. 1 day after reseeding on microscopic glass slides, the cells were fixed and stained for p21 in IF. Positive cells were quantified as described in Figure 5.10.

5.4.4 Characterization of the senescence-associated secretory phenotype

Senescence induction is commonly associated with changes in the cellular secretome, termed senescence-associated secretory phenotype (SASP) [156]. In order to further characterize our observed senescence phenotype, we designed a panel of markers for qPCR analysis based on regularly affected genes reported in the literature [156, 157, 158]. After treatment with co-culture CM, increased expression of relevant SASP factors such as IL-6, IL-8, IL-1α, IL-1β was detected on mRNA level (Fig. 5.16 A). Other markers that were significantly upregulated included the matrix metalloproteinases (MMPs) 1, 2, 3, 9, the serpins PAI-1 and PAI-2, the chemokine family members CXCL1, CXCL2, CCL2 and CCL7, the growth factors TGF-β and VEGF-A, and the adhesion protein ICAM-1. Importantly, with the exception of CXCL1 and TGF-β, the increase in mRNA levels were prevented by TNF-α and IFN-γ neutralization for all markers.

Besides mRNA expression, we expanded the SASP analysis by measuring protein concentrations for IL-6, IL-8, IL-1α, and IL-1β in melanoma cell supernatants after CM treatment. In line with the mRNA results, IL-6, IL-8, and IL-1β were significantly upregulated after CM exposure, for IL-8 even above the maximal detection limit of the assay (Fig. 5.16 B). This effect was reversed or reduced when we added TNF-α/IFN-γ neutralizing antibodies

during the CM treatment. IL-1α was expressed at very low levels. However expression was still increased by the CM and reverted by neutralization.

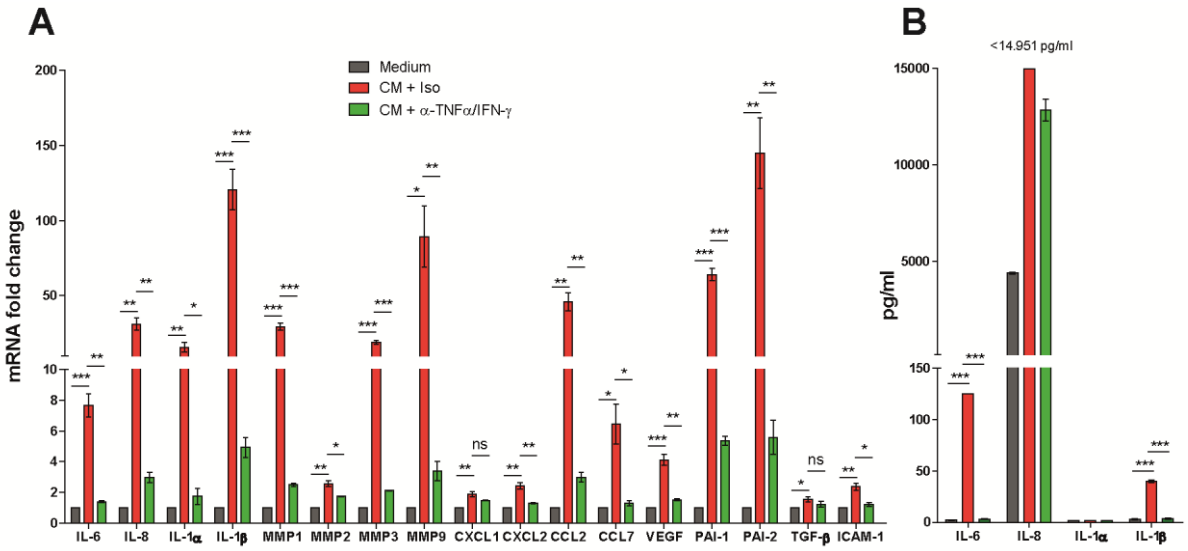

Figure 5.16 – mRNA and protein expression levels of a selected set of markers induced by CM treatment. (A) SK-Mel-28 cells were treated as described in Figure 5.13 (A) with CM + TNF-α/IFN-γ neutralization. After reseeding in fresh medium and an additional culture period of 2 days, the cells were lysed in Trizol and the expression of several genes on mRNA level was performed by qPCR. **(B)** SK-Mel-28 cells were treated as described in (A) and the cell-free supernatant was harvested prior to cell lysis for multiplex analysis of different soluble factors. For IL-8, concentrations reached the maximum threshold of the assay.

5.4.5 *In vivo* evidence for senescence in melanoma

Since we established a role for innate immunity in inducing a p21^{high} melanoma cell senescence in an elaborate *in vitro* system, we were now interested in whether we can also find evidence for this phenotype *in vivo*. Therefore, we stained FFPE melanoma samples for p21 in IHC. This resulted in a strong nuclear staining, which was absent in isotype controls (Fig. 5.17 A). In general, p21 staining was mostly restricted to melanoma cells, as morphologically different immune cells were predominantly p21 negative. However, only a fraction of melanoma cells was p21 positive and this was very donor dependent. Additionally, the staining intensity observed for p21 positive cells was not homogenous, instead we observed the presence of different melanoma cell populations ranging from absent p21 staining to weak and also very intense p21 expression.

In order to connect this to innate immunity, we co-stained p21 with slan. slan^{+} cells infiltrated p21 positive areas and were detected in close proximity to p21^{high} melanoma cells (Fig. 5.17 B, C). However, no further quantification of slan or CD56 accumulating within p21 positive melanomas was performed in this study.

With the detection of a p21^{high} expressing melanoma cell population *in vivo*, we strengthened the relevance of our finding that melanoma cells can develop a senescent state characterized by p21 overexpression.

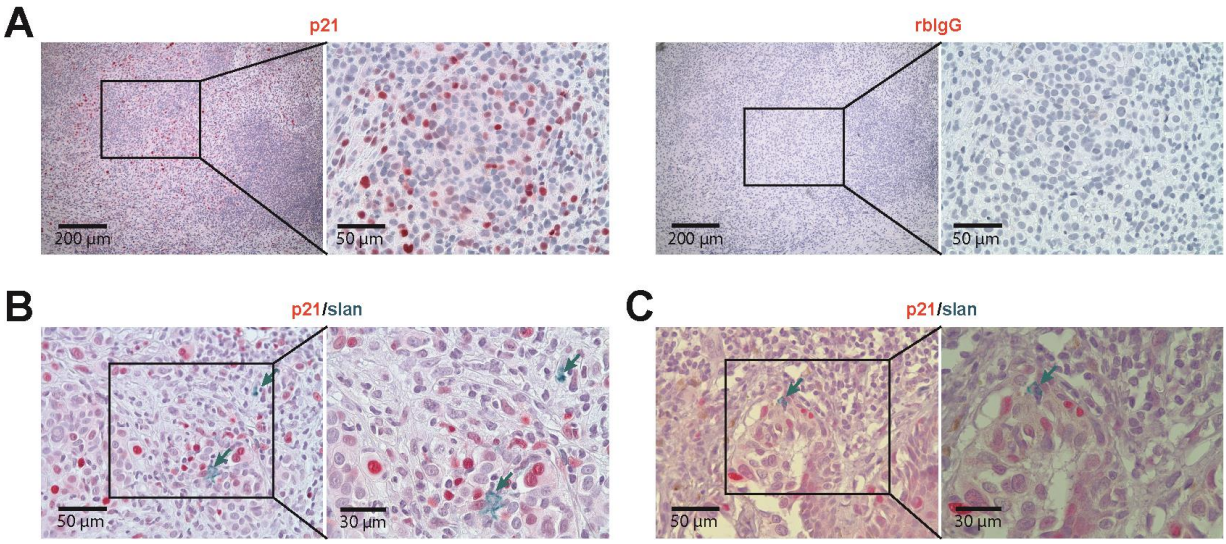

Figure 5.17 – p21 staining in melanoma patient samples. (A) FFPE samples from a stage II melanoma patient were stained with an anti-p21 antibody (left panel) and the respective rabbit IgG isotype control (right panel). Original magnification: 1st and 3rd image 100x, 2nd and 4th image 400x. **(B-C)** p21 was double-stained with slan in a stage II FFPE melanoma sample as described in the color code above. Original magnifications: left image 400x, right image 630x.

6 Discussion

6.1. slanMo and NK cells infiltrate malignant melanoma

6.1.1. Prognostive value of innate immune cell infiltration into tumors

The tumor immune microenvironment plays an important role in tumor growth, progression, and metastasis. As outlined by the concept of cancer immunosurveillance, tissues are constantly screened by immune cells not only for external threats such as pathogens, but also for the presence of malignant cancer cells. The process of malignant transformation is often accompanied by changes in the respective cells, i.e. the expression of neoantigens that enable T cell responses as well as the release of DAMPs and the upregulation of stress-induced ligands. Together, these mechanisms form the foundation for anti-tumor immune responses. NK cells at the site of initial tumor formation recognize transformed cells and lysis of individual tumor cells triggers inflammatory processes. DCs internalize tumor antigens and migrate to lymph nodes in order to prime antigen specific T cells. During the priming and affinity maturation phase required for adaptive immunity, phagocytes control proliferating tumor cells. Finally, expanded tumor-specific T cells eliminate the tumor before metastases can arise.

As outlined in 3.1.5, the process described above represents only the first stage of tumor immunology and is often followed by a relapse mediated by different escape mechanisms. It is assumed that the effectiveness of anti-tumor immune responses highly depends on the local immune TME, especially under checkpoint inhibitor therapy. Various recent reports have addressed the issue of deciphering the prognostive value of the immune cell microenvironment both in murine cancer models as well as in patient tumors [42, 43, 44, 159, 160, 161, 162, 163, 164]. Typically, most analysis focus on characterizing T cells in the TME with regard to activation and exhaustion markers, as well as for the presence of antigen-specific T cell clones [44, 48]. However, also innate immune cell populations numerously infiltrate melanoma and other tumor entitites. Our histological analysis revealed a strong infiltration of slanMo in early stages of cutaneous melanoma, followed by increased numbers of NK cells in stage III cutaneous lesions and lymph node metastasis (Fig. 5.3). NK cell infiltration in stage III melanoma was furthermore accompanied by a significant correlation with slanMo infiltration. A recent bioinformatic study utilized expression signatures to delineate the relationship between specific leukocyte subset and the survival outcomes of patients [42]. They described

various markers and associated immune cell populations that correlate with favorable or adverse effects over 39 malignancies including solid cancers and blood cancers. Interestingly, a rare innate immune cell population was associated with the best prognosis over all tumor entities: γδ T cells. The most favorable prognostic gene discovered in the analysis was KLRB1 (CD161), which is found on T cell subsets and NK cells [165]. Another factor of positive prognosis were plasma cells (PCs), suggesting a potential relevance for tumor-specific antibody responses. Similarly, yet to a lesser extent, NK cells were associated with favorable outcome in solid cancers. Interestingly, NK cell and PC signatures correlated with regard to positive outcome, arguing for a role of NK cell ADCC in supporting PC-enabled antibody-mediated anti-tumor responses. This would be line with the general concept of tumor-specific antibodies that function via engagement of NK cells and tumor clearance via ADCC [166].

Apart from broad-scale transcriptomic analysis, NK cells can also be detected by alternative methods in tumors, such as histology and flow cytometry. NK cells were previously described to be rather absent from primary tumors but to exert anti-metastastatic functions in tumor-draining lymph nodes [111, 113, 167, 168, 169]. In this regard, our results that demonstrated NK cell infiltration in advanced stage cutaneous melanoma inspire more detailed investigation of the mechanisms and modulation possibilities of NK cell infiltration into solid tumors. However, it needs to be considered that NK cells are often dysfunctional in tumor tissues. In this regard, NK cells are reported to be associated with a worse outcome in hepatocellular carcinoma [170]. Similarly, Carrega *et al.* and Platonova *et al.* showed severly reduced cytotoxic capabilities of intratumoral NK cells in non-small cell lung cancer patients [103, 171]. Besides inactivity due to exhaustion in tissues, Balsamo *et al.* suggested that melanoma cells acquire resistence to NK cell mediated killing under conditions that mirror NK cell to tumor cell ratios in the TME. The authors argued for increased HLA I expression as well as NKG2D ligand downregulation as resistence mechanisms for this phenotype [172]. Furthermore, NK cells are reported to execute pro-tumorigenic functions by facilitating tumor cell epithelial to mesenchymal transistion (EMT), which can support metastasis formation [173]. On the other hand, EMT can increase susceptibility to NK cell lysis, thereby reducing metastatic efficacy [174]. Together, this argues for a potential mechanism where NK cells modulate the phenotype of tumor cells in a direction that facilitates subsequent elimination. Our data are not offering a prognostic follow-up or a description of the activation status of NK cells *in situ*. It is therefore difficult to judge the effectiveness of NK cells infiltrating in late stage cutaneous melanoma. Regardless, elucidation of the conditions and specific chemokines that guide NK cells to tumors are of high interest. Mechanistic insights open up avenues for recruiting NK cells to newly formed tumors or metastasis, where they can exert their widely accepted anti-metastatic potential.

NK cells are defined by several genes that identify their cellular origin and can therefore be studied in broad-scale transcriptomic analyses. The diversity of monocytes and macrophages however often cannot be studied adequately. In particular the subset of non-classical monocytes, that also encompasses slanMo, is usually neglected due to a lack of precise gene signatures robustly identifying these cells in tissues. This hampers the broad-scale transcriptomic investigation of monocyte subsets in tumors. Since also the specific marker slan merely represents a carbohydrate modification not exclusively related to a single gene, quantification of slanMo in tumors relies on histological stainings. We observed a high density of slanMo, particularly in stage I melanoma, which cannot be considered a homeostatic cutaneous condition, since healthy skin was virtually devoid of slanMo. These results extend previous reports that have described high numbers of slanMo in metastatic tumor-draining lymph nodes of carcinoma patients but absence of slanMo in the primary tumor [73] . Increased slanMo cell numbers in early melanoma development suggests immediate recruitment to the tumor site. This is in line with the reported patrolling function of human slanMo as a sub-group of non-classical monocytes [59, 175]. Constant monitoring for vascular damage allows slanMo to immediately sense any disturbances in the endothelial composition that are triggered by tumor initiation. Recently, Headley *et al.* visualized and quantified the arrival of phagocytic immune cells immediately after generation of micrometastastes in the lung [176]. They found that patrolling monocytes arrive very rapidly and concomitant with neutrophils and classical monocytes, despite in lower frequencies compared to neutrophils and classical monocytes. Importantly, patrolling monocytes remained in the vicinity of tumor sites for a prolonged time, which was not observed for neutrophils and classical monocytes.

In the TME, monocytes can develop into polarized macrophages, either resembling anti-tumorigenic M1 or pro-tumorigenic M2 macrophages [54, 55]. The attempt to translate this phenotypic discrimination to slanMo in tissues is difficult due to the fact that no mouse homolog exists that would permit functional studies. However, slanMo in tissues were previously described as TNF-α producing [66, 73, 75, 177], CD68 positive [58, 73], IL-23 positive [65], iNOS positive [65], and actively phagocytosing [72], suggesting the tendency to develop an anti-tumor M1 phenotype after leaving the circulation [178]. In accordance with this hypothesis, a recent report suggested the coexistence of two separate slanMo tissue phenotypes; a macrophage-like $CD163^{hi}/CD14^{hi}/CD64^{hi}/CD16^{hi}$ phenotype and a DC-like $CD163^{low}/CD14^{low}/CD64^{low}/CD16^{low}$ phenotype [72]. Interestingly, we observed the presence of two morphologically distinct slanMo populations in the melanoma biopsies. In line with the study by Vermi *et al.*, DD2 stained round, monocytic cells inside or in the vicinity of vessels, arguing for ongoing or recent transmigration. Alternatively, DD2 stained cells displaying macrophage features or dendritic-like cells (Fig. 5.1) [72]. Our histological stainings lacked

functional markers such as TNF-α or IL-12, which precludes a characterization of the *in situ* slanMo activation status. However, our *in vitro* and the previously mentioned preferential M1 macrophage polarization in tissues suggests also a high inflammatory potential in the melanoma microenvironment.

Interestingly, the correlation of slanMo and NK cell numbers may suggest linked migratory mechanisms. Furthermore, when also considering the differential infiltration pattern in stage I and II melanoma, this argues for a hypothesis that slanMo, after becoming fully activated in the advanced stage TME, aid in NK cell recruitment. However, since we were not normalizing the numbers of slanMo and NK cells to the total immune cell infiltrate, it is so far difficult to assess whether the correlation is specific for slanMo and NK cells or mirrors increased overall leukocyte infiltration.

6.1.2. Chemokine production by slanMo

In an attempt to identify the mechanisms behind the correlated slanMo and NK cell infiltration, we pursued the hypothesis that slanMo, present in high levels in early tumor development, might account for the increasing levels of NK cells in stage III. Besides low to intermediate level CCL3 and CCL4 expression, we found that slanMo are prominent producers of IL-8 with intermediate steady state scretion and strongly elevated expression after R848-stimulation (Fig. 5.4 B, C). This is in contrast to previous studies that reported only minor IL-8 as well as CCL3 production [59, 69]. However, these studies were not adhering to a 6 h maturation phase before stimulation by TLR ligands, which is important for achieving efficient slanMo cytokine production. IL-8 binds to the receptors CXCR1 and CXCR2, mostly expressed on neutrophils, monocytes, NK cells and CD8 T cells. Neutrophils are often considered tumor promoting, which is why IL-8 is repeatedly associated with tumor progression [179, 180, 181]. Additionally, IL-8 is reported to represent a major melanoma-derived factor in the TME, suggesting that IL-8 potentially has direct pro-tumorigenic effects [182, 183] or that IL-8 modulates the immune composition towards a immunosuppressive bias by recruitment of MDSCs [184, 185]. However, since CXCR1 and CXCR2 are also expressed by other immune cell subsets typically associated with a positive outcome, such as CD8 T cells and NK cells [42], it can be assumed that IL-8 additionally exerts positive functions in the TME. Nevertheless, it will be challenging to dissect the positive from the negative effects and to find therapies to manipulate the system.

6.1.3. Recruitment of NK cells to the TME

We were able to demonstrate IL-8 dependent migration of NK cells towards activated slanMo supernatants, demonstrating that IL-8 can also exert positive functions in the TME by recruitment of cytotoxic NK cells. Our results are consistent with the current literature, where it is reported that NK cells express CXCR1 and CXCR2 coupled to the ability to migrate towards the chemokine IL-8 derived from different sources, i.e. dendritic cells [105, 186]. Besides IL-8, CCL3 and CCL4 were also present in slanMo supernatants, yet in lower concentrations. Despite reports that state expression of CCR5 on $CD56^{bright}$ NK cells [105], we consistently detected only around 1 % of NK cells expressing CCR5 (data not shown) and migrating towards CCL3 or CCL4 (Fig. 5.4 E). Accordingly, blocking experiments using anti-human CCR5 neutralizing antibodies showed only a marginal reduction in migrated NK cells (Fig. 5.5 C). Together with successful inhibition of NK cell migration with IL-8 neutralization, this demonstrates the instrumental role of IL-8 in the slanMo – NK cell migratory axis. We corroborated the receptor-ligand interaction by analysis of migrated cells, revealing that exposure to the slanMo CM completely removes the receptors from the cell surface. This can be explained by receptor internalization as a result of CXCR1 and CXCR2 signaling in NK cells, which subsequently leads to receptor internalization [154, 155, 187, 188]. However, it needs to be demonstrated that the presence of chemotactic factors suffices for active NK cell infiltration into melanoma, since another report states that NK cells are absent from colorectal cancer despite ample expression of chemokine ligands in the tissue [189]. Nevertheless, the discovery of novel potential innate migration axis is highly relevant for the understanding and initiation of immune responses in tissues. In addition, this recruitment hierarchy could further be expanded by the results recently published by Böttcher *et al.* [190]*.* Using a melanoma mouse model, they demonstrated that tumor infiltrating NK cells can recruit cDC1 via XCL1 and CCL5. Infiltrated cDC1 then aid in initiating adaptive immune responses through recruitment and priming of T cells. In this line of thought, our results argue for a mechanism in which slanMo extravasate at the site of newly formed tumors or metastasis and recruit NK cells to facilitate influx of cDC1.

6.2. The slanMo/NK cell crosstalk induces melanoma cell senescence

The role of cellular senescence in tumorigenesis and tumor progression is still a topic of debate. While it is widely accepted that senescence is a major tumor suppressor mechanisms preventing cell cycling after mutagenesis, the function and the associated prognostic relevance of senescence in fully established tumors is controversial. For one, it is

unclear whether senescence represents a ultimately irreversible proliferation stop. Similar to senescence, tumor dormancy, as it is described during the equilibrium phase (3.1.5.2), is potentially characterized by a low proliferative status of the tumor [30]. Interestingly, this would be in line with the hypothesis that senescence, besides representing a tumor suppressor mechanism, can facilitate immune escape through maintenance of individual, temporarily non-cycling tumor clones.

6.2.1. Comparison of different immune cell cytokine profiles

The tumor immune microenvironment affects many areas of tumor growth, progression, and metastasis [191]. Many questions arise when trying to model immune interactions in the TME: What immune cells are present? Which type of immune cells co-localize? How is the interaction taking place? And what is the prognostic value of this immune crosstalk? Studies often rely on histological analysis when trying to pursue these questions, since only histological staining combines single-cell identification with spatial information. In line with previous reports, we observed co-localization of slanMo and $CD56^+$ NK cells in tumor-draining lymph nodes of stage III melanoma patients [73]. This led us to further characterize the slanMo and NK cell crosstalk with regard to their cytokine profile. Cytokines and their effects on tumor cells are believed to play a important role in the TME. Similar to the ramifications different immune compositions account for, the effects that different cytokine milieus can exert are discussed controversially. For example, while IFN-γ is reported to represent a gene that is essential for cancer immunotherapy and tumor clearance [192], there are also studies suggesting a contribution to immunoevasion and cancer progression [193].

Consistent with previous reports, we found that the slanMo/NK cell crosstalk excels at producing the proinflammatory cytokines TNF-α, IFN-γ, and IL-12, after stimulation with TLR ligands. In contrast, NK cell mono-cultures were not producing meaningful amounts of any of the cytokines tested, regardless of TLR-activation. This is not unexpected, since NK cells are typically activated by other means such as pro-inflammatory cytokines or stress-induced ligands, whereas studies on the potency of TLR activation in NK cells are still not providing unambiguous results [194]. On the other hand, slanMo are known for high TLR expression, which is why we observed similar TNF-α levels after TLR stimulation irrespective of mono- or co-culture setup [65, 66]. To be able to put this into context with the TME, we included $CD14^+$ monocytes and T cells in our experiments. Surprisingly, the slanMo/NK cell crosstalk proved to be superior in TNF-α, IFN-γ, and IL-12 production compared to $CD14^+$ monocyte/NK cell and slanMo/T cell co-cultures (Fig. 5.9). This is consistent with the previously described differential IL-12 producing potential between slanMo and CD14+ Mo, since IL-12 limits NK cell IFN-γ production [58]. The difference between NK cell and T cell co-cultures with slanMo

highlights the role of NK cells as innate source of IFN-γ, because T cells typically require additional antigen-specific stimulation to reach full activation [195].

6.2.2. Supernatants from slanMo/NK cell co-cultures arrest melanoma growth

The cytokine milieu generated by slanMo and NK cells arrested tumor growth over several culture passages. We compared the inhibition by TLR activated slanMo and NK cell mono-culture CM with the activated co-culture CM. Besides slightly reduced melanoma cell growth numbers observed with slanMo CM, which might be due to TNF receptor mediated apoptosis, we only observed a consistent growth arrest with co-culture CM treatment. Together with TNF-α and IFN-γ neutralization experiments, this demonstrated the requirement of the slanMo/NK cell crosstalk in order to facilitate synergistic high level IFN-γ and TNF-α production capable of limiting melanoma growth. TNF-α/IFN-γ neutralization restored exponential growth to around 80 % when considering cell numbers at day 8 after seeding. An explanation for this could be provided by insufficient neutralization efficiency. However, analogous experiments where TNF-α/IFN-γ neutralizing antibodies were added to recombinant TNF-α + IFN-γ resulted in complete restoration of SK-Mel 28 growth rates (data not shown), arguing against this as the cause for the incomplete reversal of the CM-induced growth inhibition. Another explanation is that additional factors produced in the slanMo/NK cell crosstalk influence melanoma cell proliferation or induce apoptosis. Apart from IL-12, for which no direct effects on tumor cells are reported, IL-6 and IL-8 are highly expressed by slanMo [58] and studies indicated their involvement in senescence [196, 197, 198]. It is therefore conceivable that IL-6 and IL-8 account for the incomplete growth restoration after CM treatment with TNF-α/IFN-γ neutralization. This would also be coherent with the observation of reduced cell numbers and increased SA β-Gal positive cells after slanMo mono-culture CM treatment (Fig. 5.7 B, Fig. 5.14 C). Another soluble factor typically associated with senescence is TGF-β [199, 200]. Since neither concentration measurement nor neutralization was performed for TGF-β, we cannot completely rule out an additional effect of TGF-β in our system.

The detection of stable cell numbers is not directly indicating a stop in proliferation. Other aspects can mimic the effect of stagnant growth curves, i.e. apoptosis of cells. CM treatment clearly increased apoptosis rates in SK-Mel-28, as visualized by Annexin V staining (Fig. 5.13 A). However, as Ki67 staining and ^{3}H-Thymidine incorporation revealed reduced proportions of proliferating cells induced by CM as well as recombinant TNF-α + IFN-γ, it appears that both apoptosis and reduced proliferation together result in the virtually complete arrest up to day 8. It is difficult to extract and assess the isolated effect of

TNF-α/IFN-γ-mediated growth inhibition without influences stemming from apoptosis. However, as also the Ki67 staining revealed, cytokine treatment affects only a fraction of melanoma cells, since ~40 % of cells remained in a proliferative state. It is therefore also understandable that the growth curves start to resemble exponential growth after several passages, since unaffected melanoma cells rapidly outnumber non-proliferating cells. In addition, single-cell tracking in kinetic studies revealed that the majority of SK-Mel 28 cells were actively dividing. Confluency analysis showed a steady, yet significantly lower increase in confluency compared to control conditions. Morphologically, only a minor subpopulation appeared remarkable, which was demonstrated by an enlarged and flattenend morphology. This morphological appearance is described as a major feature of senescence, interestingly also for the cell line used here, SK-Mel-28 [201]. It was therefore reasonable to further investigate the possibility of senescence as the proliferation-limiting mechanism.

6.2.3. Phenotype of the senescence induced by the slanMo/NK cell crosstalk

SA β-Gal is repeatedly used to identify senescent cells. We detected significant upregulation of SA β-Gal staining in SK-Mel 28 cells after treatment with co-culture CM. By performing neutralization experiments and recombinant cytokines, we could trace the effect back to TNF-α and IFN-γ. TNF-α and IFN-γ were previously associated with senescence. In detail, Braumüller *et al.* described senescence induction in a β-cell cancer mouse model that was also characterized by elevated SA β-Gal positive cells [123]. The senescence effect Braumüller *et al.* investigated was dependent on Th1-derived TNF-α/IFN-γ acting directly on β-cancer cells. Additionally, they described reduced *in vitro* growth of cell lines derived from various cancer types, including one melanoma cell line. However, the study lacked a characterization of the cytokine induced senescence phenotype in a broader setting including different tumor entitites. In this regard, our study in melanoma increases the knowledge about the translation of this phenotype to anti-tumor immunity in general. In detail, we expand this concept by two important characteristics: (1) we describe an innate immune crosstalk composed of slanMo and NK cells as mediators of TNF-α/IFN-γ induced senescence; (2) we discover that the slanMo/NK cell crosstalk exclusively upregulated p21 in melanoma cells, suggesting activation of the p53/p21 pathway. This was in contrast to the observations made in Th1-mediated cytokine induced senescence, where senescence was triggered by the p16Ink4a/Rb pathway. However, our results are reasonable when considering that melanoma cells regularly carry mutations in the CDKN2A locus. p21 acts downstream of p53, however, it can also function in an p53-independent manner. Since p53 is commonly mutated in melanoma cell lines and in particular in the cell lines SK-Mel-25 and SK-Mel-30

used in this study (Broad Institute Cancer Cell Line Encyclopedia), it appears that we discovered a novel TNF-α + IFN-γ triggered p53-independent mechanism for p21-mediated senescence in melanoma cells.

Similarly, a recent report stated NK cell-mediated cell cycle arrest of melanoma cells after appropriate stimulation with PDGF-DD, which triggered Nkp44 signaling [124]. The growth arrest was dependent on NK cell derived TNF-α + IFN-γ, however no connection to senescence was provided. The concept of NK cell involvement in tumor senescence extends NK cell mediated anti-tumor functions, which are most prominently focused on tumor-directed cytotoxicity. Yet, senescent tumor cells potentially still pose a threat since tumors can re-emerge after periods of dormancy. Interestingly, NK cells are known to recognize and eliminate senescent cells. This is enabled through expression of stress induced ligands such as DNAM-1 ligands or ULBP proteins on the surface of senescent tumor cells [202, 203].

The concept of cancer stem cells describes individual tumor clones that acquire a stem-cell like phenotype, which equips them with increased tumor-initiating potential. In melanoma, this was demonstrated by simple serial dilution injection experiments into immunocompromised mice, showing that particular subpopulations differ strikingly in their ability to establish tumors [204]. A recent study described a connection between senescence and stemness in a way that senescence facilitates the acquisition of a cancer stem cell phenotype, which is associated with increased aggressiveness and tumorigenic potential after relapse [205]. Additionally, cancer stem cells are assumed to represent a major cause for therapy failure. Due to low cycling and reduction of MHC-I expression, cancer stem cells excel at evading destruction by chemotherapy and T cell-mediated immunotherapy, respectively [206, 207, 208]. In this line of thought, cancer stem cells are also often considered to represent a state of tumor dormancy and therefore mediate the escape from the immune system during relapse [208, 209]. Inflammatory environments in melanoma are reported to lead to reversible melanoma cell dedifferentiation associated with modulation of T cell antigens [210]. Similar to recognition of senescent cells, NK cells are reported to preferentially kill stem-cell like cancer cells [211, 212, 213, 214]. This creates an intriguing concept in which NK cells facilitate both the generation as well as subsequent clearance of senescenct and stem-like, therapy-resistant, tumor clones. However, as demonstrated by the negligible cytokine profile of unstimulated NK cells, this requires the presence and adequate activation status of NK cells in the TME. Of note, contradictory results were previously published by Stokes *et al.* that described limited clearance of senescent cancer cells mediated by NK cells [215].

Another interesting link between tumor senescence and NK cells can be drawn with regard to chemokine-mediated NK cell recruitment. As will be discussed below, senescence in tumor cells is associated with the secretion of an array of cytokines, chemokines, and growth

factors. In this regard, it was reported that senescent tumor cells are eliminated by NK cells recruited via tumor-derived CCL2 [216]. Interestingly, there is an additional connection between p53 and CCL2 proposed, wherein p53 directly binds to a CCL2 enahncer region and regulates gene expression [217]. Similarly, CX_3CL1, another chemokine that mediates NK cell migration, is also suggested to be a target gene of p53 [218]. Together, these results strengthen the previous assumption of NK cells as specialized senescence-targeting cells, as senescence induction is accompanied by upregulation of NK cell recruiting factors.

6.2.4. Functions of the SASP in the TME

Not only immune cells contribute to the TME cytokine milieu, but also other cellular components such as fibroblasts, endothelial cells, and tumor cells majorly shape the composition of soluble factors in the microenvironment. We observed increased expression of various cytokines generally considered in the literature to represent SASP components (Fig. 5.17) [144]. Secretion of inflammatory cytokines such as IL-6, IL-8, IL-1α, and IL-1β have the potential to modulate the tumor microenvironment towards anti-tumor immune responses, as described for M1 macrophage polarization after exposure to pro-inflammatory SASP factors. Consistent with the role of M1 macrophages, this resulted in reduced tumorigenesis in a mouse model of liver fibrosis induced hepatocellular carcinoma [219]. Furthermore, the strong IL-8 upregulation we observed is intriguing when considering an additive effect on NK cell recruitment. Nevertheless, chronic inflammation that is induced by continuous SASP expression argues for major pro-tumorigenic functions [156, 220]. Our observation of increased mRNA levels for MMPs also signals pro-tumorigenic and pro-metastatic activity (Fig. 5.17 A). Active extracellular matrix remodeling is often considered a prerequisite of metastasis. In this regard, elevated MMPs might skew melanoma cells towards higher metastatic potential, similar to as described for thyroid cancer cells [221]. In addition to IL-8, several other chemokines where upregulated in a TNF-α/IFN-γ-dependent fashion, including CXCL1, CXCL2, CCL2, and CCL7 (Fig. 5.17 A). The first three chemokines argue for increased attraction of CXCR2 expressing cells such as NK cells or neutrophils, whereas CCL2 and CCL7 potentially attract CCR2-expressing monocytes to the TME. However, it is difficult to predict the *in vivo* effect on shaping the local immune microenvironment. The marginal increase in TGF-β transcripts in contrast to striking pro-inflammatory cytokine upregulation might suggest a tendency towards anti-tumorigenic immune responses in our system. Interestingly, we found upregulation of ICAM-1 transcripts. This is coherent with our *in vitro* observations that CM- and recombinant TNF-α/IFN-γ-treated cells required longer times to loosen from culture plates during incubation with trypsin (data not shown).

With the list of SASP molecules in mind, a current debate focuses on whether the SASP is actually beneficial for tumor development or not. The expression of angiogenic and matrix modifying enzymes is related to heightened metastatic potential and maintaining chronic tumor-promoting inflammation represents a hallmark of tumor biology. On the other hand, secretion of chemotactic SASP factors by senescent cells was shown to facilitate NK recruitment and clearance of senescent cells [216]. Thus it is still difficult to fully assess the impact of the SASP in the TME and in tumor progression. In addition, it was postulated that the SASP requires continuous DNA-damage response signaling [144] and that isolated overexpression of p16 or p21 does not involve secretion of SASP factors [222]. This would imply that constant DNA-damage occurs through TNF- and IFN-receptor signaling in our system, since we observe p21 upregulation co-existing with SASP factor upregulation. However, we were not investigating DNA-damage markers in CM-induced senescence and thus we cannot rule out the possibility of DNA-damage response signaling.

All pro- and anti-tumorigenic aspects considered, to be physiologically relevant in limiting melanoma progression, cytokine induced senescence should represent a temporary condition that provides time for NK cell and cytotoxic T cell mediated tumor clearance.

6.3. Clinical relevance of patrolling monocytes and NK cells in melanoma

Despite major differences between artificial mouse models and the situation in human patients, development of cancer immunotherapeutics typically originates from basic research. Hanna *et al.* described strongly increased metastasis formation in the absence of murine patrolling monocytes [53]. In their model, patrolling Ly6C^{low} monocytes extravasated at early metastatic sites, ingested tumor material, and contributed to tumor clearance through recruitment of NK cells. Together with other reports that focus on the anti-metastatic role of the murine patrolling monocyte and NK cell crosstalk, this strenghtens the relevance of innate immune responses in tumor immunology [127, 223]. However, patrolling monocytes were also previously associated with immunesuppressive, even pro-tumorigenic functions related to anti-angiogenic therapy [224]. Without doubt, unleashing the full synergy of slanMo and NK cells *in vivo* would require adequate stimulation in the TME.

6.3.1. Evaluation of innate immune cell stimulation in the TME

Besides manipulation of the immune activation status in the TME by tumor cells, other conditions that often render immune cells exhausted and futile include lack of stimulatory

factors, hypoxia, and spatial exclusion of immune cells. Immune-stimulating agents are often scarce in developed tumors where little apoptosis and cytotoxicity occurs. Besides NK cells, which are well studied regarding recognition of malignant cells, precise mechanisms for activation of for example monocytes or DCs in the TME are still not clear. Certain apoptosis related molecules are assumed to trigger PRR signaling and thereby activate innate immune cells. The nuclear protein HMGB1 is released during cell death but can also be produced by other immune cells such as NK cells. Interestingly, besides perforin/granzyme-mediated release of tumor cell HMGB1, it was found that NK cells secrete a chemotactic HMGB1 variant after co-culture with tumor cells. NK cell-derived HMGB1 then recruits additional RAGE-expressing NK cells, resulting in amplified NK cell responses [225]. Since HMGB1 is reported to trigger TLRs and activate monocytes and DCs, tumor- and immune cell-derived HMGB1 together has the potential to initiate immune responses in the TME [31]. Surprisingly, HMGB1 expression in melanoma cells is reported to correlate with poor prognosis in patients, despite its pro-inflammatory functions. In detail, Li *et al.* described senescence induction in melanoma cells as a response to HMGB1 suppression by RNA interference [226]. Constant HMGB1 expression prevented p21 upregulation and maintained a cycling state, which was abrogated in the absence of HMGB1. Similarly, HMGB1 is reported as a factor secreted by senescent cells and abnormal HMGB1 expression was associated with supporting a senescent state [227]. In this line of thought, it would be conceivable that NK cells further modulate tumor cell senescence through endogenous HMGB1 as well as tumor cell-derived HMGB1 released through cell lysis.

Recently, it was stated that tumor-derived exosomes activate patrolling monocytes and thereby facilitate immunosurveillance [128]. Similar to the function of tumor exosomes in modulating and preparing metastatic seeding [228], Plebanek *et al.* demonstrated that successful metastasizing depended on exosome composition, notably the presence of PEDF on exosomes. Interestingly, PEDF stimulated patrolling monocytes and expression of PEDF was the factor that differentiated metastatic from non-metastatic melanomas. Similarly, PEDF was shown to activate human macrophages *in vitro*, arguing for PEDF as a innate immune stimulus in the TME.

Together, these results outline the potential of innate immune cell activation in TME. Ensuring optimal stimulation however might require therapeutic intervention. One option to achieve this is by the use of TLR 7/8 ligand therapeutics such as imiquimod, which is studied for treatment of cutaneous melanoma lesions and metastasis. Topic imiquimod application has been reported to induce melanoma regression and is also investigated for supportive treatment after initial melanoma excision [138, 139, 140]. Since slanMo express TLR 7 and 8,

imiquimod therapy can potentially activate those cells in the TME and thereby initiate a senescence-inducing slanMo/NK cell crosstalk.

6.3.2. Relevance of melanoma cell senescence for cancer therapy

Senescence in tumors is associated with both pro- and anti-tumorigenic properties. Nevertheless, senescent cells are rendered in a unproliferative state that potentially renders them susceptible to other treatment options as well as to destruction by NK cells. In this regard, current lines of therapeutic inventions aim at disturbing tumor-intrinsic modulation of the cell cycle. Most prominently, CDK inhibitors are currently tested for their ability to arrest tumor cell growth. Recently, Goel *et al.* investigated the CDK4/6 inhibitor Ademaciclib in different mouse tumor models and found that inhibition of G1 CDKs induced a senescence-like phenotype [229]. Interestingly, CDK4/6 inihbition was associated with increased T cell-mediated anti-tumor immunity, enabled through increased expression of antigen-presentation machinery components. In a similar line of thought, Ruscetti *et al.* demonstrated senescence as a result of combination treatment with MAPK and CDK4/6 inhibitors [230]. In this study, clearance of senescent cells was found to be dependent on NK cells becoming activated by tumor-derived SASP factors. Together, these data suggest that cell cycle proteins offer attractive targets for novel therapeutics, in particular for combination therapies with immune checkpoint inhibitors and targeted therapies [151].

6.4. Conclusion

Innate immune cells are instrumental in anti-tumor responses as first line of defense and initiators of adaptive immune responses. Here, we demonstrate the senescence-inducing capability of innate immune cells represented by slanMo and NK cells undergoing a synergistic crosstalk. We observed correlating numbers of infiltrating slanMo and NK cells in stage III melanoma. Furthermore, we provided an explanation for this finding by demonstrating that slanMo can recruit NK cells. This migration axis was dependent on slanMo-derived IL-8 signaling via CXCR1 and CXCR2 on NK cells. Regarding functional aspects of the slanMo/NK cell crosstalk, we showed that the cytokine milieu generated by TLR 7/8-activated slanMo and NK cells limits melanoma cell growth characterized by reduced cell numbers and reduced proliferation. Mechanistically, we found that the growth arrest is mediated by senescence induction in melanoma cells. We validated this by demonstrating increased SA β-Gal staining, increased p21 expression, and the secretion of SASP factors, together strongly arguing for a senescence phenotype.

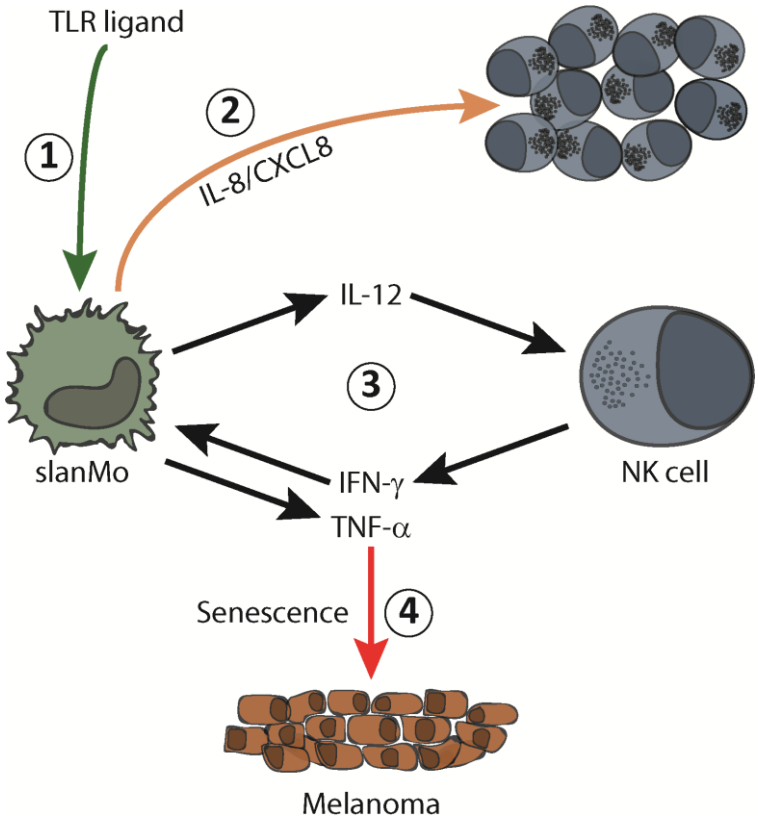

Figure 6.1 - Schematic summarizing the actions of the slanMo/NK cell crosstalk in melanoma. (1) slanMo become stimulated by TLR ligands in the TME or provided by TLR ligand therapy. (2) slanMo produce IL-8/CXCL8 that recruits NK cells to the TME. (3) slanMo and NK cell undergo a synergistic crosstalk that yields high levels of IL-12, IFN-γ and TNF-α. (4) slanMo/NK cell crosstalk derived TNF-α and IFN-γ can induce a senescence phenotype in melanoma cells.

Combining the insights gained from this study with recent reports provides a hypothesis for the initial contact between newly formed melanoma tumors or metastasis with the innate immune system (Fig. 6.1). In detail, we provide evidence for a hierarchical order involving (1) strong early infiltration and activation of slanMo followed by (2) subsequent recruitment of NK cells. The resulting intratumoral slanMo/NK cell crosstalk (3) generates very high levels of TNF-α and IFN-γ that (4) induce senescence in melanoma cells. This order can be extended by the mouse model study of Böttcher *et al.* that described recruitment of T cell-priming cDC1 by intratumoral NK cells. Furthermore, our results can potentially be translated to checkpoint inhibitor therapy when considering the study by Barry *et al.* demonstrating that the presence of NK cells and cDC1 is a major determinant of checkpoint inhibitor therapy responsiveness[231].

Taken together, we broaden the concept of cytokine-induced senescence by including innate immune responses. Our results indicate that therapies providing optimal monocyte and DC stimulation through TLR 7/8 ligands, such as topical imiquimod treatment, strongly activate slanMo present in primary melanoma and metastasis and fuel a slanMo/NK cell synergistic crosstalk that reduces tumor progression through TNF-α/ IFN-γ-mediated senescence induction.

7 References

1. Wong, K.L. *et al.* The three human monocyte subsets: implications for health and disease. *Immunol Res* **53**, 41-57 (2012).

2. Schakel, K. *et al.* A novel dendritic cell population in human blood: one-step immunomagnetic isolation by a specific mAb (M-DC8) and in vitro priming of cytotoxic T lymphocytes. *Eur J Immunol* **28**, 4084-4093 (1998).

3. Davies, L.C. & Taylor, P.R. Tissue-resident macrophages: then and now. *Immunology* **144**, 541-548 (2015).

4. Perdiguero, E.G. & Geissmann, F. The development and maintenance of resident macrophages. *Nat Immunol* **17**, 2-8 (2016).

5. Bopst, M., Haas, C., Car, B. & Eugster, H.P. The combined inactivation of tumor necrosis factor and interleukin-6 prevents induction of the major acute phase proteins by endotoxin. *Eur J Immunol* **28**, 4130-4137 (1998).

6. Thomas, G., Tacke, R., Hedrick, C.C. & Hanna, R.N. Nonclassical patrolling monocyte function in the vasculature. *Arterioscler Thromb Vasc Biol* **35**, 1306-1316 (2015).

7. Janeway, C.A., Jr. & Medzhitov, R. Innate immune recognition. *Annu Rev Immunol* **20**, 197-216 (2002).

8. Barton, G.M. & Medzhitov, R. Toll-like receptors and their ligands. *Curr Top Microbiol Immunol* **270**, 81-92 (2002).

9. Aderem, A. & Ulevitch, R.J. Toll-like receptors in the induction of the innate immune response. *Nature* **406**, 782-787 (2000).

10. Kawai, T. & Akira, S. The role of pattern-recognition receptors in innate immunity: update on Toll-like receptors. *Nat Immunol* **11**, 373-384 (2010).

11. Medzhitov, R., Preston-Hurlburt, P. & Janeway, C.A., Jr. A human homologue of the Drosophila Toll protein signals activation of adaptive immunity. *Nature* **388**, 394-397 (1997).

12. Ganguly, D. *et al.* Self-RNA-antimicrobial peptide complexes activate human dendritic cells through TLR7 and TLR8. *J Exp Med* **206**, 1983-1994 (2009).

13. Taniguchi, M., Seino, K. & Nakayama, T. The NKT cell system: bridging innate and acquired immunity. *Nat Immunol* **4**, 1164-1165 (2003).

14. Branzk, N., Gronke, K. & Diefenbach, A. Innate lymphoid cells, mediators of tissue homeostasis, adaptation and disease tolerance. *Immunol Rev* **286**, 86-101 (2018).

15. Hayday, A.C. gammadelta T Cell Update: Adaptate Orchestrators of Immune Surveillance. *J Immunol* **203**, 311-320 (2019).

16. Di Cesare, A., Di Meglio, P. & Nestle, F.O. The IL-23/Th17 axis in the immunopathogenesis of psoriasis. *J Invest Dermatol* **129**, 1339-1350 (2009).

17. Ley, K., Laudanna, C., Cybulsky, M.I. & Nourshargh, S. Getting to the site of inflammation: the leukocyte adhesion cascade updated. *Nat Rev Immunol* **7**, 678-689 (2007).

18. Simon, S.I., Hu, Y., Vestweber, D. & Smith, C.W. Neutrophil tethering on E-selectin activates beta 2 integrin binding to ICAM-1 through a mitogen-activated protein kinase signal transduction pathway. *J Immunol* **164**, 4348-4358 (2000).

19. Berlin, C. *et al.* alpha 4 integrins mediate lymphocyte attachment and rolling under physiologic flow. *Cell* **80**, 413-422 (1995).

20. Murdoch, C. & Finn, A. Chemokine receptors and their role in inflammation and infectious diseases. *Blood* **95**, 3032-3043 (2000).

21. Barreiro, O. *et al.* Dynamic interaction of VCAM-1 and ICAM-1 with moesin and ezrin in a novel endothelial docking structure for adherent leukocytes. *J Cell Biol* **157**, 1233-1245 (2002).

22. Carman, C.V. & Springer, T.A. A transmigratory cup in leukocyte diapedesis both through individual vascular endothelial cells and between them. *J Cell Biol* **167**, 377-388 (2004).

23. Griffith, J.W., Sokol, C.L. & Luster, A.D. Chemokines and chemokine receptors: positioning cells for host defense and immunity. *Annu Rev Immunol* **32**, 659-702 (2014).

24. Yoshida, R. *et al.* Molecular cloning of a novel human CC chemokine EBI1-ligand chemokine that is a specific functional ligand for EBI1, CCR7. *J Biol Chem* **272**, 13803-13809 (1997).

25. Campbell, J.J. *et al.* 6-C-kine (SLC), a lymphocyte adhesion-triggering chemokine expressed by high endothelium, is an agonist for the MIP-3beta receptor CCR7. *J Cell Biol* **141**, 1053-1059 (1998).

26. Forster, R. *et al.* CCR7 coordinates the primary immune response by establishing functional microenvironments in secondary lymphoid organs. *Cell* **99**, 23-33 (1999).

27. Sharma, N., Benechet, A.P., Lefrancois, L. & Khanna, K.M. CD8 T Cells Enter the Splenic T Cell Zones Independently of CCR7, but the Subsequent Expansion and Trafficking Patterns of Effector T Cells after Infection Are Dysregulated in the Absence of CCR7 Migratory Cues. *J Immunol* **195**, 5227-5236 (2015).

28. Proudfoot, A.E. Chemokine receptors: multifaceted therapeutic targets. *Nat Rev Immunol* **2**, 106-115 (2002).

29. Dunn, G.P., Old, L.J. & Schreiber, R.D. The three Es of cancer immunoediting. *Annu Rev Immunol* **22**, 329-360 (2004).

30. Mittal, D., Gubin, M.M., Schreiber, R.D. & Smyth, M.J. New insights into cancer immunoediting and its three component phases--elimination, equilibrium and escape. *Curr Opin Immunol* **27**, 16-25 (2014).

31. Scaffidi, P., Misteli, T. & Bianchi, M.E. Release of chromatin protein HMGB1 by necrotic cells triggers inflammation. *Nature* **418**, 191-195 (2002).

32. Sims, G.P., Rowe, D.C., Rietdijk, S.T., Herbst, R. & Coyle, A.J. HMGB1 and RAGE in inflammation and cancer. *Annu Rev Immunol* **28**, 367-388 (2010).

33. Krysko, D.V. *et al.* Immunogenic cell death and DAMPs in cancer therapy. *Nat Rev Cancer* **12**, 860-875 (2012).

34. Koebel, C.M. *et al.* Adaptive immunity maintains occult cancer in an equilibrium state. *Nature* **450**, 903-907 (2007).

35. Uyttenhove, C. *et al.* Evidence for a tumoral immune resistance mechanism based on tryptophan degradation by indoleamine 2,3-dioxygenase. *Nat Med* **9**, 1269-1274 (2003).

36. Groh, V., Wu, J., Yee, C. & Spies, T. Tumour-derived soluble MIC ligands impair expression of NKG2D and T-cell activation. *Nature* **419**, 734-738 (2002).

37. Naidoo, J., Page, D.B. & Wolchok, J.D. Immune modulation for cancer therapy. *Br J Cancer* **111**, 2214-2219 (2014).

38. Schlecker, E. *et al.* Tumor-infiltrating monocytic myeloid-derived suppressor cells mediate CCR5-dependent recruitment of regulatory T cells favoring tumor growth. *J Immunol* **189**, 5602-5611 (2012).

39. Vignali, D.A., Collison, L.W. & Workman, C.J. How regulatory T cells work. *Nat Rev Immunol* **8**, 523-532 (2008).

40. Bonaventura, P. *et al.* Cold Tumors: A Therapeutic Challenge for Immunotherapy. *Front Immunol* **10**, 168 (2019).

41. Joyce, J.A. & Fearon, D.T. T cell exclusion, immune privilege, and the tumor microenvironment. *Science* **348**, 74-80 (2015).

42. Gentles, A.J. *et al.* The prognostic landscape of genes and infiltrating immune cells across human cancers. *Nat Med* **21**, 938-945 (2015).

43. Azizi, E. *et al.* Single-Cell Map of Diverse Immune Phenotypes in the Breast Tumor Microenvironment. *Cell* **174**, 1293-1308 e1236 (2018).

44. Tirosh, I. *et al.* Dissecting the multicellular ecosystem of metastatic melanoma by single-cell RNA-seq. *Science* **352**, 189-196 (2016).

45. Fridman, W.H., Pages, F., Sautes-Fridman, C. & Galon, J. The immune contexture in human tumours: impact on clinical outcome. *Nat Rev Cancer* **12**, 298-306 (2012).

46. Sade-Feldman, M. *et al.* Defining T Cell States Associated with Response to Checkpoint Immunotherapy in Melanoma. *Cell* **175**, 998-1013 e1020 (2018).

47. Zheng, C. *et al.* Landscape of Infiltrating T Cells in Liver Cancer Revealed by Single-Cell Sequencing. *Cell* **169**, 1342-1356 e1316 (2017).

48. Thommen, D.S. & Schumacher, T.N. T Cell Dysfunction in Cancer. *Cancer Cell* **33**, 547-562 (2018).

49. Schreiber, R.D., Old, L.J. & Smyth, M.J. Cancer immunoediting: integrating immunity's roles in cancer suppression and promotion. *Science* **331**, 1565-1570 (2011).

50. Qian, B.Z. *et al.* CCL2 recruits inflammatory monocytes to facilitate breast-tumour metastasis. *Nature* **475**, 222-225 (2011).

51. Kitamura, T. *et al.* CCL2-induced chemokine cascade promotes breast cancer metastasis by enhancing retention of metastasis-associated macrophages. *J Exp Med* **212**, 1043-1059 (2015).

52. Qian, B.Z. *et al.* FLT1 signaling in metastasis-associated macrophages activates an inflammatory signature that promotes breast cancer metastasis. *J Exp Med* **212**, 1433-1448 (2015).

53. Hanna, R.N. *et al.* Patrolling monocytes control tumor metastasis to the lung. *Science* **350**, 985-990 (2015).

54. Murray, P.J. Macrophage Polarization. *Annu Rev Physiol* **79**, 541-566 (2017).

55. Biswas, S.K. *et al.* A distinct and unique transcriptional program expressed by tumor-associated macrophages (defective NF-kappaB and enhanced IRF-3/STAT1 activation). *Blood* **107**, 2112-2122 (2006).

56. Franklin, R.A. *et al.* The cellular and molecular origin of tumor-associated macrophages. *Science* **344**, 921-925 (2014).

57. Schakel, K. *et al.* 6-Sulfo LacNAc, a novel carbohydrate modification of PSGL-1, defines an inflammatory type of human dendritic cells. *Immunity* **17**, 289-301 (2002).

58. Schakel, K. *et al.* Human 6-sulfo LacNAc-expressing dendritic cells are principal producers of early interleukin-12 and are controlled by erythrocytes. *Immunity* **24**, 767-777 (2006).

59. Cros, J. *et al.* Human CD14dim monocytes patrol and sense nucleic acids and viruses via TLR7 and TLR8 receptors. *Immunity* **33**, 375-386 (2010).

60. Schakel, K. Dendritic cells--why can they help and hurt us. *Exp Dermatol* **18**, 264-273 (2009).

61. Patel, A.A. *et al.* The fate and lifespan of human monocyte subsets in steady state and systemic inflammation. *J Exp Med* **214**, 1913-1923 (2017).

62. Yona, S. *et al.* Fate mapping reveals origins and dynamics of monocytes and tissue macrophages under homeostasis. *Immunity* **38**, 79-91 (2013).

63. Carlin, L.M. *et al.* Nr4a1-dependent Ly6C(low) monocytes monitor endothelial cells and orchestrate their disposal. *Cell* **153**, 362-375 (2013).

64. Hanna, R.N. *et al.* The transcription factor NR4A1 (Nur77) controls bone marrow differentiation and the survival of Ly6C- monocytes. *Nat Immunol* **12**, 778-785 (2011).

65. Hansel, A. *et al.* Human slan (6-sulfo LacNAc) dendritic cells are inflammatory dermal dendritic cells in psoriasis and drive strong TH17/TH1 T-cell responses. *J Allergy Clin Immunol* **127**, 787-794 e781-789 (2011).

66. Hansel, A. *et al.* Human 6-sulfo LacNAc (slan) dendritic cells have molecular and functional features of an important pro-inflammatory cell type in lupus erythematosus. *J Autoimmun* **40**, 1-8 (2013).

67. de Baey, A. *et al.* A subset of human dendritic cells in the T cell area of mucosa-associated lymphoid tissue with a high potential to produce TNF-alpha. *J Immunol* **170**, 5089-5094 (2003).

68. Kunze, A., Forster, U., Oehrl, S., Schmitz, M. & Schakel, K. Autocrine TNF-alpha and IL-1beta prime 6-sulfo LacNAc(+) dendritic cells for high-level production of IL-23. *Exp Dermatol* **26**, 314-316 (2017).

69. van Leeuwen-Kerkhoff, N. *et al.* Human Bone Marrow-Derived Myeloid Dendritic Cells Show an Immature Transcriptional and Functional Profile Compared to Their Peripheral Blood Counterparts and Separate from Slan+ Non-Classical Monocytes. *Front Immunol* **9**, 1619 (2018).

70. Ahmad, F., Dobel, T., Schmitz, M. & Schakel, K. Current Concepts on 6-sulfo LacNAc Expressing Monocytes (slanMo). *Front Immunol* **10**, 948 (2019).

71. Sidibe, A. *et al.* Angiogenic factor-driven inflammation promotes extravasation of human proangiogenic monocytes to tumours. *Nat Commun* **9**, 355 (2018).

72. Vermi, W. *et al.* slan(+) Monocytes and Macrophages Mediate CD20-Dependent B-cell Lymphoma Elimination via ADCC and ADCP. *Cancer Res* **78**, 3544-3559 (2018).

73. Vermi, W. *et al.* slanDCs selectively accumulate in carcinoma-draining lymph nodes and marginate metastatic cells. *Nat Commun* **5**, 3029 (2014).

74. Thomas, K. *et al.* Accumulation and therapeutic modulation of 6-sulfo LacNAc(+) dendritic cells in multiple sclerosis. *Neurol Neuroimmunol Neuroinflamm* **1**, e33 (2014).

75. Olaru, F. *et al.* Intracapillary immune complexes recruit and activate slan-expressing CD16+ monocytes in human lupus nephritis. *JCI Insight* **3** (2018).

76. Baran, W. *et al.* Phenotype, Function, and Mobilization of 6-Sulfo LacNAc-Expressing Monocytes in Atopic Dermatitis. *Front Immunol* **9**, 1352 (2018).

77. Bippes, C.C. *et al.* A novel modular antigen delivery system for immuno targeting of human 6-sulfo LacNAc-positive blood dendritic cells (SlanDCs). *PLoS One* **6**, e16315 (2011).

78. Schmitz, M. *et al.* Tumoricidal potential of native blood dendritic cells: direct tumor cell killing and activation of NK cell-mediated cytotoxicity. *J Immunol* **174**, 4127-4134 (2005).

79. Schmitz, M. *et al.* Native human blood dendritic cells as potent effectors in antibody-dependent cellular cytotoxicity. *Blood* **100**, 1502-1504 (2002).

80. Lamarthee, B. *et al.* Quantitative and functional alterations of 6-sulfo LacNac dendritic cells in multiple myeloma. *Oncoimmunology* **7**, e1444411 (2018).

81. Wehner, R. *et al.* Impact of chemotherapeutic agents on the immunostimulatory properties of human 6-sulfo LacNAc+ (slan) dendritic cells. *Int J Cancer* **132**, 1351-1359 (2013).

82. Nagler, A., Lanier, L.L., Cwirla, S. & Phillips, J.H. Comparative studies of human FcRIII-positive and negative natural killer cells. *J Immunol* **143**, 3183-3191 (1989).

83. Cooper, M.A. *et al.* Human natural killer cells: a unique innate immunoregulatory role for the CD56(bright) subset. *Blood* **97**, 3146-3151 (2001).

84. Chiossone, L., Dumas, P.Y., Vienne, M. & Vivier, E. Natural killer cells and other innate lymphoid cells in cancer. *Nat Rev Immunol* **18**, 671-688 (2018).

85. Diefenbach, A., Colonna, M. & Romagnani, C. The ILC World Revisited. *Immunity* **46**, 327-332 (2017).

86. Lanier, L.L. NK cell recognition. *Annu Rev Immunol* **23**, 225-274 (2005).

87. Vivier, E., Nunes, J.A. & Vely, F. Natural killer cell signaling pathways. *Science* **306**, 1517-1519 (2004).

88. Vivier, E. *et al.* Innate or adaptive immunity? The example of natural killer cells. *Science* **331**, 44-49 (2011).

89. Mrozek, E., Anderson, P. & Caligiuri, M.A. Role of interleukin-15 in the development of human CD56+ natural killer cells from CD34+ hematopoietic progenitor cells. *Blood* **87**, 2632-2640 (1996).

90. Becknell, B. & Caligiuri, M.A. Interleukin-2, interleukin-15, and their roles in human natural killer cells. *Adv Immunol* **86**, 209-239 (2005).

91. Dubois, S., Mariner, J., Waldmann, T.A. & Tagaya, Y. IL-15Ralpha recycles and presents IL-15 In trans to neighboring cells. *Immunity* **17**, 537-547 (2002).

92. Kobayashi, M. *et al.* Identification and purification of natural killer cell stimulatory factor (NKSF), a cytokine with multiple biologic effects on human lymphocytes. *J Exp Med* **170**, 827-845 (1989).

93. Cooper, M.A. *et al.* Cytokine-induced memory-like natural killer cells. *Proc Natl Acad Sci U S A* **106**, 1915-1919 (2009).

94. Ni, J., Miller, M., Stojanovic, A., Garbi, N. & Cerwenka, A. Sustained effector function of IL-12/15/18-preactivated NK cells against established tumors. *J Exp Med* **209**, 2351-2365 (2012).

95. Leong, J.W. *et al.* Preactivation with IL-12, IL-15, and IL-18 induces CD25 and a functional high-affinity IL-2 receptor on human cytokine-induced memory-like natural killer cells. *Biol Blood Marrow Transplant* **20**, 463-473 (2014).

96. Ross, M.E. & Caligiuri, M.A. Cytokine-induced apoptosis of human natural killer cells identifies a novel mechanism to regulate the innate immune response. *Blood* **89**, 910-918 (1997).

97. Borrego, F. *et al.* Structure and function of major histocompatibility complex (MHC) class I specific receptors expressed on human natural killer (NK) cells. *Mol Immunol* **38**, 637-660 (2002).

98. De Maria, A., Bozzano, F., Cantoni, C. & Moretta, L. Revisiting human natural killer cell subset function revealed cytolytic CD56(dim)CD16+ NK cells as rapid producers of abundant IFN-gamma on activation. *Proc Natl Acad Sci U S A* **108**, 728-732 (2011).

99. Dunn, G.P., Koebel, C.M. & Schreiber, R.D. Interferons, immunity and cancer immunoediting. *Nat Rev Immunol* **6**, 836-848 (2006).

100. Castriconi, R. *et al.* Molecular Mechanisms Directing Migration and Retention of Natural Killer Cells in Human Tissues. *Front Immunol* **9**, 2324 (2018).

101. Berahovich, R.D., Lai, N.L., Wei, Z., Lanier, L.L. & Schall, T.J. Evidence for NK cell subsets based on chemokine receptor expression. *J Immunol* **177**, 7833-7840 (2006).

102. Gregoire, C. *et al.* The trafficking of natural killer cells. *Immunol Rev* **220**, 169-182 (2007).

103. Carrega, P. *et al.* CD56(bright)perforin(low) noncytotoxic human NK cells are abundant in both healthy and neoplastic solid tissues and recirculate to secondary lymphoid organs via afferent lymph. *J Immunol* **192**, 3805-3815 (2014).

104. Fehniger, T.A. *et al.* CD56bright natural killer cells are present in human lymph nodes and are activated by T cell-derived IL-2: a potential new link between adaptive and innate immunity. *Blood* **101**, 3052-3057 (2003).

105. Lima, M. *et al.* Chemokine Receptor Expression on Normal Blood CD56(+) NK-Cells Elucidates Cell Partners That Comigrate during the Innate and Adaptive Immune Responses and Identifies a Transitional NK-Cell Population. *J Immunol Res* **2015**, 839684 (2015).

106. Parolini, S. *et al.* The role of chemerin in the colocalization of NK and dendritic cell subsets into inflamed tissues. *Blood* **109**, 3625-3632 (2007).

107. Campbell, J.J. *et al.* Unique subpopulations of CD56+ NK and NK-T peripheral blood lymphocytes identified by chemokine receptor expression repertoire. *J Immunol* **166**, 6477-6482 (2001).

108. Biron, C.A., Byron, K.S. & Sullivan, J.L. Severe herpesvirus infections in an adolescent without natural killer cells. *N Engl J Med* **320**, 1731-1735 (1989).

109. Textor, S. *et al.* Activating NK cell receptor ligands are differentially expressed during progression to cervical cancer. *Int J Cancer* **123**, 2343-2353 (2008).

110. Frazao, A. *et al.* CD16(+)NKG2A(high) Natural Killer Cells Infiltrate Breast Cancer-Draining Lymph Nodes. *Cancer Immunol Res* **7**, 208-218 (2019).

111. Ali, T.H. *et al.* Enrichment of CD56(dim)KIR + CD57 + highly cytotoxic NK cells in tumour-infiltrated lymph nodes of melanoma patients. *Nat Commun* **5**, 5639 (2014).

112. Cristiani, C.M. *et al.* Accumulation of Circulating CCR7(+) Natural Killer Cells Marks Melanoma Evolution and Reveals a CCL19-Dependent Metastatic Pathway. *Cancer Immunol Res* **7**, 841-852 (2019).

113. Lopez-Soto, A., Gonzalez, S., Smyth, M.J. & Galluzzi, L. Control of Metastasis by NK Cells. *Cancer Cell* **32**, 135-154 (2017).

114. Simoni, Y. *et al.* Human Innate Lymphoid Cell Subsets Possess Tissue-Type Based Heterogeneity in Phenotype and Frequency. *Immunity* **46**, 148-161 (2017).

115. Vivier, E., Tomasello, E., Baratin, M., Walzer, T. & Ugolini, S. Functions of natural killer cells. *Nat Immunol* **9**, 503-510 (2008).

116. Prager, I. & Watzl, C. Mechanisms of natural killer cell-mediated cellular cytotoxicity. *J Leukoc Biol* **105**, 1319-1329 (2019).

117. Balaji, K.N., Schaschke, N., Machleidt, W., Catalfamo, M. & Henkart, P.A. Surface cathepsin B protects cytotoxic lymphocytes from self-destruction after degranulation. *J Exp Med* **196**, 493-503 (2002).

118. Cohnen, A. *et al.* Surface CD107a/LAMP-1 protects natural killer cells from degranulation-associated damage. *Blood* **122**, 1411-1418 (2013).

119. van den Broek, M.E. *et al.* Decreased tumor surveillance in perforin-deficient mice. *J Exp Med* **184**, 1781-1790 (1996).

120. Takeda, K. *et al.* Critical role for tumor necrosis factor-related apoptosis-inducing ligand in immune surveillance against tumor development. *J Exp Med* **195**, 161-169 (2002).

121. Chin, Y.E. *et al.* Cell growth arrest and induction of cyclin-dependent kinase inhibitor p21 WAF1/CIP1 mediated by STAT1. *Science* **272**, 719-722 (1996).

122. Wang, S. *et al.* Interferon-gamma induces senescence in normal human melanocytes. *PLoS One* **9**, e93232 (2014).

123. Braumuller, H. *et al.* T-helper-1-cell cytokines drive cancer into senescence. *Nature* **494**, 361-365 (2013).

124. Barrow, A.D. *et al.* Natural Killer Cells Control Tumor Growth by Sensing a Growth Factor. *Cell* **172**, 534-548 e519 (2018).

125. Tufa, D.M., Chatterjee, D., Low, H.Z., Schmidt, R.E. & Jacobs, R. TNFR2 and IL-12 coactivation enables slanDCs to support NK-cell function via membrane-bound TNF-alpha. *Eur J Immunol* **44**, 3717-3728 (2014).

126. Wehner, R. *et al.* Reciprocal activating interaction between 6-sulfo LacNAc+ dendritic cells and NK cells. *Int J Cancer* **124**, 358-366 (2009).

127. Kubo, H., Mensurado, S., Goncalves-Sousa, N., Serre, K. & Silva-Santos, B. Primary Tumors Limit Metastasis Formation through Induction of IL15-Mediated Cross-Talk between Patrolling Monocytes and NK Cells. *Cancer Immunol Res* **5**, 812-820 (2017).

128. Plebanek, M.P. *et al.* Pre-metastatic cancer exosomes induce immune surveillance by patrolling monocytes at the metastatic niche. *Nat Commun* **8**, 1319 (2017).

129. Hodis, E. *et al.* A landscape of driver mutations in melanoma. *Cell* **150**, 251-263 (2012).

130. Munoz-Couselo, E., Adelantado, E.Z., Ortiz, C., Garcia, J.S. & Perez-Garcia, J. NRAS-mutant melanoma: current challenges and future prospect. *Onco Targets Ther* **10**, 3941-3947 (2017).

131. Hanahan, D. & Weinberg, R.A. Hallmarks of cancer: the next generation. *Cell* **144**, 646-674 (2011).

132. Williams, A.B. & Schumacher, B. p53 in the DNA-Damage-Repair Process. *Cold Spring Harb Perspect Med* **6** (2016).

133. Karimian, A., Ahmadi, Y. & Yousefi, B. Multiple functions of p21 in cell cycle, apoptosis and transcriptional regulation after DNA damage. *DNA Repair (Amst)* **42**, 63-71 (2016).

134. Cayrol, C., Knibiehler, M. & Ducommun, B. p21 binding to PCNA causes G1 and G2 cell cycle arrest in p53-deficient cells. *Oncogene* **16**, 311-320 (1998).

135. Bieging, K.T., Mello, S.S. & Attardi, L.D. Unravelling mechanisms of p53-mediated tumour suppression. *Nat Rev Cancer* **14**, 359-370 (2014).

136. Gershenwald, J.E. *et al.* Melanoma staging: Evidence-based changes in the American Joint Committee on Cancer eighth edition cancer staging manual. *CA Cancer J Clin* **67**, 472-492 (2017).

137. Luke, J.J., Flaherty, K.T., Ribas, A. & Long, G.V. Targeted agents and immunotherapies: optimizing outcomes in melanoma. *Nat Rev Clin Oncol* **14**, 463-482 (2017).

138. Ellis, L.Z., Cohen, J.L., High, W. & Stewart, L. Melanoma in situ treated successfully using imiquimod after nonclearance with surgery: review of the literature. *Dermatol Surg* **38**, 937-946 (2012).

139. Fan, Q., Cohen, S., John, B. & Riker, A.I. Melanoma in Situ Treated with Topical Imiquimod for Management of Persistently Positive Margins: A Review of Treatment Methods. *Ochsner J* **15**, 443-447 (2015).

140. Steinmann, A., Funk, J.O., Schuler, G. & von den Driesch, P. Topical imiquimod treatment of a cutaneous melanoma metastasis. *J Am Acad Dermatol* **43**, 555-556 (2000).

141. Ito, Y., Hoare, M. & Narita, M. Spatial and Temporal Control of Senescence. *Trends Cell Biol* **27**, 830-842 (2017).

142. Dimri, G.P. *et al.* A biomarker that identifies senescent human cells in culture and in aging skin in vivo. *Proc Natl Acad Sci U S A* **92**, 9363-9367 (1995).

143. Malaquin, N. *et al.* Senescent fibroblasts enhance early skin carcinogenic events via a paracrine MMP-PAR-1 axis. *PLoS One* **8**, e63607 (2013).

144. Faget, D.V., Ren, Q. & Stewart, S.A. Unmasking senescence: context-dependent effects of SASP in cancer. *Nat Rev Cancer* (2019).

145. Serrano, M., Hannon, G.J. & Beach, D. A new regulatory motif in cell-cycle control causing specific inhibition of cyclin D/CDK4. *Nature* **366**, 704-707 (1993).

146. Cerqueira, A. *et al.* Genetic characterization of the role of the Cip/Kip family of proteins as cyclin-dependent kinase inhibitors and assembly factors. *Mol Cell Biol* **34**, 1452-1459 (2014).

147. Mello, S.S. & Attardi, L.D. Deciphering p53 signaling in tumor suppression. *Curr Opin Cell Biol* **51**, 65-72 (2018).

148. Witkiewicz, A.K., Knudsen, K.E., Dicker, A.P. & Knudsen, E.S. The meaning of p16(ink4a) expression in tumors: functional significance, clinical associations and future developments. *Cell Cycle* **10**, 2497-2503 (2011).

149. Bailey, M.H. *et al.* Comprehensive Characterization of Cancer Driver Genes and Mutations. *Cell* **173**, 371-385 e318 (2018).

150. Malumbres, M. & Barbacid, M. Cell cycle, CDKs and cancer: a changing paradigm. *Nat Rev Cancer* **9**, 153-166 (2009).

151. Otto, T. & Sicinski, P. Cell cycle proteins as promising targets in cancer therapy. *Nat Rev Cancer* **17**, 93-115 (2017).

152. Santamaria, D. *et al.* Cdk1 is sufficient to drive the mammalian cell cycle. *Nature* **448**, 811-815 (2007).

153. Hydbring, P. *et al.* Phosphorylation by Cdk2 is required for Myc to repress Ras-induced senescence in cotransformation. *Proc Natl Acad Sci U S A* **107**, 58-63 (2010).

154. Richardson, R.M., Pridgen, B.C., Haribabu, B., Ali, H. & Snyderman, R. Differential cross-regulation of the human chemokine receptors CXCR1 and CXCR2. Evidence for time-dependent signal generation. *J Biol Chem* **273**, 23830-23836 (1998).

155. Nasser, M.W. *et al.* Differential activation and regulation of CXCR1 and CXCR2 by CXCL8 monomer and dimer. *J Immunol* **183**, 3425-3432 (2009).

156. Coppe, J.P., Desprez, P.Y., Krtolica, A. & Campisi, J. The senescence-associated secretory phenotype: the dark side of tumor suppression. *Annu Rev Pathol* **5**, 99-118 (2010).

157. Mrazkova, B. *et al.* Induction, regulation and roles of neural adhesion molecule L1CAM in cellular senescence. *Aging (Albany NY)* **10**, 434-462 (2018).

158. Rapisarda, V. *et al.* Integrin Beta 3 Regulates Cellular Senescence by Activating the TGF-beta Pathway. *Cell Rep* **18**, 2480-2493 (2017).

159. Bindea, G. *et al.* Spatiotemporal dynamics of intratumoral immune cells reveal the immune landscape in human cancer. *Immunity* **39**, 782-795 (2013).

160. Bezzi, M. *et al.* Diverse genetic-driven immune landscapes dictate tumor progression through distinct mechanisms. *Nat Med* **24**, 165-175 (2018).

161. Lavin, Y. *et al.* Innate Immune Landscape in Early Lung Adenocarcinoma by Paired Single-Cell Analyses. *Cell* **169**, 750-765 e717 (2017).

162. Pfannstiel, C. *et al.* The Tumor Immune Microenvironment Drives a Prognostic Relevance That Correlates with Bladder Cancer Subtypes. *Cancer Immunol Res* **7**, 923-938 (2019).

163. Varn, F.S., Wang, Y., Mullins, D.W., Fiering, S. & Cheng, C. Systematic Pan-Cancer Analysis Reveals Immune Cell Interactions in the Tumor Microenvironment. *Cancer Res* **77**, 1271-1282 (2017).

164. Thorsson, V. *et al.* The Immune Landscape of Cancer. *Immunity* **48**, 812-830 e814 (2018).

165. Kurioka, A. *et al.* CD161 Defines a Functionally Distinct Subset of Pro-Inflammatory Natural Killer Cells. *Front Immunol* **9**, 486 (2018).

166. Wang, W., Erbe, A.K., Hank, J.A., Morris, Z.S. & Sondel, P.M. NK Cell-Mediated Antibody-Dependent Cellular Cytotoxicity in Cancer Immunotherapy. *Front Immunol* **6**, 368 (2015).

167. Stoll, G., Zitvogel, L. & Kroemer, G. Differences in the composition of the immune infiltrate in breast cancer, colorectal carcinoma, melanoma and non-small cell lung cancer: A microarray-based meta-analysis. *Oncoimmunology* **5**, e1067746 (2016).

168. Vuletic, A. *et al.* Distribution of several activating and inhibitory receptors on CD3(-)CD56(+) NK cells in regional lymph nodes of melanoma patients. *J Surg Res* **183**, 860-868 (2013).

169. Messaoudene, M. *et al.* Characterization of the Microenvironment in Positive and Negative Sentinel Lymph Nodes from Melanoma Patients. *PLoS One* **10**, e0133363 (2015).

170. Sun, H. *et al.* Accumulation of tumor-infiltrating CD49a+ NK cells correlates with poor prognosis for human hepatocellular carcinoma. *Cancer Immunol Res* (2019).

171. Platonova, S. *et al.* Profound coordinated alterations of intratumoral NK cell phenotype and function in lung carcinoma. *Cancer Res* **71**, 5412-5422 (2011).

172. Balsamo, M. *et al.* Melanoma cells become resistant to NK-cell-mediated killing when exposed to NK-cell numbers compatible with NK-cell infiltration in the tumor. *Eur J Immunol* **42**, 1833-1842 (2012).

173. Huergo-Zapico, L. *et al.* NK-cell Editing Mediates Epithelial-to-Mesenchymal Transition via Phenotypic and Proteomic Changes in Melanoma Cell Lines. *Cancer Res* **78**, 3913-3925 (2018).

174. Chockley, P.J. *et al.* Epithelial-mesenchymal transition leads to NK cell-mediated metastasis-specific immunosurveillance in lung cancer. *J Clin Invest* **128**, 1384-1396 (2018).

175. Collison, J.L., Carlin, L.M., Eichmann, M., Geissmann, F. & Peakman, M. Heterogeneity in the Locomotory Behavior of Human Monocyte Subsets over Human Vascular Endothelium In Vitro. *J Immunol* **195**, 1162-1170 (2015).

176. Headley, M.B. *et al.* Visualization of immediate immune responses to pioneer metastatic cells in the lung. *Nature* **531**, 513-517 (2016).

177. Brunner, P.M. *et al.* Infliximab induces downregulation of the IL-12/IL-23 axis in 6-sulfo-LacNac (slan)+ dendritic cells and macrophages. *J Allergy Clin Immunol* **132**, 1184-1193 e1188 (2013).

178. Martinez, F.O. & Gordon, S. The M1 and M2 paradigm of macrophage activation: time for reassessment. *F1000Prime Rep* **6**, 13 (2014).

179. Singh, S., Nannuru, K.C., Sadanandam, A., Varney, M.L. & Singh, R.K. CXCR1 and CXCR2 enhances human melanoma tumourigenesis, growth and invasion. *Br J Cancer* **100**, 1638-1646 (2009).

180. Holzel, M. & Tuting, T. Inflammation-Induced Plasticity in Melanoma Therapy and Metastasis. *Trends Immunol* **37**, 364-374 (2016).

181. Bald, T. *et al.* Ultraviolet-radiation-induced inflammation promotes angiotropism and metastasis in melanoma. *Nature* **507**, 109-113 (2014).

182. Schadendorf, D. *et al.* IL-8 produced by human malignant melanoma cells in vitro is an essential autocrine growth factor. *J Immunol* **151**, 2667-2675 (1993).

183. Srivastava, S.K. *et al.* Interleukin-8 is a key mediator of FKBP51-induced melanoma growth, angiogenesis and metastasis. *Br J Cancer* **112**, 1772-1781 (2015).

184. Singh, S., Singh, A.P., Sharma, B., Owen, L.B. & Singh, R.K. CXCL8 and its cognate receptors in melanoma progression and metastasis. *Future Oncol* **6**, 111-116 (2010).

185. Peng, H.H., Liang, S., Henderson, A.J. & Dong, C. Regulation of interleukin-8 expression in melanoma-stimulated neutrophil inflammatory response. *Exp Cell Res* **313**, 551-559 (2007).

186. Vujanovic, L., Ballard, W., Thorne, S.H., Vujanovic, N.L. & Butterfield, L.H. Adenovirus-engineered human dendritic cells induce natural killer cell chemotaxis via CXCL8/IL-8 and CXCL10/IP-10. *Oncoimmunology* **1**, 448-457 (2012).

187. Barlic, J. *et al.* beta-arrestins regulate interleukin-8-induced CXCR1 internalization. *J Biol Chem* **274**, 16287-16294 (1999).

188. Feniger-Barish, R., Ran, M., Zaslaver, A. & Ben-Baruch, A. Differential modes of regulation of cxc chemokine-induced internalization and recycling of human CXCR1 and CXCR2. *Cytokine* **11**, 996-1009 (1999).

189. Halama, N. *et al.* Natural killer cells are scarce in colorectal carcinoma tissue despite high levels of chemokines and cytokines. *Clin Cancer Res* **17**, 678-689 (2011).

190. Bottcher, J.P. *et al.* NK Cells Stimulate Recruitment of cDC1 into the Tumor Microenvironment Promoting Cancer Immune Control. *Cell* **172**, 1022-1037 e1014 (2018).

191. Binnewies, M. *et al.* Understanding the tumor immune microenvironment (TIME) for effective therapy. *Nat Med* **24**, 541-550 (2018).

192. Patel, S.J. *et al.* Identification of essential genes for cancer immunotherapy. *Nature* **548**, 537-542 (2017).

193. Mojic, M., Takeda, K. & Hayakawa, Y. The Dark Side of IFN-gamma: Its Role in Promoting Cancer Immunoevasion. *Int J Mol Sci* **19** (2017).

194. Adib-Conquy, M., Scott-Algara, D., Cavaillon, J.M. & Souza-Fonseca-Guimaraes, F. TLR-mediated activation of NK cells and their role in bacterial/viral immune responses in mammals. *Immunol Cell Biol* **92**, 256-262 (2014).

195. Smith-Garvin, J.E., Koretzky, G.A. & Jordan, M.S. T cell activation. *Annu Rev Immunol* **27**, 591-619 (2009).

196. Mosteiro, L. *et al.* Tissue damage and senescence provide critical signals for cellular reprogramming in vivo. *Science* **354** (2016).

197. Mosteiro, L., Pantoja, C., de Martino, A. & Serrano, M. Senescence promotes in vivo reprogramming through p16(INK)(4a) and IL-6. *Aging Cell* **17** (2018).

198. Ortiz-Montero, P., Londono-Vallejo, A. & Vernot, J.P. Senescence-associated IL-6 and IL-8 cytokines induce a self- and cross-reinforced senescence/inflammatory milieu strengthening tumorigenic capabilities in the MCF-7 breast cancer cell line. *Cell Commun Signal* **15**, 17 (2017).

199. Senturk, S. *et al.* Transforming growth factor-beta induces senescence in hepatocellular carcinoma cells and inhibits tumor growth. *Hepatology* **52**, 966-974 (2010).

200. Wu, S. *et al.* TGF-beta enforces senescence in Myc-transformed hematopoietic tumor cells through induction of Mad1 and repression of Myc activity. *Exp Cell Res* **315**, 3099-3111 (2009).

201. Haferkamp, S. *et al.* Vemurafenib induces senescence features in melanoma cells. *J Invest Dermatol* **133**, 1601-1609 (2013).

202. Antonangeli, F., Zingoni, A., Soriani, A. & Santoni, A. Senescent cells: Living or dying is a matter of NK cells. *J Leukoc Biol* **105**, 1275-1283 (2019).

203. Textor, S. *et al.* Human NK cells are alerted to induction of p53 in cancer cells by upregulation of the NKG2D ligands ULBP1 and ULBP2. *Cancer Res* **71**, 5998-6009 (2011).

204. Quintana, E. *et al.* Phenotypic heterogeneity among tumorigenic melanoma cells from patients that is reversible and not hierarchically organized. *Cancer Cell* **18**, 510-523 (2010).

205. Milanovic, M. *et al.* Senescence-associated reprogramming promotes cancer stemness. *Nature* **553**, 96-100 (2018).

206. Batlle, E. & Clevers, H. Cancer stem cells revisited. *Nat Med* **23**, 1124-1134 (2017).

207. Maccalli, C., Volonte, A., Cimminiello, C. & Parmiani, G. Immunology of cancer stem cells in solid tumours. A review. *Eur J Cancer* **50**, 649-655 (2014).

208. Miao, Y. *et al.* Adaptive Immune Resistance Emerges from Tumor-Initiating Stem Cells. *Cell* **177**, 1172-1186 e1114 (2019).

209. Maccalli, C., Rasul, K.I., Elawad, M. & Ferrone, S. The role of cancer stem cells in the modulation of anti-tumor immune responses. *Semin Cancer Biol* **53**, 189-200 (2018).

210. Landsberg, J. *et al.* Melanomas resist T-cell therapy through inflammation-induced reversible dedifferentiation. *Nature* **490**, 412-416 (2012).

211. Tallerico, R., Garofalo, C. & Carbone, E. A New Biological Feature of Natural Killer Cells: The Recognition of Solid Tumor-Derived Cancer Stem Cells. *Front Immunol* **7**, 179 (2016).

212. Tallerico, R. *et al.* Human NK cells selective targeting of colon cancer-initiating cells: a role for natural cytotoxicity receptors and MHC class I molecules. *J Immunol* **190**, 2381-2390 (2013).

213. Tseng, H.C. *et al.* Increased lysis of stem cells but not their differentiated cells by natural killer cells; de-differentiation or reprogramming activates NK cells. *PLoS One* **5**, e11590 (2010).

214. Ames, E. *et al.* NK Cells Preferentially Target Tumor Cells with a Cancer Stem Cell Phenotype. *J Immunol* **195**, 4010-4019 (2015).

215. Stokes, K.L. *et al.* Natural killer cells limit the clearance of senescent lung adenocarcinoma cells. *Oncogenesis* **8**, 24 (2019).

216. Iannello, A., Thompson, T.W., Ardolino, M., Lowe, S.W. & Raulet, D.H. p53-dependent chemokine production by senescent tumor cells supports NKG2D-dependent tumor elimination by natural killer cells. *J Exp Med* **210**, 2057-2069 (2013).

217. Hacke, K. *et al.* Regulation of MCP-1 chemokine transcription by p53. *Mol Cancer* **9**, 82 (2010).

218. Shiraishi, K. *et al.* Identification of fractalkine, a CX3C-type chemokine, as a direct target of p53. *Cancer Res* **60**, 3722-3726 (2000).

219. Lujambio, A. *et al.* Non-cell-autonomous tumor suppression by p53. *Cell* **153**, 449-460 (2013).

220. Schosserer, M., Grillari, J. & Breitenbach, M. The Dual Role of Cellular Senescence in Developing Tumors and Their Response to Cancer Therapy. *Front Oncol* **7**, 278 (2017).

221. Kim, Y.H. *et al.* Senescent tumor cells lead the collective invasion in thyroid cancer. *Nat Commun* **8**, 15208 (2017).

222. Coppe, J.P. *et al.* Tumor suppressor and aging biomarker p16(INK4a) induces cellular senescence without the associated inflammatory secretory phenotype. *J Biol Chem* **286**, 36396-36403 (2011).

223. Beffinger, M. *et al.* CSF1R-dependent myeloid cells are required for NKmediated control of metastasis. *JCI Insight* **3** (2018).

224. Jung, K. *et al.* Ly6Clo monocytes drive immunosuppression and confer resistance to anti-VEGFR2 cancer therapy. *J Clin Invest* **127**, 3039-3051 (2017).

225. Parodi, M. *et al.* Natural Killer (NK)/melanoma cell interaction induces NK-mediated release of chemotactic High Mobility Group Box-1 (HMGB1) capable of amplifying NK cell recruitment. *Oncoimmunology* **4**, e1052353 (2015).

226. Li, Q. *et al.* Overexpression of HMGB1 in melanoma predicts patient survival and suppression of HMGB1 induces cell cycle arrest and senescence in association with p21 (Waf1/Cip1) up-regulation via a p53-independent, Sp1-dependent pathway. *Oncotarget* **5**, 6387-6403 (2014).

227. Davalos, A.R. *et al.* p53-dependent release of Alarmin HMGB1 is a central mediator of senescent phenotypes. *J Cell Biol* **201**, 613-629 (2013).

228. Hoshino, A. *et al.* Tumour exosome integrins determine organotropic metastasis. *Nature* **527**, 329-335 (2015).

229. Goel, S. *et al.* CDK4/6 inhibition triggers anti-tumour immunity. *Nature* **548**, 471-475 (2017).

230. Ruscetti, M. *et al.* NK cell-mediated cytotoxicity contributes to tumor control by a cytostatic drug combination. *Science* **362**, 1416-1422 (2018).

231. Barry, K.C. *et al.* A natural killer-dendritic cell axis defines checkpoint therapy-responsive tumor microenvironments. *Nat Med* **24**, 1178-1191 (2018).

8 Abbreviations

°C	degree
µg	microgram
A488	Alexa Fluor 488
A647	Alexa Fluor 647
ADCC	antibody-dependent cellular cytotoxicity
AP	alkaline phosphatase
APC	antigen-presenting cell
BCA	bicinchoninic acid
Bcl-XL	B-cell lymphoma-extra large
BCR	B cell receptor
CCL	CC chemokine ligand
CCR	CC chemokine receptor
CD	Cluster of Differentiation
cDC	conventional dendritic cell
CDK	cyclin-dependent kinase
CDKI	CDK inhibitor
cDNA	complementary DNA
CLR	C-type lectin-like receptor
CM	conditioned medium
cpm	counts per minute
CTLA-4	cytotoxic T-lymphocyte-associated Protein 4
CXCL	C-X-C chemokine ligand
CXCR	C-X-C chemokine receptor
DAMP	damage-associated molecular pattern
DC	dendritic cell
DD1	Dresden 1; monoclonal antibody directed against slan
DD2	Dresden 2; monoclonal antibody directed against slan
ECL	electrochemiluminescence
ECM	extracellular matrix

EDTA	ethylenediaminetetraacetic acid
EMT	epithelial to mesenchymal transition
FACS	fluorescence-activated cell sorting
FCS	fetal calf serum
FFPE	Formalin-fixed paraffin-embedded
g	gram
GPCR	g-protein coupled receptor
HMGB1	high mobility group box 1
HRP	horseradish peroxidase
ICAM1	intercellular adhesion molecule 1
IDO	Indoleamine 2,3-deoxygenase
IF	Immunofluorescence
IFNGR1	Interferon gamma receptor 1
IFN-γ	Interferon gamma
IgG	Immunoglobulin
IHC	Immunohistochemistry
IL	Interleukin
ILC	Innate lymphoid cell
Iso	Isotype
ITAM	immunoreceptor tyrosine-based activation motifs
ITIM	immunoreceptor tyrosine-based inhibitory motifs
JAK1/2	Janus kinase 1/2
KLRB1	Killer Cell Lectin Like Receptor B1
KLRG1	Killer cell lectin-like receptor subfamily G member 1
LFA-1	lymphocyte function-associated antigen 1
LPS	Lipopolysaccharid
Ly6C	lymphocyte Ag 6C
MAPK	mitogen-activated protein kinase
M-DC8	Munich – dendritic cell 8; monoclonal antibody against slan
MDSC	myeloid-derived suppressor cell
mg	milligram

MHC	major histocompatibility complex
MIC-A	MHC class I chain-related gene A
MMP	matrix metalloproteinases
NF-κB	nuclear factor k-light-chain-enhancer of activated B cells
ng	nanogram
NK cell	natural killer cell
NLR	NOD-like receptor
NR4A1	nuclear receptor subfamily 4 group A member 1
OIS	oncogene-induced senescence
p16	$p16^{INK4a}$
p21	$p21^{cip1}$
PAMP	pathogen-associated molecular pattern
PBMCs	peripheral blood mononuclear cells
PBS	Phosphate buffered saline
pDC	plasmacytoid dencritic cell
PDGF	platelet-derived growth factor
PD-L1	Programmed cell death 1 ligand 1
PEDF	pigment epithelium-derived factor
pg	picogram
PLC2	phospholipase Cβ2
PSGL-1	P-selectin glycoprotein ligand-1
RAGE	receptor for advanced glycation enproducts
Rb	Retinoblastom
rcf	relative centrifugal force
RLR	RIG-like receptor
RPMI 1640	Roswell Park Memorial Institute 1630 medium
RT	room temperature
SA β-Gal	senescence-associated β-Galactosidase
SASP	senescence-associated secretory phenotype
SDF-1	stromal-derived-factor 1
SIRPα	signal-regulatory protein α

slan	6-sulfo LacNAc
slanMo	slan positive monocyte
SLO	secondary lymphoid organs
ssRNA	single stranded RNA
STAT1	Signal transducer and activator of transcription 1
T reg	T regulatory cell
TAM	tumor-associated macrophage
TCR	T cell receptor
TGF-β	transforming growth factor beta
Th	T helper
TIGIT	T cell immunoreceptor with Ig and ITIM domains
TLR	Toll-like receptor
TMB	3,3´,5,5´-Tetramethylbenzidine
TME	tumor microenvironment
TNF-α	tumor necrosis factor-alpha
TRAIL	TNF-related apoptosis-inducing ligand
TT	Tetanus toxoid
ULBP	UL16 binding protein
VCAM1	vascular cell-adhesion molecule 1
VEGF	vascular endothelial growth factor
VLA4	very late antigen 4
WB	Western Blot
β2m	β2-Microglobulin

9 Acknowledgements

I would like to thank my supervisors Prof. Knut Schäkel and Prof. Heidi Cerwenka for providing me the opportunity to perform my PhD thesis in their laboratories. Their feedback and support guided me through the years as a PhD and shaped my scientific development.

Additionally, I want to thank Prof. Viktor Umansky, who not only agreed to be the first examiner for my thesis, but also supported me over the years during TAC meetings and RTG events. I am thankful to Prof. Georg Stöckling for serving as chair for my defense and Dr. Guoliang Cui to complete the committee as fourth examiner.

For the support during TAC meetings and the opportunity to come to London, I want to thank Prof. Adrian Hayday. Further, I want to acknowledge the help of all collaborators that helped me during my PhD. In particular I want to thank Jasmin Roth, Lenka Kyjacova, and Prof. Jessica Hassel for supporting me with experiments and with providing samples.

A special thanks also goes to Jens and the group in Mannheim, who helped and supported me a lot during my first steps in the PhD. Even though I spent only a short time in the lab there, I am glad for all the shared lab outings and Christmas parties.

I am very grateful for the time in the Hautklinik lab and I am happy to have met so many funny, crazy, amazing friends during my PhD there. I want to thank my Jingi for a billion high-fives and involuntary chair rides, Hao for all the Chinese traditions he introduced us to, Yutaka for all the funny moments in and around the lab, Frauhammer for all the crazy stories we had together, Florina for always being so nice and supportive, Carmen for all the short chats, Florian for joining all the lab events, the spanish guys Cinthia and Adriana for a lot of very funny beer hours, and Lukas for all the help in the lab, the Skat and board game nights, and all the funny moments. Thanks Silvi, Stefan and Galina for helping me so much with experiments and for making it a nice atmosphere in the lab. I am thankful to Karsten and Sabine for the help and support with experiments. I will also remember all the people that only stayed for a short time in lab: Sophie, Julius, Martin, Danny, Priscilla, Mustafa, Meihong, Akira, and many more. Thanks a lot to Fareed for all the help and support. It was great to have you in the lab and I will miss our little coffee breaks and your minimum essential medium.

I am especially thankful to Diego and the Steffi's, Oehrli and Häberli. I will always remember the time we had in the lab, all the crazy actions, late night dinners in the lab, parties, vacations, and Bärchi missions. You all supported me a lot during my struggles in the PhD, every one of you in their own way. Thank you Steffi Häberle for always listening to my problems and for trying to cheer me up when I needed it.

Zum Abschluss möchte ich mich bei meiner Mutter und meiner Freundin Melanie bedanken. Dorit, du hast das alles möglich gemacht. Du hast mich da hingebracht wo ich jetzt bin, und dafür bin ich dir unendlich dankbar.

Melli, ich weiß nicht wo ich anfangen soll dir zu danken. Du warst und bist immer für mich da und ich weiß nicht wie ich es ohne dich geschafft hätte. Ich liebe Dich.